

**ENVIRONMENTAL CHAMBER STUDIES OF ATMOSPHERIC  
REACTIVITIES OF VOLATILE ORGANIC COMPOUNDS.  
EFFECTS OF VARYING ROG SURROGATE AND NO<sub>x</sub>**

Final Report to

California Air Resources Board, Contract A032-096  
Coordinating Research Council, Inc., Project ME-9  
National Renewable Energy Laboratory, Contract ZF-2-12252  
South Coast Air Quality Management District, Contract C91323

by

William P. L. Carter, Dongmin Luo,  
Irina L. Malkina, and John A. Pierce

March 24, 1995

Statewide Air Pollution Research Center, and  
College of Engineering, Center for Environmental Research and Technology  
University of California, Riverside, CA 92521

## **PREFACE**

This report describes work carried out at the University of California under funding from the California Air Resources Board (CARB) through contract number A032-096, the Coordinating Research Council, Inc. (CRC) through project number ME-9, the National Renewable Energy Laboratory (NREL) through contract ZF-2-12252, and the California South Coast Air Quality Management District (SCAQMD) through contract no. C91323. CARB, CRC and NREL funded most of the experimental work, and the SCAQMD funded the building where the experiments were conducted.

The opinions and conclusions in this document are entirely those of the authors. Mention of trade names and commercial products does not constitute endorsement or recommendation for use.

## ABSTRACT

A series of indoor environmental chamber experiments were conducted to measure incremental reactivities of representative volatile organic compounds (VOCs) in irradiations of various reactive organic gas (ROG) surrogate -  $\text{NO}_x$  - air mixtures designed to represent or approximate conditions of urban photochemical smog. Incremental reactivities are defined as the change in to ozone formation or OH radical levels caused by adding the VOC to a "base case" experiment, divided by the amount added. The base case included irradiations, at both relatively high and low  $\text{NO}_x$  levels, of a surrogate mixture of 8 VOCs which model calculations predicted would yield the same results as use of a full ambient ROG mixture, and high  $\text{NO}_x$  experiments where ethylene alone represented the ambient ROGs. The test VOCs included carbon monoxide, n-butane, n-hexane, n-octane, ethylene, propene, trans-2-butene, benzene, toluene, m-xylene, formaldehyde, and acetaldehyde. The data obtained show that VOC have a greater range of incremental reactivities when simplified base case ROG surrogates are used than with the more realistic 8-component surrogate. Reducing  $\text{NO}_x$  reduced incremental reactivities by differing amounts for different VOCs, with ozone reactivities of propene, trans-2-butene, acetaldehyde, and the aromatics becoming negative in the low  $\text{NO}_x$  experiments. These results are consistent with model predictions. The model simulated reactivities in experiments with the more complex surrogate reasonably well, though it was more variable in the simulations of the simpler systems, which are more sensitive to differences among the VOCs. Model calculations indicated that experimentally measured incremental reactivities may correlate well with those in the atmosphere under high  $\text{NO}_x$  conditions, but not when  $\text{NO}_x$  is low. Thus the best use for data from incremental reactivity experiments is evaluating the models used to predict reactivities in the atmosphere.

## ACKNOWLEDGEMENTS

The authors wish to acknowledge and thank Mr Bart Croes of the CARB, Mr. Tim Belian of the CRC, Dr. Alan Lloyd of the SCAQMD, Mr. Brent Bailey of NREL, and the members of the CRC/APRAC reactivity committee for their support of this project and their patience with the delays in completing this report. We also gratefully acknowledge Dr. Joseph Norbeck, Director of the University of California, Riverside's College of Engineering Center for Environmental Research and Technology (CE-CERT) for providing significant salary support and equipment used in this project.

Valuable assistance in constructing the chamber facility and conducting the experiments for this program was provided by Mr William D. Long. Mr. Robert Walters assisted in improvements to the pure air and temperature control system used in this project. Assistance in conducting the experiments was provided by Ms. Kathalena M. Smihula and Mr. Armando D. Avallone. Mr. Dennis Fitz assisted in the preparation of this report. Dr. Harvey Jeffries of the University of North Carolina provided the ambient VOC data and assignments used in the analysis discussed in Section II.

## EXECUTIVE SUMMARY

### Introduction

The formation of ground-level ozone is caused by the gas-phase interactions of emitted volatile organic compounds (VOCs) and oxides of nitrogen ( $\text{NO}_x$ ) in the presence of sunlight. Although traditional VOC control strategies to reduce ozone have focused on reducing the total mass of VOC emissions, not all VOCs are equal in the amount of ozone formation they cause. Control strategies which take into account these differences in "reactivities" of VOCs might provide a means for additional ozone reduction which could supplement mass-based controls. Examples include conversion of motor vehicles to alternative fuels and solvent substitutions. However, before reactivity-based strategies can be implemented, there must be a means to quantify VOC reactivity which is sufficiently reliable that it can be used in regulatory applications.

The most direct quantitative measure of the degree to which a VOC contributes to ozone formation in a photochemical air pollution episode is its "incremental reactivity". This is defined as the amount of additional ozone formation resulting from the addition of a small amount of the compound to the emissions in the episode, divided by the amount of compound added. This depends both on the VOC and on the conditions of the environment where it emitted, such as  $\text{NO}_x$  levels and the nature and level of other reactive organic gases (ROGs) which are present. Incremental reactivities in the atmosphere can be calculated using computer airshed models, given a model for airshed conditions and a mechanism for the VOCs' atmospheric chemical reactions. This approach was used in the development of the "Maximum Incremental Reactivity" (MIR) scale (Carter, 1993, 1994), which has been adopted by the California Air Resources Board (ARB) for the derivation of reactivity adjustment factors for use in vehicle emissions standards (CARB 1991).

However, model calculations of reactivity can be no more reliable than the chemical mechanisms upon which they are based. Therefore, mechanisms must be evaluated under controlled conditions by comparing their predictions against results of environmental chamber experiments. The Statewide Air Pollution Research Center (SAPRC), in conjunction with the College of Engineering, Center for Environmental Research and Technology (CE-CERT), has been conducting a multi-year environmental chamber program to address these data needs. This program is being carried out in several phases, as discussed below.

In the first phase of this program, we measured the incremental reactivities of 36 representative VOCs under relatively high  $\text{NO}_x$  conditions using a simplified "surrogate" mixture to represent ROGs in the atmosphere and a blacklight light source (Carter et al., 1993a). These data were important in providing experimental reactivity data for a large variety of VOCs under conditions where  $\text{O}_3$  formation is most sensitive to VOC emissions. However, they

provided no information concerning the effect on VOC reactivity on variations of environmental conditions, such as varying NO<sub>x</sub> levels or the nature of the other ROG<sub>s</sub> present. In addition, the 3-component mixture used to represent the other reactive organics in the atmosphere (referred to as the "base ROG surrogate") greatly oversimplified actual atmospheric systems.

The second phase of this program had two major components. The first consisted of measuring incremental reactivities of representative VOCs using different base ROG surrogate mixtures and under lower NO<sub>x</sub> conditions. The second consisted of obtaining experimental data to assess the effect of varying the light source on the ability of models to simulate the results of environmental chamber experiments. The second component is discussed in a separate report "Environmental Chamber Studies of Atmospheric Reactivities of Volatile Organic Compounds. Effects of Varying Chamber and Light Source" (Carter et al., 1995a). This report describes our study of the effects of varying base ROG surrogate and NO<sub>x</sub> conditions on experimentally measured incremental reactivities.

#### **Modeling Effects of Base ROG Surrogates on Incremental Reactivity Experiments**

Incremental reactivity experiments consist of measuring the effect of adding a test VOC to a "base case" experiment designed to simulate an already polluted atmosphere. The base case experiment consists of a one-day irradiation of NO<sub>x</sub> and a "base ROG surrogate" designed to represent the mixture of reactive organic pollutants in the atmosphere. Use of highly simplified mixtures as the base ROG surrogate, such as the 3-component mixture employed in our Phase I study, has the important advantages of experimental simplicity and more straightforward use of the results for mechanism evaluation. However, if the chemical conditions of the experiments are too unrealistic, the data may not provide an appropriate test to the parts of the mechanism which are important in affecting predictions of atmospheric reactivity. To determine the most appropriate surrogates to use for such a study, we conducted a modeling study of the effects of varying ROG surrogates on experimental measurements of incremental reactivity, and how experimental incremental reactivities correlate with those in the atmosphere.

The results of this modeling study indicated that an 8-component surrogate designed to represent a similar level of chemical detail as used in current airshed models provides an excellent representation of the ambient ROG mixture for reactivity experiments, and that use of more complex mixtures would not yield experimentally distinguishable results. The effect of ignoring unreactive carbon in the ROG surrogate was calculated to be negligible. However, the calculations also showed that even if the exact same ROG mixture is used in the experiments as occurs in the atmosphere, reactivities in environmental chamber experiments would not necessarily be the same or even correlate with those in the atmosphere. The best correlations are obtained with reactivities under maximum reactivity conditions and with IntOH reactivities under various conditions. No correlation

is obtained with ozone reactivities under maximum ozone or NO<sub>x</sub>-limited conditions.

The 3-component "mini-surrogate" used in the Phase I study was calculated to yield measurable differences in reactivities for many species, and significantly higher reactivities for formaldehyde and acetone. However, the calculations also indicated that experiments using the simpler 3-component mini-surrogates are more sensitive to effects of differences among VOCs, and thus potentially more useful for mechanism evaluation. Since such mechanism evaluations are complicated by uncertainties in the m-xylene mechanism, calculations were conducted to determine whether use of an even simpler surrogate consisting of ethylene alone might provide equivalent information while minimizing problems due to ROG surrogate mechanism uncertainties. It was found that the ethylene surrogate gives almost equivalent maximum reactivity results as the "mini-surrogate", but tends to be more sensitive to NO<sub>x</sub>-sink species under NO<sub>x</sub>-limited conditions. The latter may be an advantage from the point of view of evaluating this aspect of VOC mechanisms.

Based on these results, it was determined that incremental reactivity experiments using both the lumped surrogate, and ethylene alone as the surrogate, would, in conjunction with the mini-surrogate experiments already conducted, provide useful and complementary information concerning the effect of ROG surrogate on incremental reactivity. These experiments are discussed in the following sections.

#### **Environmental Chamber Experiments**

Incremental reactivity experiments were carried out using two different ROG surrogates and two different NO<sub>x</sub> levels. The "ethene surrogate" experiments used ethene as the base ROG surrogate and were carried out at the relatively high NO<sub>x</sub> levels where VOCs have their highest incremental reactivities. The "full surrogate" experiments used the 8-component mixture derived as a result of the modeling study discussed above, and were carried out at both the relatively high "maximum incremental reactivity" NO<sub>x</sub> levels and at ~4 times lower NO<sub>x</sub> levels where O<sub>3</sub> formation is NO<sub>x</sub>-limited. The compounds studied under all three conditions were carbon monoxide, n-butane, n-octane, propene, trans-2-butene, m-xylene, and formaldehyde. Experiments with ethane, ethene, benzene, toluene, and acetaldehyde were carried out under a subset of these conditions.

The results were analyzed to derive the following measures of reactivity: (1) the effect of the VOC on the total amount of O<sub>3</sub> formed and NO oxidized, which is referred to as its "total" reactivity; (2) the effect of the VOC on integrated radical levels, or its "IntOH" reactivity; and (3) the "direct" reactivity of the VOC, which is an estimate of the amount of O<sub>3</sub> formation and NO oxidation caused directly by radicals formed in the reactions of the test VOC or its direct reaction products. The latter can be estimated under high NO<sub>x</sub> conditions based on the assumption that the total effect of the VOC on O<sub>3</sub> formation and NO oxidation is the direct reactivity plus the effect of the VOC on the amount of

reaction of the components of the base ROG surrogate, which in turn can be estimated from the IntOH reactivities and the correspondence between O<sub>3</sub> formation, NO oxidation, and IntOH levels in the "base case" experiments where the test VOC is not present. Derivation of these separate components of reactivity are useful for understanding the mechanistic basis behind the observed reactivities, and for evaluating whether the current mechanisms appropriate represent these components.

The results of these experiments are expressed in terms of "mechanistic reactivities", which are analogous to incremental reactivities except they are relative to the amount of test VOC reacted up to the time of the observation, rather than the amount added. Mechanistic reactivities are useful because, to a first approximation, they are independent on how rapidly the VOC reacts, and thus allow comparisons of reactivity characteristics of VOCs which react at different rates. It is the most uncertain component of incremental reactivity because atmospheric reaction rate constants are reasonably well characterized for most VOCs.

Table EX-1 gives a summary of selected total and direct mechanistic reactivity results obtained using the different ROG surrogates and NO<sub>x</sub> levels from this work. Comparable results from our Phase I study are also shown for comparison. It can be seen that decreasing the NO<sub>x</sub> levels causes the total mechanistic reactivities to decrease, but the extent of decrease varies depending on the type of compound. In addition, the nature of the base ROG surrogate

Table EX-1. Summary of experimentally measured total and direct mechanistic reactivities for selected VOCs[a].

Compound	--- Total Mechanistic Reactivity ---				Direct Mechanistic React'y		
	----- High NO <sub>x</sub> -----		----- Low NO <sub>x</sub> -----		----- High NO <sub>x</sub> -----		
	Ethene	Mini Srg	Full Srg	Full Srg	Ethene	Mini Srg	Full Srg
CO	1.1±0.2	0.7±0.2	0.5	0.3±0.1	1.2±0.3	0.8±0.1	0.7
n-Butane	1.2±0.4	0.8±0.3	1.2±0.1	0.6±0.1	1.7±0.6	2.2±0.4	1.9±0.1
n-Octane	-0.8±0.2	-4.4±1.2	0.8±0.2	0.3±0.2	1.8±0.4	2.3±1.0	2.3±0.3
Propene	2.3±0.3	2.7±0.7	1.0±0.1	0.0±0.1		[b]	0.2±0.1
t-2-Butene	6.0±1.1	5.4±1.0	1.0±0.1	-0.1±0.2			0.2±0.1
Toluene		7.0±1.0	2.8±0.5	-0.5±0.1			1.0±0.4
m-Xylene	7.6±0.7	7.6±2.5	4.9±0.8	-0.7±0.3			
Acetald.		0.4±0.2	0.6±0.2	-0.2±0.1		1.4±0.2	1.7±0.4

[a] Units are moles of O<sub>3</sub> per mole VOC reacted. Most values are weighted averages of results of several experiments. "Ethene", "Mini Srg" and "Full Srg" refer to the base ROG surrogate, where "Full Srg" refers to the 8-component mixture derived in this work, and "Mini Srg" refers to experiments from the Phase I study using the 3-component mixture. The "Ethene" and "Full Srg" data are from this study.

[b] Blank means that direct mechanistic reactivities could not be determined with sufficient precision to be meaningful.

significantly affects total mechanistic reactivities for some compounds, particularly n-octane, whose total reactivity is positive with the full surrogate but negative with the simplified ones, with the data using the mini-surrogate being more similar to those using the ethene surrogate than those using the 8-component mixture. On the other hand, the nature of the base ROG surrogate does not appear to have a significant effect on direct mechanistic reactivities, at least for those compounds where this could be determined. These observations are generally consistent with results of model simulations using an updated version of the SAPRC detailed chemical mechanism.

## Discussion and Conclusions

The experimental data and model simulations have shown that the presence of other VOC pollutants can significantly affect the incremental reactivities of added VOCs. For example, the model predicted, and the experimental data confirmed, that the incremental reactivity of n-octane could change sign, and the absolute reactivities of species such as alkenes, aromatics, and formaldehyde could change significantly, depending on the mixture used to represent the base ROG. VOCs were found to have much smaller differences in ozone effects when reacting in the presence of a more complex mixture designed to represent ambient ROG pollutants than when reacting in the presence of more simplified mixtures such as the 3-component "mini-surrogate" used in our Phase I study. This is attributed to species in the more complex mixture, such as formaldehyde and (perhaps to a lesser extent) internal alkenes, which provide radical sources early in the irradiations, and tend to make the system less sensitive to the radical input or termination processes caused by the test VOC.

On the other hand, model simulations showed that it is probably not necessary to use a highly complex mixture to adequately represent the effects of other ROG pollutants in experimental studies of incremental reactivity. Use of a simple 8-component mixture, containing approximately the level of chemical detail as incorporated in condensed "lumped molecule" mechanisms in airshed models, was calculated to provide indistinguishable reactivity results in chamber experiments as use of an ambient ROG mixture containing the full set of compounds measured in the atmosphere. But simplifying this 8-component mixture further was found to have non-negligible effects on reactivity.

Using a realistic ROG surrogate is obviously necessary if experimental reactivity data are to correspond to reactivities in the atmosphere. However, it is not sufficient. Model calculations showed that even if the ambient mixture itself is used as the ROG surrogate, the extent to which chamber reactivities correlate with those in the atmosphere depended significantly on  $\text{NO}_x$  conditions. Under high  $\text{NO}_x$  conditions, experimental incremental reactivities correlate moderately well with atmospheric reactivities in the MIR scale, though the correlation was poor for acetaldehyde, and the correlation with the chamber data could only predict the atmosphere reactivities for the other VOCs to within  $\pm 50\%$ . Under low  $\text{NO}_x$  conditions, there was *no correlation at all* between atmospheric

reactivity and reactivity in the chamber experiments. This was true whether using real chamber data or chamber data simulated by the model. Reactivities under low NO<sub>x</sub> conditions are influenced by differing and often opposing factors, and apparently balances among these factors are quite different in the chamber experiments than in the atmosphere.

It may be possible someday to design an experimental system which gives better correlations between experimental and atmospheric reactivities, but we suspect it would be extremely difficult and expensive, and may yield data with large experimental uncertainties. In the meantime, we must rely on model simulations to predict reactivities in the atmosphere. The role of the chamber data is thus not to directly measure atmospheric reactivity, but rather to evaluate and if necessary calibrate the models which must be used for this purpose.

Experiments with both realistic and simplified ROG surrogates are necessary for an adequate evaluation of the ability of models to predict reactivity. Use of realistic surrogates are obviously necessary to test the ability of the mechanism to simulate reactivities in chemically realistic conditions. However, experiments with simpler surrogates are more sensitive to differences among VOCs, particularly in terms of their effects on radical levels. This means that model simulations of those experiments would be more sensitive to errors in the mechanisms of the VOCs. This is consistent with the results of this study, where in general the mechanism performed better in simulating reactivity in the experiments using the more complex surrogate than it did in the experiments using the mini-surrogate or ethylene alone.

The experimental data in this study confirmed the model predictions concerning the importance of NO<sub>x</sub> in affecting a VOC's incremental reactivity. As expected, the incremental and mechanistic reactivities of all VOCs were reduced under low NO<sub>x</sub> conditions. As also expected, this reduction was the greatest for VOCs, such as aromatics, acetaldehyde, and the higher alkenes, which are believed to have significant NO<sub>x</sub> sinks in their mechanisms. All these NO<sub>x</sub> sink species were found to have negative reactivities in our low NO<sub>x</sub> experiments. This includes species, such as alkenes and acetaldehyde, which are calculated to have positive reactivities under low NO<sub>x</sub> conditions in the atmosphere (Carter, 1993, 1994). Thus, low NO<sub>x</sub> chamber reactivity experiments appear to be highly sensitive to effects of NO<sub>x</sub> sinks in VOC's mechanisms - much more so than is apparently the case in the atmosphere. This high sensitivity may be the cause of the poor correlation between low NO<sub>x</sub> chamber data and atmospheric reactivities. However, this also means that the chamber data should provide a highly sensitive test to this aspect of the mechanism.

The current detailed chemical mechanism was found to perform remarkably well in simulating the reactivities of the VOCs with the realistic 8-component surrogate, both under high and low NO<sub>x</sub> conditions. An exception was that the

model did not correctly predict the effects of aromatics on radical levels under low NO<sub>x</sub> conditions. In addition, the model did not give totally satisfactory performance in simulating the incremental reactivity of formaldehyde and performed poorly in simulating the incremental reactivity of n-octane using the ethene surrogate. In general, the model performance was more variable in simulating the experiments with the highly simplified (ethylene only) surrogate, though the observed reactivity trends were correctly predicted. The greater variability is attributable in part to the greater sensitivity of the simpler systems to mechanism differences, as indicated above. However, it can also be attributable to the greater sensitivity of simulations of the ethene reactivity experiments to uncertainties in reaction conditions and the ethene mechanism. With more base ROG components present, errors in the mechanisms and amounts of each individual component becomes relatively less important in affecting the result.

While problems and uncertainties with the mechanisms remain, the results of this study generally give a fairly optimistic picture of the ability of the model to simulate reactivities under atmospheric conditions. This optimism is in part due to the fact that systems with realistic mixtures tend to be less sensitive to errors in the mechanisms than systems that are perhaps most useful for mechanism evaluation. However, one would clearly have more confidence in the fundamental validity of reactivity predictions if the model could satisfactorily predict reactivities in simple as well as complex chemical systems. The data obtained thus far indicate that if the model can simulate reactivity with simple ROG surrogates, it should be able to do so in the more realistic chemical system.

Although this study, in conjunction with our Phase I work, has provided a large experimental data base on VOC reactivity, it is not comprehensive. For example, only a relatively small number of VOCs have been studied using the more realistic 8-component surrogate. The mini-surrogate provide a more comprehensive data set, but the data quality for some important VOCs was not as good as can be obtained using the present facility, and many important VOCs, such as branched alkane isomers, have been inadequately studied. No information has been obtained concerning the effect of temperature on reactivity, and there is only limited information concerning the effects of varying the light sources. Experiments which address some of these issues are discussed in a separate report (Carter et al., 1995a), or are now underway as part of our ongoing studies.



## TABLE OF CONTENTS

<u>Section</u>	<u>Page</u>
ABSTRACT . . . . .	iii
ACKNOWLEDGEMENTS . . . . .	iv
EXECUTIVE SUMMARY . . . . .	v
LIST OF TABLES . . . . .	xv
LIST OF FIGURES . . . . .	xvi
I. INTRODUCTION . . . . .	xx
II. MODELING ANALYSIS OF ROG SURROGATES . . . . .	4
A. Derivation of Ambient ROG Mixture . . . . .	4
1. Hydrocarbon Portion . . . . .	5
2. Oxygenate Portion . . . . .	10
B. Derivation of the Lumped Molecule (Lumped) Surrogate . . . . .	10
C. Calculated Effects of Complexity of ROG Surrogate on Mechanistic Reactivities . . . . .	13
D. Comparison of Predicted Experimental Reactivities with the Maximum Reactivity and Maximum Ozone Reactivity Scales. . . . .	22
E. Summary . . . . .	27
III. EXPERIMENTAL FACILITY AND METHODS . . . . .	29
A. Facility . . . . .	29
1. New Indoor and Outdoor Chamber Laboratory Facility . . . . .	29
2. Indoor Teflon Chamber #2 (ETC) . . . . .	31
3. Dividable Teflon Chamber (DTC) . . . . .	31
B. Experimental Procedures . . . . .	34
C. Analytical Methods . . . . .	34
D. Characterization Data . . . . .	35
1. Light Source . . . . .	35
2. Temperature . . . . .	36
3. Dilution . . . . .	36
4. Control Experiments . . . . .	36
IV. EXPERIMENTAL ANALYSIS METHODS AND RESULTS . . . . .	37
A. Reactivity Analysis Methods . . . . .	37
1. NO oxidized and Ozone Formed, [d(O <sub>3</sub> -NO)] . . . . .	37
2. Integrated OH Radicals (IntOH) . . . . .	41
3. Base Case d(O <sub>3</sub> -NO) and IntOH . . . . .	42
4. Amounts of Test VOC Added and Reacted . . . . .	42
5. Dilution . . . . .	43
6. Total or d(O <sub>3</sub> -NO) incremental reactivities . . . . .	44
7. IntOH Incremental Reactivities . . . . .	44
8. Direct and Indirect Incremental Reactivities . . . . .	45
9. Mechanistic Reactivities . . . . .	46
B. Ethene Surrogate Reactivity Results . . . . .	47
1. Base Case results . . . . .	47
2. Reactivity Results . . . . .	49
C. Lumped Surrogate Reactivity Results . . . . .	66
1. Base Case results . . . . .	66
2. High NO <sub>x</sub> Reactivity Results . . . . .	72
3. Low NO <sub>x</sub> Reactivity Results . . . . .	80

<u>Section</u>	<u>Page</u>
V. MODEL SIMULATIONS . . . . .	105
A. Chemical Mechanism . . . . .	105
B. Chamber Modeling Procedures . . . . .	107
1. Photolysis Rates . . . . .	107
2. Run Conditions . . . . .	108
3. Chamber Effects Parameters . . . . .	109
4. Modeling Experimental Incremental Reactivities . . . . .	110
C. Model Simulation Results . . . . .	111
1. Base Case Experiments . . . . .	111
2. Ethene Surrogate Reactivity Experiments . . . . .	115
3. High NO <sub>x</sub> Lumped Surrogate Reactivity Experiments . . . . .	115
4. Low NO <sub>x</sub> Lumped Surrogate Reactivity Experiments . . . . .	116
VI. DISCUSSION . . . . .	119
A. Effect of ROG Surrogate on Reactivity . . . . .	119
B. Effect of NO <sub>x</sub> on Reactivity . . . . .	124
C. Mechanism Evaluation Results . . . . .	125
D. Correlations Between Experimental and Atmospheric Reactivities . . . . .	127
VII. CONCLUSIONS . . . . .	131
VIII. REFERENCES . . . . .	135

## LIST OF TABLES

<u>Number</u>		<u>page</u>
1.	Detailed composition of the ambient air ROG mixture. . . . .	5
2.	EPA All City Average hydrocarbon data used to derive ambient ROG Mixture, and assignments to SAPRC Model Species. . . . .	6
3.	Comparison of Lumped Model Species for various ambient air hydrocarbon mixtures or hydrocarbon surrogates. . . . .	9
4.	Composition of the "Lumped Molecule" ROG Surrogate . . . . .	12
5.	Listing of all environmental chamber experiments relevant to this report. . . . .	38
6.	Summary of reactivity experiments carried out for this program. . .	40
7.	Summary of conditions and selected results of the ETC ethene surrogate reactivity experiments. . . . .	48
8.	Derivation of hourly d(O <sub>3</sub> -NO) reactivities from the results of the ethene surrogate experiments. . . . .	51
9.	Derivation of hourly IntOH reactivities from the results of the ethene surrogate experiments. . . . .	53
10.	Derivation of the hourly direct reactivities from the results of the ethene surrogate reactivity experiments. . . . .	55
12.	Derivation of hourly d(O <sub>3</sub> -NO) reactivities from the results of the lumped molecule surrogate experiments. . . . .	74
13.	Derivation of hourly IntOH reactivities from the results of the lumped molecule surrogate experiments. . . . .	77
14.	Derivation of the hourly direct reactivities from the results of the lumped molecule surrogate reactivity experiments. . . . .	81
15.	Summary of selected results for reactivity experiments using different ROG surrogates and NO <sub>x</sub> levels. . . . .	120

## LIST OF FIGURES

<u>Number</u>	<u>page</u>
1.	Plots of Calculated Mechanistic Reactivities of Representative Species in Chamber Experiments Using the Lumped ROG Surrogate Against those for Experiments using the Ambient ROG Mixture. . . . . 17
2.	Plots of calculated mechanistic reactivities of selected species in maximum reactivity chamber experiments using various ROG surrogates, against those for similar experiments using the ambient ROG Mixture. . . . . 18
3.	Plots of calculated mechanistic reactivities of selected species in maximum ozone chamber experiments using various ROG surrogates, against those for similar experiments using the ambient ROG mixture. . . . . 18
4.	Plots of calculated mechanistic reactivities of selected species in NO <sub>x</sub> -limited chamber experiments using various ROG surrogates, against those for similar experiments using the ambient ROG mixture. . . . . 19
5.	Plots of calculated mechanistic reactivities of selected species in maximum reactivity chamber experiments using the 3-component mini-surrogate, against those for similar experiments using the ambient ROG mixture. . . . . 19
6.	Plots of calculated mechanistic reactivities of selected species in maximum ozone chamber experiments using the 3-component mini-surrogate, against those for similar experiments using the ambient ROG mixture. . . . . 20
7.	Plots of calculated mechanistic reactivities of representative species in NO <sub>x</sub> -limited chamber experiments using the 3-component mini-surrogate, against calculated mechanistic reactivities for similar experiments using the ambient ROG mixture. . . . . 20
8.	Plots of maximum ozone in base case experiments and of mechanistic reactivities for selected VOCs as a function of initial NO <sub>x</sub> from model simulations of reactivity experiments employing the ambient ROG mixture and selected ROG surrogates. . . . . 23
9.	Plots of calculated mechanistic reactivities of selected species in chamber experiments using the ethene as the ROG surrogate against those for experiments using the mini-surrogate ROG mixture. . . . . 24
10.	Plots of calculated mechanistic reactivities for chamber conditions, using either the airshed ROG or the 3-component mini-surrogate, against those calculated for airshed conditions. . . . . 25
11.	Diagram of SCAQMD-Funded SAPRC indoor and outdoor chamber laboratory for VOC reactivity studies. . . . . 30
12.	Diagram of SAPRC Dividable Teflon Chamber (DTC). . . . . 32
13.	Concentration time plots of selected species in a representative "base case" ethene surrogate run. Results of model simulations are also shown. . . . . 49

<u>Number</u>		<u>page</u>
14.	Plots of observed vs regression predicted 6-hour $d(O_3-NO)$ , IntOH and $d(O_3-NO)/IntOH$ ratios for the base case ethene surrogate experiments. . . . .	50
15.	Plots of selected results of ethene surrogate reactivity experiments for <b>carbon monoxide</b> . . . . .	56
16.	Plots of selected results of ethene surrogate reactivity experiments for <b>Ethane</b> . . . . .	57
17.	Plots of selected results of ethene surrogate reactivity experiments for <b>n-Butane</b> . . . . .	58
18.	Plots of selected results of ethene surrogate reactivity experiments for <b>n-Hexane</b> . . . . .	59
19.	Plots of selected results of ethene surrogate reactivity experiments for <b>n-Octane</b> . . . . .	60
20.	Plots of selected results of ethene surrogate reactivity experiments for <b>Propene</b> . . . . .	61
21.	Plots of selected results of ethene surrogate reactivity experiments for <b>trans-2-Butene</b> . . . . .	62
22.	Plots of selected results of ethene surrogate reactivity experiments for <b>m-Xylene</b> . . . . .	63
23.	Plots of selected results of ethene surrogate reactivity experiments for <b>Formaldehyde</b> . . . . .	64
24.	Concentration - time plots for selected species in the base case high $NO_x$ lumped surrogate run DTC013. This run is a side equivalency test with the same mixture irradiated on both sides. . . . .	68
25.	Concentration - time plots for selected species in the base case low $NO_x$ lumped surrogate run DTC032A. . . . .	69
26.	Base case $d(O_3-NO)$ , IntOH, and $d(O_3-NO)/IntOH$ results for the high $NO_x$ lumped surrogate runs. . . . .	70
27.	Base case $d(O_3-NO)$ , IntOH, and $d(O_3-NO)/IntOH$ results for the low $NO_x$ lumped surrogate runs. . . . .	71
28.	Differences in $d(O_3-NO)$ and IntOH in a DTC side equivalency test experiment. . . . .	73
29.	Plots of selected results of the high $NO_x$ lumped molecule surrogate reactivity experiments for <b>carbon monoxide</b> . . . . .	83
30.	Plots of selected results of the high $NO_x$ lumped molecule surrogate reactivity experiment for <b>n-butane</b> . . . . .	84
31.	Plots of selected results of the high $NO_x$ lumped molecule surrogate reactivity experiments for <b>n-octane</b> . . . . .	85
32.	Plots of selected results of the high $NO_x$ lumped molecule surrogate reactivity experiment for <b>ethene</b> . . . . .	86

<u>Number</u>		<u>page</u>
33.	Plots of selected results of the high NO <sub>x</sub> lumped molecule surrogate reactivity experiment for <b>propene</b> . . . . .	87
34.	Plots of selected results of the high NO <sub>x</sub> lumped molecule surrogate reactivity experiments for <b>trans-2-Butene</b> . . . . .	88
35.	Plots of selected results of the high NO <sub>x</sub> lumped molecule surrogate reactivity experiment for <b>toluene</b> . . . . .	89
36.	Plots of selected results of the high NO <sub>x</sub> lumped molecule surrogate reactivity experiments for <b>m-xylene</b> . . . . .	90
37.	Plots of selected results of the high NO <sub>x</sub> lumped molecule surrogate reactivity experiment for <b>formaldehyde</b> . . . . .	91
38.	Plots of selected results of the high NO <sub>x</sub> lumped molecule surrogate reactivity experiment for <b>acetaldehyde</b> . . . . .	92
39.	Plots of selected results of the low NO <sub>x</sub> lumped molecule surrogate reactivity experiment for <b>carbon monoxide</b> . . . . .	94
40.	Plots of selected results of the low NO <sub>x</sub> lumped molecule surrogate reactivity experiment for <b>n-butane</b> . . . . .	95
41.	Plots of selected results of the low NO <sub>x</sub> lumped molecule surrogate reactivity experiments for <b>n-octane</b> . . . . .	96
42.	Plots of selected results of the low NO <sub>x</sub> lumped molecule surrogate reactivity experiment for <b>ethene</b> . . . . .	97
43.	Plots of selected results of the low NO <sub>x</sub> lumped molecule surrogate reactivity experiment for <b>propene</b> . . . . .	98
44.	Plots of selected results of the low NO <sub>x</sub> lumped molecule surrogate reactivity experiment for <b>trans-2-Butene</b> . . . . .	99
45.	Plots of selected results of the low NO <sub>x</sub> lumped molecule surrogate reactivity experiment for <b>toluene</b> . . . . .	100
46.	Plots of selected results of the low NO <sub>x</sub> lumped molecule surrogate reactivity experiment for <b>benzene</b> . . . . .	101
47.	Plots of selected results of the low NO <sub>x</sub> lumped molecule surrogate reactivity experiments for <b>m-xylene</b> . . . . .	102
48.	Plots of selected results of the low NO <sub>x</sub> lumped molecule surrogate reactivity experiment for <b>formaldehyde</b> . . . . .	103
49.	Plots of selected results of the low NO <sub>x</sub> lumped molecule surrogate reactivity experiment for <b>acetaldehyde</b> . . . . .	104
50.	Experimental and calculated concentration-time profiles for selected species in selected Phase I base-case mini-surrogate experiments, and plots of relative errors in model calculations of the Set 3 runs against average temperature. . . . .	112
51.	Comparisons of experimental and calculated 6-hour d(O <sub>3</sub> -NO) for the base case experiments. . . . .	113

<u>Number</u>		<u>page</u>
52.	Plots of experimental <u>vs</u> calculated 6-hour d(O <sub>3</sub> -NO) mechanistic reactivities for the various types of reactivity runs. . . . .	116
53.	Plots of experimental <u>vs</u> calculated 6-hour IntOH mechanistic reactivities for the various types of reactivity experiments. . .	117
54.	Plots of experimental <u>vs</u> calculated 6-hour direct d(O <sub>3</sub> -NO) mechanistic reactivities for the various types of high NO <sub>x</sub> reactivity experiments. . . . .	118
55.	Comparisons of weighed averages of the direct, indirect, and overall mechanistic reactivities for high NO <sub>x</sub> conditions for the three base ROG surrogates. . . . .	122
56.	Plots of atmospheric incremental reactivities (carbon basis) against incremental reactivities in the environmental chamber experiments using the lumped surrogate. . . . .	128



## I. INTRODUCTION

The formation of ground-level ozone is caused by the gas-phase interactions of emitted volatile organic compounds (VOCs) and oxides of nitrogen ( $\text{NO}_x$ ) in the presence of sunlight. Traditional VOC control strategies to reduce ozone have focused on reducing the total mass of VOC emissions, but not all VOCs are equal in the amount of ozone formation they cause. Control strategies which take into account these differences in "reactivities" of VOCs might provide a means for additional ozone reduction which could supplement mass-based controls. Examples of such control strategies include conversion of motor vehicles to alternative fuels and solvent substitutions. However, before reactivity-based VOC strategies can be implemented, there must be a means to quantify VOC reactivity which is sufficiently reliable that it can be used in regulatory applications.

The most direct quantitative measure of the degree to which a VOC contributes to ozone formation in a photochemical air pollution episode is its "incremental reactivity" (Carter and Atkinson, 1987; 1989; Chang and Rudy, 1990; Russell, 1990; Carter, 1991, 1993, 1994). This is defined as the amount of additional ozone formation resulting from the addition of a small amount of the compound to the emissions in the episode, divided by the amount of compound added. This depends not only on the VOC and its atmospheric reactions, but also on the conditions of the environment in which the VOC is emitted, such as  $\text{NO}_x$  levels and the nature and level of other reactive organic gases (ROGs) which are present. Incremental reactivities of VOCs in the atmosphere cannot be measured experimentally because it is not feasible to duplicate in the laboratory all the environmental factors which affect reactivity. They can, however, be calculated using computer airshed models, given a model for airshed conditions and a mechanism for the VOCs' atmospheric chemical reactions. For example, a set of models for airshed conditions throughout the U.S. and a detailed chemical mechanism were used to calculate a "Maximum Incremental Reactivity" (MIR) scale (Carter, 1993, 1994). Reactivities in this scale were calculated based on effects of VOCs on ozone formation under relatively high  $\text{NO}_x$  conditions where changes in VOC emissions have the greatest effect on ozone formation (Carter, 1991, 1994). This scale has been adopted by the California Air Resources Board (ARB) for the derivation of reactivity adjustment factors for use in vehicle emissions standards (CARB 1991).

However, such calculations can be no more reliable than the chemical mechanisms upon which they are based. To be minimally suitable for this purpose, such mechanisms need to be evaluated under controlled conditions by comparing their predictions against results of environmental chamber experiments in which the VOCs react in the presence of  $\text{NO}_x$  to form ozone. Although the MIR scale gives reactivity factors for over 100 compounds (Carter, 1993, 1994), at the time the chemical mechanism used to calculate it was developed, less than a dozen compounds had been tested against results of environmental chamber experiments.

Furthermore, only a few of those experiments provided direct tests of the mechanisms' ability to predict incremental reactivities.

The Statewide Air Pollution Research Center (SAPRC), in conjunction with the College of Engineering, Center for Environmental Research and Technology (CE-CERT), has been conducting a multi-year environmental chamber program to address these data needs. In the first phase of this program, we measured the incremental reactivities of 36 representative VOCs under maximum incremental reactivity conditions using a simplified "surrogate" mixture to represent ROGs in the atmosphere and a blacklight light source. The results have been described previously (Carter et al., 1993a). As expected, it was found that incremental reactivities of VOCs varied widely, even after differences in their atmospheric reaction rates were taken into account. A large part of these differences could be attributed to differences among VOCs in their effects on radical levels, and in addition VOCs were found to differ in the amounts of O<sub>3</sub> formation and NO oxidation estimated to be caused by their direct reactions. The current chemical mechanism was found to be able to simulate the experimental reactivity data to within the experimental uncertainty for approximately half the VOCs studied, and qualitatively predicted the observed reactivity trends. However, the results indicated that refinements are needed to the mechanisms for a number of compounds, including branched alkanes, alkenes, aromatics, acetone, and possibly even formaldehyde. The possibility that some of the discrepancies were due to uncertainties in the model for the base case experiment could not be ruled out, and the data for some of the compounds provided an imprecise test of the mechanism because of run-to-run variability of conditions.

These Phase I data were important in providing experimental reactivity data for a large variety of VOCs under conditions where O<sub>3</sub> formation is most sensitive to VOC emissions. However, they provided no information concerning the effect on VOC reactivity on variations of environmental conditions, such as relative NO<sub>x</sub> levels or the nature of the other ROGs which are present. All the Phase I experiments employed "maximum reactivity" conditions where NO<sub>x</sub> was in excess, an 3-component ROG surrogate mixture which oversimplifies the complex mixture of ROGs in actual atmospheres, and employed a blacklight light source which does not give a good representation of sunlight in some wavelength regions. In addition, there appeared to be an inconsistency between the results of this study and past environmental chamber data concerning the mechanism for m-xylene which provided the best fits to the results of the base case experiments.

Phase II of this project had two major components. The first consisted of measuring incremental reactivities of representative VOCs using different ROG surrogate mixtures and under lower NO<sub>x</sub> conditions. The second consisted of obtaining experimental data to assess the consistency and utility of the entire environmental chamber data base used to evaluate the chemical mechanisms. The major effort in this regard was to determine the effect of varying the light source on the ability of models to simulate the results of environmental chamber

experiments. The work on the second component is discussed in the document entitled "Environmental Chamber Studies of Atmospheric Reactivities of Volatile Organic Compounds. Effects of Varying Chamber and Light Source" (Carter et al., 1995a). In this document, we describe the work on the effects of varying ROG surrogate and  $\text{NO}_x$  conditions on experimentally measured incremental reactivities.

As indicated above, the ROG surrogate used in the Phase I study is a highly simplified approximation of the ROGs actually emitted into the atmosphere. Although the main purpose of the Phase I study was not to simulate atmospheric conditions exactly, but instead to provide data for mechanism evaluation, if the chemical conditions of the experiments are too unrealistic, the data may not provide an appropriate test to the parts of the mechanism which are important in affecting predictions of atmospheric reactivity. On the other hand, it can be argued that use of even simpler ROG surrogates may be preferable for mechanism evaluation, since if mechanisms for important components of the base ROG are uncertain, one is unsure if poor fits of calculated to experimental reactivities may be due in errors of the base ROGs' mechanisms rather than that of the test VOC, or (worse) whether good fits may be due to compensating errors. The best way to evaluate this would be to measure incremental reactivities using differing ROG surrogates, both to determine the effect of changing the ROG surrogate on incremental reactivity, and how use of different types of ROG surrogates affect the model's ability to predict reactivity.

To determine the most appropriate surrogates to use for such a study, we first conducted a modeling study of the effects of varying ROG surrogates on experimental measurements of incremental reactivity, and how experimental incremental reactivities correlate with those in the atmosphere. The results of the initial modeling study, the subsequent experimental measurements, and the evaluation of the current detailed mechanism using the experiments, are discussed in this report.

Another limitation of the Phase I study was that it measured incremental reactivities only under relatively high  $\text{NO}_x$ , "maximum reactivity" conditions. Previous modeling work (e.g., Carter and Atkinson, 1989; Carter, 1991, 1994) indicate that VOC reactivities can be quite different under lower  $\text{NO}_x$  conditions, because they are affected by different aspects of a VOC's reaction mechanism. In particular, reactivities under low  $\text{NO}_x$  conditions are highly sensitive to  $\text{NO}_x$  sinks in the VOCs' oxidation mechanisms, but this aspect of the mechanism has no effect on high  $\text{NO}_x$  or maximum reactivities. Therefore, as part of this phase of the program, we measured incremental reactivities of representative VOCs under low  $\text{NO}_x$  conditions, using the most realistic of the ROG surrogates employed. The results of these experiments, and the performance of the current mechanisms, are also presented in this report.

## II. MODELING ANALYSIS OF ROG SURROGATES

Incremental reactivity determinations involve measuring (or calculating) the effect of adding a particular VOC to a mixture containing  $\text{NO}_x$  and other reactive organic gases. Previous modeling analyses have shown that the other reactive organic species which are present might affect the incremental reactivity of the added VOC (e.g., Carter, 1991). Because of this, when using environmental chamber experiments to measure incremental reactivity, it is important that the ROG mixture employed in the experiment to represent VOCs in the atmosphere (the "ROG surrogate") be good representation of atmospheric VOCs in terms of their effect on reactivity results. It is also important that the effect that differences between the experimental ROG surrogate and atmospheric mixtures be understood. One approach in conducting such experiments is to use a highly complex mixture designed simulate closely as possible those measured in the atmosphere. However, this has experimental difficulties, and the complexity of the system reduces the utility of the data for detailed mechanism evaluation. Another approach is to use highly simplified mixtures which is experimentally more tractable and provides a better test for mechanism evaluation, and allow the mechanism to take into account the effects of the different VOCs present in the atmosphere. This is essentially the approach employed in our Phase I study (Carter et al., 1993a). However, to have confidence in this approach, reactivity data using different ROG surrogates must be obtained so the ability of the mechanism to account for these effects to be evaluated. This necessarily includes experiments with more realistic ROG surrogates, for comparison with results with simpler mixture.

Before conducting experiments with varying ROG surrogates, a modeling analyses was carried out to evaluate alternative ROG surrogates for use in environmental chamber experiments to measure incremental reactivities of VOCs. One objective was to find a ROG surrogate mixture which is as simple as possible, yet would yield results which are equivalent to use of realistic ambient ROG mixtures. A second objective was to evaluate how closely reactivities measured using the 3-component mini-surrogate employed in the previous studies would correspond to reactivities measured using more realistic surrogates. A third objective was to evaluate the use of an even simpler surrogates than this mini-surrogate, which might reduce some of the uncertainties and potential for compensating errors when using reactivity data for evaluating mechanisms. This study and its findings are described in this section.

### A. Derivation of Ambient ROG Mixture

The composition of the ambient ROG mixture used as the basis for deriving the ROG surrogate for chamber experiments is given on Table 1. The derivation of this mixture is summarized below.

Table 1. Detailed composition of the ambient air ROG mixture.

SAPRC Species	Description	ppb/ppmC	Carbon %	SAPRC Species	Description	ppb/ppmC	Carbon %
ETHANE	Ethane	19.1	3.83	C7-OLE2	C7 Internal Alkenes	0.4	0.27
PROPANE	Propane	15.6	4.69	C8-OLE2	C8 Internal Alkenes	0.2	0.17
N-C4	n-Butane	19.5	7.80	C9-OLE2	C9 Internal Alkenes	0.2	0.20
N-C5	n-Pentane	6.0	3.01	C10-OLE2	C10 Internal Alkenes	0.1	0.11
N-C6	n-Hexane	2.1	1.28	C11-OLE2	C11 Internal Alkenes	0.1	0.11
N-C7	n-Heptane	1.0	0.71				
N-C8	n-Octane	0.7	0.54		Total Alkenes	33.5	13.29
N-C9	n-Nonane	0.8	0.73				
N-C10	n-Decane	2.2	2.25	BENZENE	Benzene	3.3	1.98
N-C11	n-Undecane	0.4	0.39	TOLUENE	Toluene	9.0	6.27
2-ME-C3	Isobutane	8.1	3.26	C2-BENZ	Ethyl Benzene	1.2	0.98
2-ME-C4	Iso-Pentane	15.4	7.68	N-C3-BEN	n-Propyl Benzene	0.4	0.33
22-DM-C4	2,2-Dimethyl Butane	0.4	0.25	I-C3-BEN	Isopropyl Benzene	0.3	0.24
23-DM-C4	2,3-Dimethyl Butane	1.0	0.58	C9-BEN1	C9 Monosub. Benzenes	0.2	0.19
24-DM-C5	2,4-Dimethyl Pentane	0.6	0.41	S-C4-BEN	s-Butyl Benzene	0.3	0.30
23-DM-C5	2,3-Dimethyl Pentane	1.1	0.76	C10-BEN1	C10 Monosub. Benzenes	0.2	0.19
CYCC5	Cyclopentane	0.8	0.39	C11-BEN1	C11 Monosub. Benzenes	0.6	0.63
ME-CYCC5	Methylcyclopentane	1.6	0.98	C12-BEN1	C12 Monosub. Benzenes	0.0	0.06
CYCC6	Cyclohexane	0.8	0.46	O-XYLENE	o-Xylene	1.8	1.45
ME-CYCC6	Methylcyclohexane	0.7	0.52	M-XYLENE	m-Xylene	4.2	3.37
ET-CYCC6	Ethylcyclohexane	0.2	0.14	C9-BEN2	C9 Disub. Benzenes	2.6	2.37
BR-C6	Branched C6 Alkanes	6.2	3.72	C10-BEN2	C10 Disub. Benzenes	2.0	2.03
BR-C7	Branched C7 Alkanes	3.6	2.49	C11-BEN2	C11 Disub. Benzenes	0.1	0.10
BR-C8	Branched C8 Alkanes	4.3	3.47	C12-BEN2	C12 Disub. Benzenes	0.0	0.04
BR-C9	Branched C9 Alkanes	1.8	1.65	135-TMB	1,3,5-Trimethyl Benzene	0.7	0.67
BR-C10	Branched C10 Alkanes	2.1	2.08	123-TMB	1,2,3-Trimethyl Benzene	0.6	0.55
BR-C12	Branched C12 Alkanes	0.2	0.24	124-TMB	1,2,4-Trimethyl Benzene	2.5	2.28
BR-C13	Branched C13 Alkanes	0.1	0.08	C9-BEN3	C9 Trisub. Benzenes	0.1	0.06
CYC-C7	C7 Cycloalkanes	0.1	0.09	C10-BEN3	C10 Trisub. Benzenes	1.0	0.98
	Total Alkanes	173.1	54.48	C11-BEN3	C11 Trisub. Benzenes	0.1	0.10
				C12-BEN3	C12 Trisub. Benzenes	0.0	0.04
ETHENE	Ethene	13.4	2.68	C10-BEN4	C10 Tetrasub. Benzenes	0.4	0.40
PROPENE	Propene	3.0	0.90	C9-STYR	C9 Styrenes	0.3	0.31
1-BUTENE	1-Butene	2.5	0.98	C10-STYR	C10 Styrenes	0.3	0.30
3M-1-BUT	3-Methyl-1-Butene	0.3	0.14		Total Aromatic HC's	32.3	26.19
1-PENTEN	1-Pentene	0.8	0.39				
1-HEXENE	1-Hexene	0.6	0.34	FORMALD	Formaldehyde	7.9	0.79
2M-1-BUT	2-Methyl-1-Butene	0.8	0.41	ACETALD	Acetaldehyde	4.8	0.95
T-2-BUTE	trans-2-Butene	1.0	0.41	PROPLD	C3 Aldehydes	0.7	0.21
C-2-BUTE	cis-2-Butene	0.8	0.34	C4-RCHO	C4 Aldehydes	0.3	0.12
13-BUTDE	1,3-Butadiene	0.5	0.21	C5-RCHO	C5 Aldehydes	1.1	0.53
ISOPRENE	Isoprene	0.5	0.24	C6-RCHO	C6 Aldehydes	0.7	0.44
CYC-HEXE	Cyclohexene	0.2	0.12		Total Aldehydes	15.5	3.05
A-PINENE	a-Pinene	0.5	0.54	ACETONE	Acetone	3.1	0.93
3-CARENE	3-Carene	0.2	0.16	MEK	C4 Ketones	1.1	0.44
C5-OLE1	C5 Terminal Alkanes	0.3	0.17		Total Ketones	4.2	1.37
C6-OLE1	C6 Terminal Alkanes	0.4	0.26	BENZALD	Benzaldehyde	0.2	0.11
C7-OLE1	C7 Terminal Alkanes	1.5	1.06	ACETYLEN	Acetylene	7.5	1.50
C8-OLE1	C8 Terminal Alkanes	0.3	0.21				
C9-OLE1	C9 Terminal Alkanes	0.6	0.50				
C11-OLE1	C11 Terminal Alkanes	0.1	0.11				
C5-OLE2	C5 Internal Alkenes	2.9	1.43				
C6-OLE2	C6 Internal Alkenes	1.2	0.72				

### 1. Hydrocarbon Portion

After discussions with Bart Croes of the CARB, Jeffries of the University of Carolina (UNC) and others, we concluded that for the hydrocarbon portion of the ROG mixture it is appropriate to use the same data as used by Jeffries and co-workers to derive the "SynUrban" mixture for the current UNC/CRC project (Jeffries et al., 1992). This is based on EPA canister data collected in 66 US cities from 1985-1988. The averaged detailed composition data was provided by Dr. Jeffries and were assigned SAPRC detailed model species with the assistance of Bart Croes. Table 2 presents the averaged hydrocarbon data we received and our model species assignments. There are a number of ambiguities

Table 2. EPA All City Average hydrocarbon data used to derive ambient ROG Mixture, and assignments to SAPRC Model Species. Data from Jeffries et al. (1992).

ID#	ppbC/ ppmC	Description on Spreadsheet	SAPRC Model Species Assignment
Alkanes			
1	73.6	n-butane	N-C4
2	46.3	propane	PROPANE
3	39.7	ethane	ETHANE
4	31.2	n-pentane	N-C5
5	19.0	n-decane	N-C10
6	13.3	n-hexane, 2-ethyl-1-butene	N-C6
7	7.6	n-nonane	N-C9
8	7.4	n-heptane	N-C7
9	7.3	n-butane	N-C4
10	5.6	n-octane	N-C8
11	4.6	unknown	(ignored) [a]
12	4.3	c10	N-C10
13	4.0	c11	N-C11
14	3.4	unknown	(ignored)
15	2.8	c7	BR-C7
16	2.5	c12	BR-C12
17	2.3	c3	PROPANE
18	2.2	c6	BR-C6
19	1.7	c9	BR-C9
20	1.5	c8	BR-C8
21	0.8	paraffin	(ignored)
22	0.8	c4	2-ME-C3
26	79.6	isopentane	2-ME-C4
27	33.0	isobutane	2-ME-C3
28	21.6	4-methylnonane	BR-C10
29	21.1	2-methylpentane	BR-C6
30	15.3	3-methylpentane	BR-C6
31	13.3	2-methylhexane	BR-C7
32	8.3	3-methylhexane	BR-C7
33	5.4	3-methylheptane	BR-C8
34	4.5	2-methylheptane	BR-C8
36	4.0	4-methyloctane	BR-C9
37	3.1	3-methyloctane	BR-C9
38	0.8	c13	BR-C13
39	7.9	2,3-dimethylpentane	23-DM-C5
40	6.0	2,3-dimethylbutane	23-DM-C4
41	4.2	2,4-dimethylpentane	24-DM-C5
42	2.8	2,5-dimethylhexane, 3-mecyclohexen	BR-C8
44	2.8	2,4-dimethylhexane	BR-C8
45	2.6	2,2-dimethylbutane	22-DM-C4
46	2.0	2,4-dimethylheptane	BR-C9
47	1.5	2,5-dimethylhexane	BR-C8
48	1.5	2,3-dimethylheptane	BR-C9
49	1.4	3,3-dimethylpentane	BR-C7
51	0.9	2,5-dimethylheptane	BR-C9
58	12.7	2,2,4-trimethylpentane	BR-C8
59	4.8	2,3,4-trimethylpentane	BR-C8
60	3.9	2,2,5-trimethylhexane	BR-C9
63	10.2	methylcyclopentane	ME-CYCC5
64	5.4	methylcyclohexane	ME-CYCC6
65	4.8	cyclohexane	CYCC6
66	4.0	cyclopentane	CYCC5
67	1.5	ethylcyclohexane	ET-CYCC6
68	0.9	cycloheptane	CYC-C7
Aromatics			
79	20.5	benzene	BENZENE
80	65.0	toluene	TOLUENE

Table 2 (continued)

ID#	ppbC/ ppmC	Description on Spreadsheet	SAPRC Model Species Assignment
81	10.2	ethylbenzene	C2-BENZ
82	4.6	isoamylbenzene	C11-BEN1
83	3.4	n-propylbenzene	N-C3-BEN
84	3.1	sec-butylbenzene	S-C4-BEN
86	2.5	isopropylbenzene	I-C3-BEN
87	1.9	n-amylbenzene	C11-BEN1
88	0.6	n-hexylbenzene	C12-BEN1
89	34.9	m&p-xylene	M-XYLENE
90	15.0	o-xylene	O-XYLENE
91	9.6	m-ethyltoluene	C9-BEN2
92	7.1	1,3-diethylbenzene	C10-BEN2
93	7.1	p-ethyltoluene	C9-BEN2
94	6.5	o-ethyltoluene	C9-BEN2
95	5.6	1-methyl-4-isopropylbenzene	C10-BEN2
97	4.8	1,4-diethylbenzene	C10-BEN2
98	3.2	p,m,o-methylstyrene	C9-STYR
100	2.2	1,2-diethylbenzene	C10-BEN2
101	23.6	1,2,4-trimethylbenzene	124-TMB
102	7.4	1,2-dimethyl-3-ethylbenzene	C10-BEN3
103	6.9	1,3,5-trimethylbenzene	135-TMB
104	5.7	1,2,3-trimethylbenzene	123-TMB
105	4.0	c10	0.5 C10-BEN1 +0.35 C10-BEN2 +0.15 C10-BEN3
106	3.9	c9	0.5 C9-BEN1 +0.35 C9-BEN2 +0.15 C9-BEN3
107	3.1	2,6-dimethylstyrene	C10-STYR
108	2.2	1,2-dimethyl-4-ethylbenzene	C10-BEN3
109	2.0	c11	0.5 C11-BEN2 +0.50 C11-BEN3
110	1.5	1,2,4,5-tetramethylbenzene	C10-BEN4
111	1.4	1,2,3,5-tetramethylbenzene	C10-BEN4
112	1.2	1,2,3,4-tetramethylbenzene	C10-BEN4
113	0.9	c12	0.5 C12-BEN2 +0.50 C12-BEN3
Alkenes			
118	27.8	ethylene	ETHENE
119	9.3	propene	PROPENE
120	8.8	2-methylpropylene, butene-1	1-BUTENE
124	7.7	2,3,3-trimethyl-1-butene	C7-OLE1
126	4.3	2-methyl-1-butene	2M-1-BUT
127	4.2	c9	0.5 C9-OLE1 +0.5 C9-OLE2
128	4.0	1-pentene	1-PENTEN
129	3.5	c5	0.5 C5-OLE1 +0.5 C5-OLE2
130	3.5	2-methyl-1-pentene, 1-hexene	1-HEXENE
132	3.2	c6	0.5 C6-OLE1 +0.5 C6-OLE2
133	3.1	1-nonene	C9-OLE1
135	2.5	c8	0.5 C8-OLE1 +0.5 C8-OLE2
136	2.3	c10	0.5 C10-OLE1 +0.5 C10-OLE2
137	2.3	2,3,3-trimethyl-1-butene	C7-OLE1
138	2.2	c11	0.5 C11-OLE1 +0.5 C11-OLE2
139	1.4	c4	1-BUTENE
140	1.4	3-methyl-1-butene	3M-1-BUT
141	1.1	c7	0.5 C7-OLE1 +0.5 C7-OLE2
142	1.1	4-methyl-1-pentene	C6-OLE1
143	0.9	1-octene	C8-OLE1
144	0.9	olefin	(ignored)
145	0.8	c7	0.5 C7-OLE1 +0.5 C7-OLE2
146	8.5	c-2-pentene	C5-OLE2
147	4.3	t-2-butene	T-2-BUTE
148	4.3	t-2-pentene	C5-OLE2
149	3.5	c-2-butene	C-2-BUTE
150	2.2	2-methyl-2-pentene	C6-OLE2
151	1.9	t-4-methyl-2-pentene	C6-OLE2
152	1.2	c&t-3-methyl-2-pentene	C6-OLE2
154	1.1	t-heptene-2	C7-OLE2

Table 2 (continued)

ID#	ppbC/ ppmC	Description on Spreadsheet	SAPRC Model Species Assignment
155	1.1	c	(ignored)
159	0.8	c-heptene-2	C7-OLE2
163	0.6	c-4-methyl-2-pentene	C6-OLE2
166	0.5	c-2-octene	C8-OLE2
170	0.3	2-methyl-2-butene	C5-OLE2
171	2.5	isoprene	ISOPRENE
172	2.2	1,3-butadiene	13-BUTDE
177	1.2	cyclohexene	CYC-HEXE
179	5.6	a-pinene	A-PINENE
180	1.7	delta-3-carene	3-CARENE
Acetylenes			
182	15.6	acetylene	ACETYLEN

[a] Unknowns constituted 1% of the mixture. No attempt was made to assign them.

in the component descriptions, some involving unspciated aromatics and others unspciated alkenes. The assignments we used for unspciated aromatics were the same as used by Jeffries et al. (1989). However, Jeffries et al. (1989) assumed that all unspciated alkenes were terminal, while Croes (private communication) assumed equal amounts of terminal and internal alkenes for the unspciated alkanes when analyzing the earlier EPA data derive the hydrocarbon composition to use when calculating reactivity scales (Carter, 1993, 1994). The latter assumption was used in these assignments.

Table 3 shows a summary of the classes of species in the hydrocarbon mixture derived using the assignments on Table 2 and compares them with the hydrocarbon composition used in our reactivity modeling studies with the composition the "SynUrban" mixture used by Jeffries et al. (1993). These data are given in terms of moles of lumped molecule condensed model species per mole carbon hydrocarbon, because this is the basis for deriving the ROG surrogate mixture for chamber studies (see below). The percentages next to the composition data give the difference between the mixture derived in this work and the one in the first column. In some cases, the composition was derived assuming the unspciated alkenes are all terminal, as assumed by Jeffries et al. (1989) ("UNC Olefin Ass't") is shown for comparison. The following additional mixtures are shown for comparison:

- "Old EPA Mixture" is the EPA all city average data from Jeffries et al. (1989), which was used in the reactivity calculations of Carter (1991) EPA report. It was derived assuming that all the unspciated alkenes are terminal, so it is also compared with the new composition when derived with this same assumption. The new mixture has significantly less ethene and slightly more alkanes and aromatics than the old mixture. Regardless

Table 3. Comparison of Lumped Model Species for various ambient air hydrocarbon mixtures or hydrocarbon surrogates.

Lumped Model Species	Lumped Model Species / ROG Hydrocarbon (ppb/ppmC, Difference)				
	Old EPA Mixture	New Mixture		New Mixture (UNC Olefin ass't)	
Lumped Alkanes #1	73.7	74.1	1%		
Lumped Alkanes #2	21.6	23.4	8%		
Ethylene	20.3	14.0	-31%		
Terminal Alkenes	15.3	10.8	-29%	12.2	-20%
Internal & Dialkenes	8.2	10.9	32%	9.5	15%
Monoalkyl Benzenes	13.5	13.9	3%		
Higher Aromatics	16.1	17.0	6%		
	<u>ARB Mix #1</u>	<u>New Mixture</u>			
Lumped Alkanes #1	71.4	74.1	4%		
Lumped Alkanes #2	22.2	23.4	5%		
Ethylene	14.1	14.0	0%		
Terminal Alkenes	12.5	10.8	-14%		
Internal & Dialkenes	13.4	10.9	-19%		
Monoalkyl Benzenes	14.1	13.9	-1%		
Higher Aromatics	17.2	17.0	-1%		
	<u>UNC SynUrban</u>	<u>New Mixture</u>		<u>New Mixture (UNC Olefin ass't)</u>	
Lumped Alkane #1	73.7	74.1	1%		
Lumped Alkane #1	70.7	74.1	5%		
Lumped Alkane #2	24.8	23.4	-6%		
Ethylene	13.6	14.0	3%		
Terminal Alkenes	11.2	10.8	-3%	12.2	9%
Internal & Dialkenes	9.4	10.9	16%	9.5	1%
Monoalkyl Benzenes	14.8	13.9	-6%		
Higher Aromatics	18.4	17.0	-8%		

of how the unspciated olefins are assigned, the new mixture has a significantly higher internal to terminal olefin ratio than the older mixture, even if the unspciated olefins are processed in the same way. Note that the assignments for the unspciated olefins has a non-negligible effect on the overall olefin composition.

- "ARB Mix #1" is the hydrocarbon composition that was provided by Croes for calculating the 1991 reactivity scale for the ARB (Carter, 1993, 1994, ARB, 1991). It is based on 1987-1988 EPA air quality data. It is similar to the new mixture, except that it has an ~20% lower alkene/alkane ratio. This presumably represents the variability of the EPA data base, and it is not clear which mixture is more realistic.

- "UNC SynUrban" is the hydrocarbons in the current UNC ROG surrogate mixture, which was derived from the same data as our mixture. The agreement is within  $\pm 9\%$  when the unspciated olefins are assigned assuming they are all terminal. It is not clear why the agreement is not better than this, since the two mixtures are derived based on the same data. However, the main difference between the hydrocarbons in the UNC SynUrban mixture and the mixture we derive is the difference in the internal /terminal alkene ratio caused by different assignments for the unspciated alkenes.

## 2. Oxygenate Portion

The EPA aldehyde data base was used to derive the UNC SynUrban surrogate composition (Jeffries et al. 1989, 1992). However, that data base includes only measurements for formaldehyde and acetaldehyde, while the SCAQS data base also include data for a number of other higher aldehydes and ketones (Croes et al., 1993). The EPA and SCAQS data bases are consistent in indicating that formaldehyde and acetaldehyde each constitute  $\sim 1\%$  of the total ROG carbon, but the SCAQS data indicate that the ketones and higher aldehydes constitute almost 3% of the total ROG. Because it is more complete, we use the SCAQS rather than the EPA data base to derive the oxygenate component of the mixture. The SCAQS aldehyde data we used is the same as that used to derive the ROG mixture for calculating the ARB reactivity scale (ARB, 1991), and was provided by Bart Croes. The total oxygenates constitute 4.75% of the ROG carbon. The constituents are listed in Table 1, and the concentrations of all the hydrocarbons are reduced so the total mixture (hydrocarbon + oxygenates) is normalized to 1 carbon.

## B. Derivation of the Lumped Molecule (Lumped) Surrogate

The mixture in Table 1 was used to derive a simplified ROG surrogate which we designate the "lumped molecule", or (for simplicity) the "lumped" surrogate. Although simplified, it is designed to have the same level of chemical detail as incorporated in the current generation of airshed models. It is based on (1) aggregating the mixture into lumped model species in a condensed (lumped molecule) mechanism used in airshed models, and (2) using a single "real" compound to represent each lumped species. The condensed mechanism and lumping approach is the latest version of the SAPRC condensed mechanism, which was recently implemented in the UAM (Lurmann et al., 1991) and the SARMAP models. Since it is documented by Lurmann et al. (1991), it is not discussed in detail here. For each lumped species which does not represent a specific compound, the representative compound chosen was the one which had the most environmental chamber data available to test its mechanism. The various lumped model species, and the compound representing them, are summarized below.

The Lumped Alkanes #1 (ALK1) group consists of alkanes, alcohols, ethers, and other saturated compounds which react with OH radicals with a 300 K constant of less than  $10^4 \text{ ppm}^{-1} \text{ min}^{-1}$ . This group is derived using "reactivity weighting"

with IntOH = 110 ppt-min. [See Carter and Lurmann, 1990 and Lurmann et al., 1992 for a discussion of reactivity weighting. The IntOH of 110 ppt-min is appropriate for regional model application (Stockwell, private communication, 1989 as cited by Carter and Lurmann, 1990), but the results are not highly sensitive to this.] n-Butane is used to represent this class, since there is by far the most environmental chamber data for this compound.

The Lumped Alkanes #2 (ALK2) group consists of alkanes, alcohols, ethers, and other saturated compounds which react with OH radicals with a 300 K constant of greater than  $10^4 \text{ ppm}^{-1} \text{ min}^{-1}$ . This group represents the individual compounds on mole for mole basis, as is the case for all the other groups except ALK1 and ARO1. It is represented by n-octane, based on availability of chamber data. N-octane-NO<sub>x</sub>-air chamber experiments have been carried out in both the SAPRC and UNC chambers, and its incremental reactivity has been measured in our previous reactivity experiments.

Ethylene (ETHE) is represented explicitly.

The group designated Terminal Alkenes (OLE1) represents all alkenes which react with OH radicals with 300 K rate constants of less than  $7.5 \times 10^4 \text{ ppm}^{-1} \text{ min}^{-1}$ . (This includes isobutene but not 2-methyl-1-butene.) It is represented by propene because (1) there is by far the most chamber data for it; and (2) the mechanisms for the other terminal alkenes are derived mainly from that for propene.

The Internal + Dialkene (OLE2) group represents all alkenes which react with OH radicals with a 300 K rate constant of greater than  $7.5 \times 10^4 \text{ ppm}^{-1} \text{ min}^{-1}$ . This includes most alkenes with more than one substituent around the bond (other than isobutene), and conjugated olefins such as isoprene. It also includes styrenes, since they are lumped as alkenes in the SAPRC mechanism. Although the compound in this group with the most chamber data is probably isoprene, isoprene is usually represented by a separate model species in current models, and it is not a good representative of most of the other alkenes in this group. Trans-2-butene is used to represent this group because a fair amount of chamber data are available for it, including incremental reactivity experiments, and because the general SAPRC internal alkene mechanism is derived based on that estimated for the 2-butenes.

The Monoalkyl Benzene (ARO1) group consists of aromatic hydrocarbons which react with OH radicals with a 300 K rate constant of less than  $2 \times 10^4 \text{ ppm}^{-1} \text{ min}^{-1}$ , which include benzene and the monoalkylbenzenes. These are represented using reactivity weighting (see discussion of ALK1, above), except that the group is assigned the OH rate constant of toluene independently of the mixture being represented. (The reactivity weighting factor affects primarily the representation of benzene.) Toluene is used to represent this group, since it is both the dominant species in it, and the one with the most chamber data.

The Higher Aromatic (ARO2) group consists of aromatic hydrocarbons which react with OH radicals with a 300 K rate constant of greater than  $2 \times 10^4 \text{ ppm}^{-1} \text{ min}^{-1}$ . This includes xylenes, polyalkylbenzenes, and naphthalenes. It is represented by m-xylene, which has the most SAPRC environmental chamber data, whose rate constant is closer to the average for this group than the other xylene isomers.

Formaldehyde (HCHO) is represented explicitly.

Acetaldehyde (CCHO) and higher aldehydes (RCHO) are separate model species in the condensed SAPRC mechanism, though for most other condensed mechanisms they are lumped together. They are also lumped together for the purpose of deriving this surrogate, and are represented by acetaldehyde.

Ketones in the mixture consist of acetone and higher ketones, in amounts of 3 ppb/ppmC and 1 ppb/ppmC, respectively. Because of the relatively low amounts of ketones in this mixture and their low or moderate reactivities, the effect of including them in the surrogate is too small to justify the non-negligible additional experimental effort this would involve. Therefore, the ketones are ignored when developing the ROG surrogate.

The composition of this 9-compound surrogate is summarized on Table 4. The "Inert/Lost Carbon" include the "extra" carbons in the compounds in the ambient mixture which are represented by example compounds with fewer carbons, the fractions of species treated as inert for groups where reactivity weighting was employed, and the ketones. Although this is not strictly speaking a part of the mixture, it must be included as a "virtual reactant" when computing the effective ppmC of the mixture for the purpose of comparing with other mixtures.

It has been argued that the unrepresented "lost carbon" in this mixture may have a non-negligible effect on the system, and they should not be ignored

Table 4. Composition of the "Lumped Molecule" ROG Surrogate

Compound	ppb/ppmC
n-Butane	70.7
n-Octane	22.3
Ethylene	13.4
Propene	10.4
t-2-Butene	10.4
Toluene	13.3
m-Xylene	16.3
Formaldehyde	7.9
Acetaldehyde	7.6
( Inert/Lost Carbon )	193.1 )

(Jeffries, private communication). This is examined in model calculations discussed in the following section, and it is concluded that their effect is unlikely to be significant.

### **C. Calculated Effects of Complexity of ROG Surrogate on Mechanistic Reactivities**

Although the lumped ROG surrogate given in Table 4 has the same degree of chemical detail as the condensed mechanisms used in current urban and regional airshed models, it is still a major simplification of realistic ambient ROG mixtures. Model simulations, using the SAPRC detailed mechanism (Carter, 1990) were conducted to assess whether use of ROG surrogates with this level of detail, or even simpler surrogates such as the "mini-surrogate" used in the Phase I experiments (Carter et al., 1993a) will significantly affect results of reactivity experiments. Three types of experiments were examined:

- Maximum Reactivity experiments were based on the ROG and NO<sub>x</sub> conditions of the Phase I maximum reactivity experiments (Carter et al., 1993a), with the amount of ROG adjusted to yield comparable final ozone levels as the mini-surrogate. The initial ROG (counting "inert/lost" carbon in the surrogate, and the "inert" carbon in the ambient mixture) was 5.5 ppmC, and the initial NO<sub>x</sub> was 0.5 ppm.<sup>1</sup>
- Maximum Ozone experiments were derived by reducing the NO<sub>x</sub> in the maximum reactivity experiments to approximately the level where the highest ozone levels were achieved in the simulations of the base case runs with the ambient mixture. This turned out to be 0.2 ppm initial NO<sub>x</sub>.
- Low NO<sub>x</sub> experiments were derived by arbitrarily reducing the initial NO<sub>x</sub> in the maximum ozone experiments by another factor of 4, i.e., to 0.05 ppm.

For each type of experiment, the differences between using the following mixtures for the base ROG surrogates were examined:

The Ambient Mix was the ambient mixture used to calculate the 1991 reactivity scale for the ARB (Carter, 1993, 1994; ARB, 1991). (These calculations were conducted prior to the derivation of the new ambient mixture discussed above, but the slight differences of the mixtures should not affect the qualitative results.)

The Ambient Mix with No Lost Carbon employed the same mixture as that discussed above, but was represented by a modified version of the SAPRC mechanism

---

<sup>1</sup> Note that ROG/NO<sub>x</sub> of 11 may be maximum ozone or NO<sub>x</sub>-limited ratio in an airshed scenario, but it is maximum a reactivity ratio under the conditions of these 6-hour runs.)

was where the effects of the additional carbons on the lumped model species were not ignored. This is to examine the significance of concerns about the "lost carbon" in the ROG surrogate – the standard SAPRC mechanism does not provide a good test in this regard because it also ignores "lost carbon".

The mechanism was modified by having each "lost" carbon in the standard mechanism appear as 1/4 of an MEK molecule whenever the lumped model species reacts.<sup>2</sup> This is more appropriate than simply adding the additional carbon in some form to the initial mixture, since its effect on the initial reaction rate of the lumped model species is already taken into account.<sup>3</sup> The effect of the additional carbon is only "lost" when the lumped model species reacts, and the products are represented by model species with fewer carbons than the actual products which are formed. Since this additional carbon appears in product species, and since MEK is the generic non-aldehyde model species used for products in the SAPRC mechanism, using MEK is an appropriate way to represent the lost carbon in this mechanism. This approach probably over-estimates the effect of this extra carbon, since it uses smaller molecules to represent larger molecules, and larger molecules tend to have lower reactivity per carbon than smaller molecules of similar type. However, erring on the side of overestimating the effect of the lost carbon is useful for the purpose of this test, since if the effect is calculated to be minor, it is probably safe to conclude that it is indeed minor.

The "Full Surrogate" was derived based on the ambient mixture used to calculate the 1991 reactivity scale, using procedures which are exactly the same as the derivation of the "lumped molecule" surrogate in Table 4 from the ambient mixture in Table 1. The relative differences of the various hydrocarbon components are as indicated on Table 3. Note that for calculations where this surrogate was compared with the "ambient mix with no lost carbon", the modified (lost C = 1/4 MEK) mechanism was used for this surrogate as well. The standard mechanism was used for all other calculations.

The "without acetaldehyde" surrogate consisted of the "full surrogate" except that acetaldehyde was removed and formaldehyde was increased to yield the same total moles of aldehydes. (Removing acetaldehyde from the surrogate would simplify the experiments and remove a potential source of irreproducibility, since special procedures are necessary to prepare this compound for injection.)

---

<sup>2</sup> For example, in the standard SAPRC mechanism, the mechanism for the reaction of OH radicals with 1-pentene is represented as: "OH + 1-PENTENE → RO2-R. + RO2. + HCHO + RCHO + -C", where "-C" is an inert counter species representing lost carbon. In the modified mechanism, this reaction is represented as: OH + 1-PENTENE → RO2-R. + RO2. + HCHO + RCHO + 0.25 MEK.

<sup>3</sup> The SAPRC mechanism uses lumped group rate constants derived to represent the mixture of species being represented.

The "without acetaldehyde and n-butane" surrogate consists of the "without acetaldehyde" surrogate, but with the n-butane and n-octane replaced by an equal molar amount of n-hexane. (Simplifying the alkanes will simplify the GC analyses, and make it easier to measure the reactivities of n-butane and n-octane.)

The "without acetaldehyde and toluene" surrogate consisted of the "without acetaldehyde" surrogate but with the toluene removed and the m-xylene increased to yield an equal number of moles of aromatics. (Simplifying the aromatics would simplify the GC analyses, and remove a potential source of variability.)

The "without acetaldehyde, toluene and n-butane" surrogate consisted as the "without acetaldehyde and n-butane" surrogate but with toluene removed and m-xylene increased as with the other "without toluene" surrogate.

The "Mini-Surrogate" was the same three-component (ethene, n-hexane, and m-xylene) surrogate as used in the Phase I reactivity experiments (Carter et al., 1993a). This surrogate is more reactive than the ambient mixture on a per carbon basis. To make this more comparable to the ambient mixture in overall reactivity, 274 ppb/ppmC of "inert carbon" is added to the mixture. This number was chosen to give this mixture the same incremental reactivity in the ambient mixture as the "base case, least squares error" reactivity scale of Carter (1993, 1994).

The "Ethylene Surrogate" employed ethylene alone to represent the simplest possible surrogate which might provide at least an approximate representation of the chemical environment in which VOCs react. For a single compound to be suitable for a base ROG surrogate, it must at a minimum (1) have a reasonably well understood mechanism; (2) provide sufficient internal radical sources so its NO<sub>x</sub>-air reactions provide a reactive system, but (3) not have such high radical sources that it produces an unnaturally radical rich environment; and (4) be easy to deal with experimentally. Ethylene is the most qualified on all these counts. 456 ppb/ppmC of "inert carbon" is added to this "mixture" to yield a surrogate which gives the maximum ozone at the same nominal ROG/NO<sub>x</sub> ratio as the mini-surrogate. (I.e., 544 ppbC of ethylene is nominally 1 ppmC ROG surrogate.)

Incremental reactivities of representative VOCs were calculated for each type of experiment and ROG surrogate. The calculations consisted of model simulations of the base case experiment, combined with simulations of the experiment with a test VOC added. The results are given in terms of the effects of the VOC on ozone formed + NO oxidized,  $\Delta([O_3]-[NO])$ , and also the effect of the VOC on integrated OH radical levels, or IntOH. The former is more generally useful measure of effects of VOC on the chemical factors affecting O<sub>3</sub> than reactivity with respect to [O<sub>3</sub>] alone, since it provides a meaningful measure even when excess NO suppresses O<sub>3</sub> formation. The latter is a useful measure of

the effect of the VOC on radical levels, which affects O<sub>3</sub> reactivity by affecting how rapidly all other VOCs present react to form ozone.

The results of these calculations are given in terms of mechanistic reactivities because this normalizes out the large effects of differences of VOCs in how rapidly they react, which (in a relative sense at least) are not affected by changes in the base ROG mixture. [Mechanistic reactivities refer to the effect of adding the VOC (on  $\Delta([O_3]-[NO])$  or IntOH) relative by the amount of VOC reacted, while incremental reactivities refer to the effects relative to the amount of VOC added.] For simplicity, these model simulations calculated "true" incremental or mechanistic reactivity, i.e., the effect of adding only small amounts of the VOC to the mixture. Although this is an approximation of what can be experimentally measured, it should be sufficient for determining the magnitude of the effect of changing the ROG surrogate.

Incremental reactivities were calculated for CO, methane, propane, n-butane, n-octane, iso-octane, ethene, propene, trans-2-butene, isobutene, 1-hexene, benzene, toluene, m-xylene 135-trimethylbenzene, formaldehyde, acetaldehyde, acetone, methanol and ethanol. Although this is not a comprehensive list of all compounds of interest, they represent a full variety of types of mechanisms which might respond differently to changes in the ROG surrogate.

The comparisons of the mechanistic reactivities in the simulated experiments using the different ROG surrogate mixtures are shown on Figures 1-7. These give plots of the mechanistic reactivities calculated for runs with the simplified surrogates against those calculated for comparable using the ambient mixture. Each point represents a different VOC; for example, the highest point on the plots for the "maximum reactivity" experiments is formaldehyde, and the lowest point is n-octane. All points lying on the line would mean the mechanistic reactivities are exactly the same in the experiments with the surrogate as in the experiments with the ambient mixture, i.e., that the model predicts that using the surrogate would yield identical measured reactivities as using the ambient mixture.

Figure 1 compares the  $d(O_3-NO)$  and IntOH reactivities calculated for the three types of experiments the 9-component "lumped molecule" ROG surrogate and the ambient mixture. The circles show the reactivities calculated with the standard SAPRC mechanism, and the diamonds show the reactivities calculated with the version of the mechanism which represents lost product carbons as MEK. It can be seen that regardless of which mechanism is used, the experiments with the surrogate are calculated to yield essentially identical reactivities as experiments with the ambient mixture. The small differences that are seen would be impossible to detect experimentally. Note that the SAPRC mechanism represents the chemical detail of the complex mixture to the extent possible given the current knowledge at the time the Carter (1990) mechanism was developed, so this

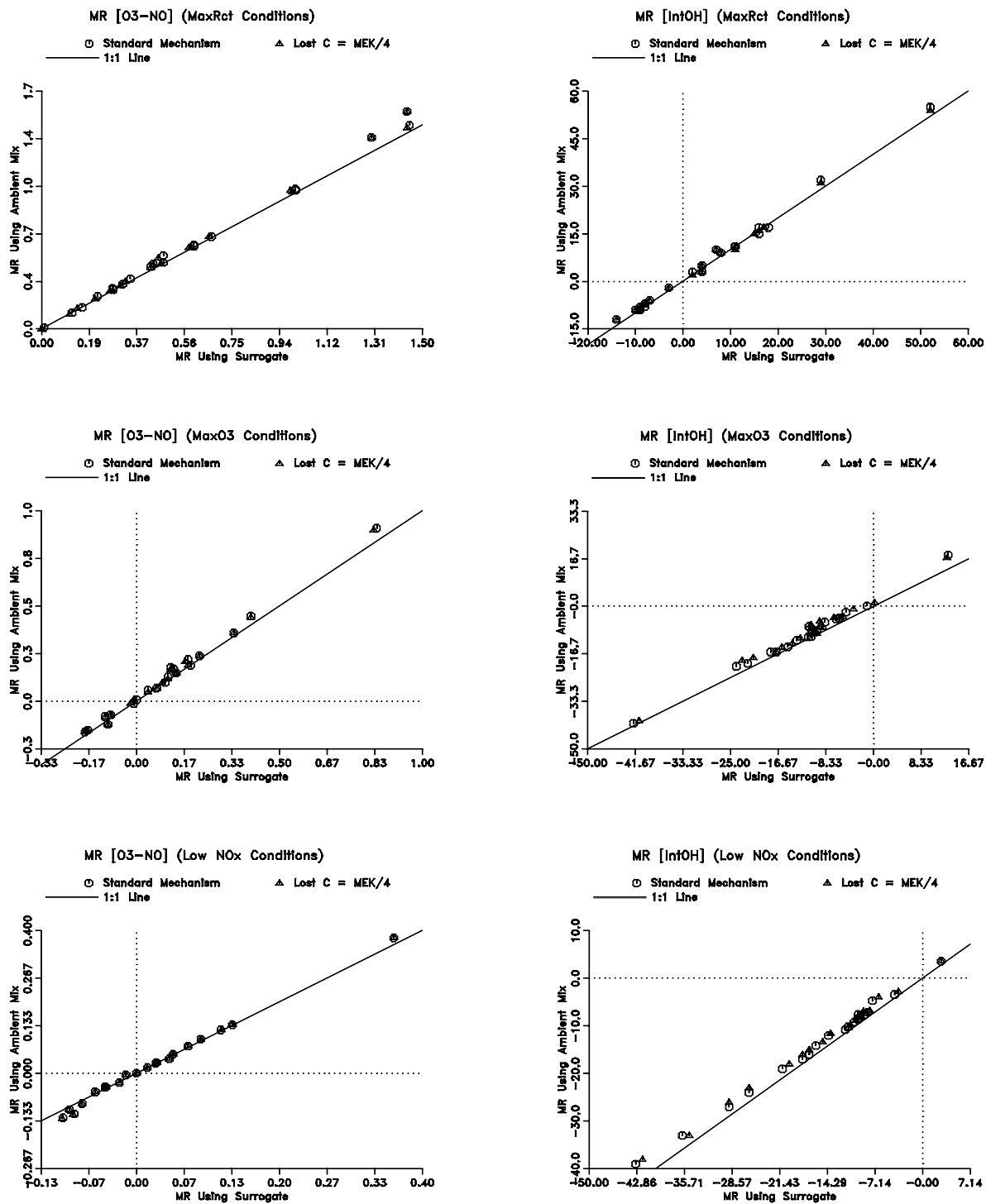


Figure 1. Plots of Calculated Mechanistic Reactivities of Representative Species in Chamber Experiments Using the Lumped ROG Surrogate Against those for Experiments using the Ambient ROG Mixture. The "Lost C = MEK/4" mechanism represents lost carbons by MEK.

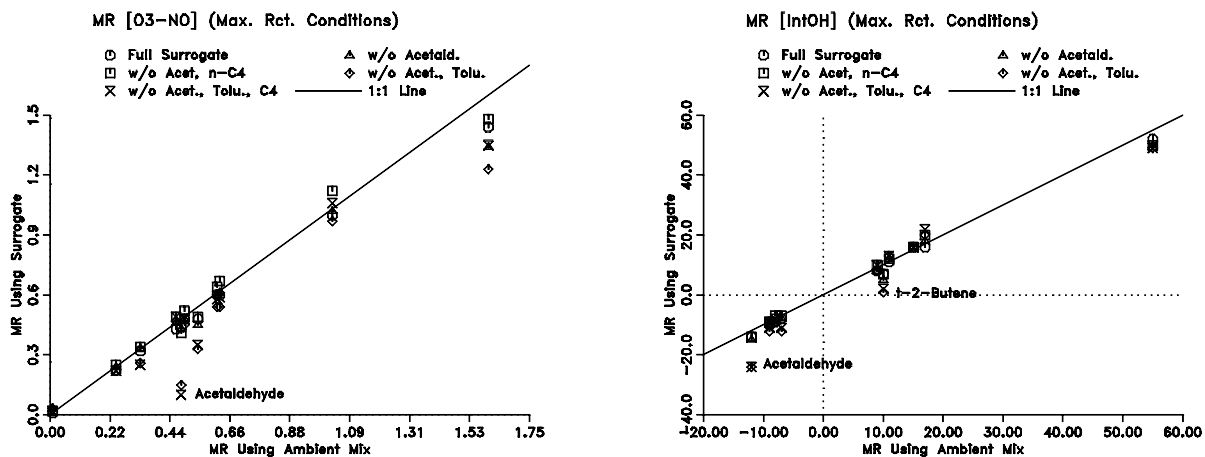


Figure 2. Plots of calculated mechanistic reactivities of selected species in maximum reactivity chamber experiments using various ROG surrogates, against those for similar experiments using the ambient ROG Mixture.

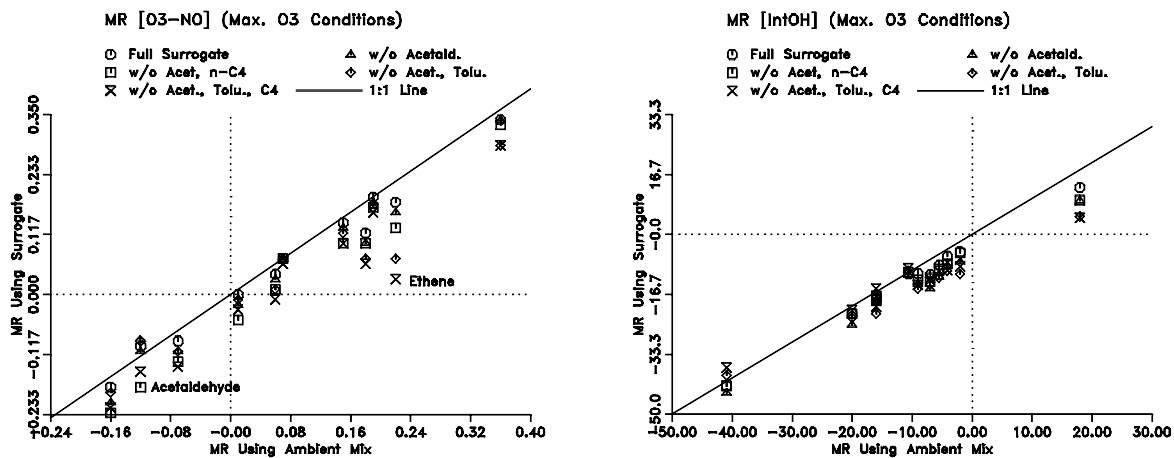


Figure 3. Plots of calculated mechanistic reactivities of selected species in maximum ozone chamber experiments using various ROG surrogates, against those for similar experiments using the ambient ROG mixture.

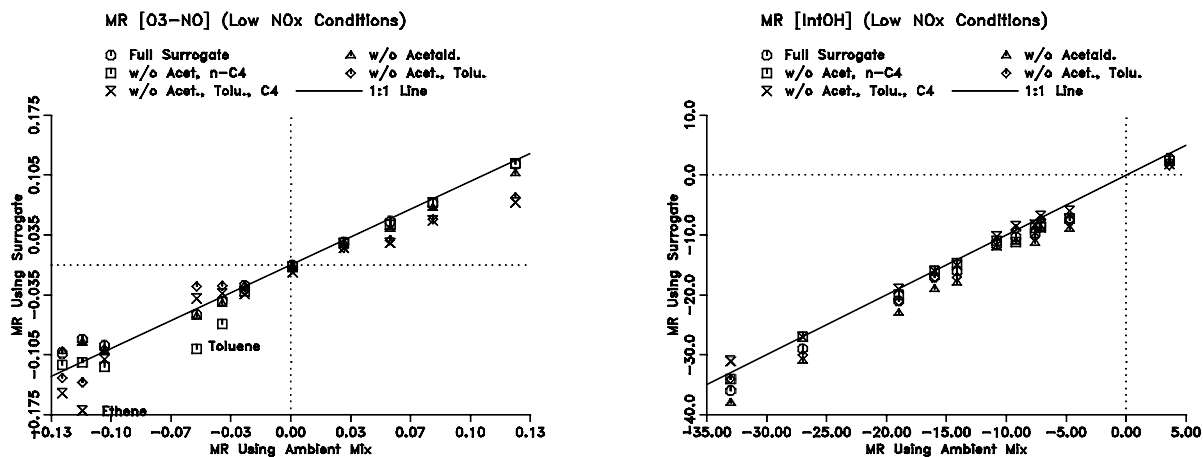


Figure 4. Plots of calculated mechanistic reactivities of selected species in NO<sub>x</sub>-limited chamber experiments using various ROG surrogates, against those for similar experiments using the ambient ROG mixture.

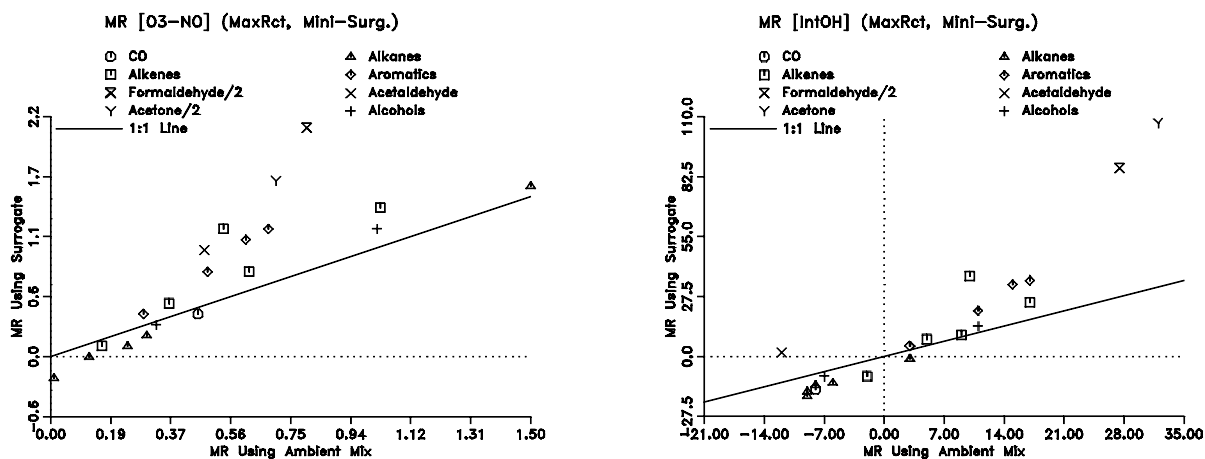


Figure 5. Plots of calculated mechanistic reactivities of selected species in maximum reactivity chamber experiments using the 3-component mini-surrogate, against those for similar experiments using the ambient ROG mixture.

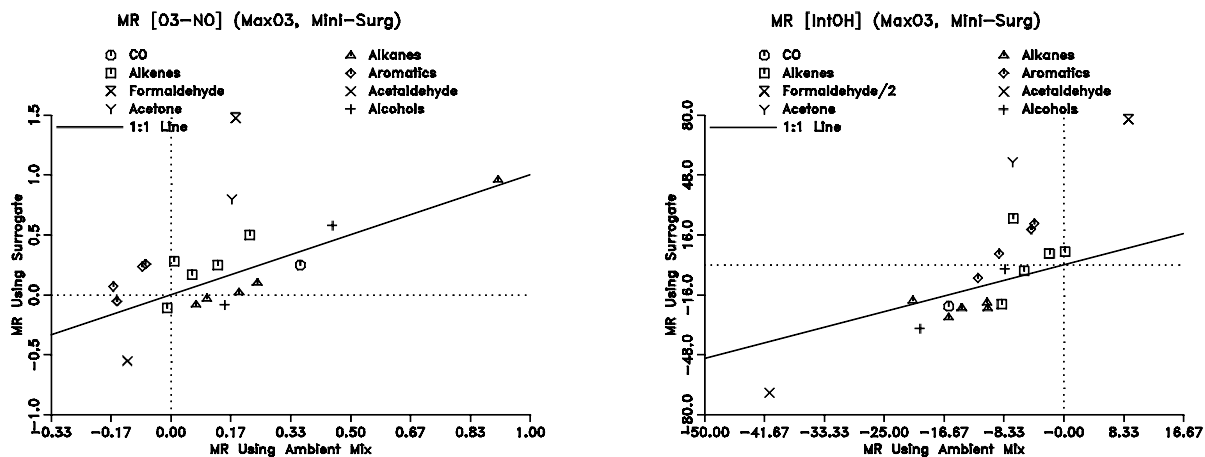


Figure 6. Plots of calculated mechanistic reactivities of selected species in maximum ozone chamber experiments using the 3-component mini-surrogate, against those for similar experiments using the ambient ROG mixture.

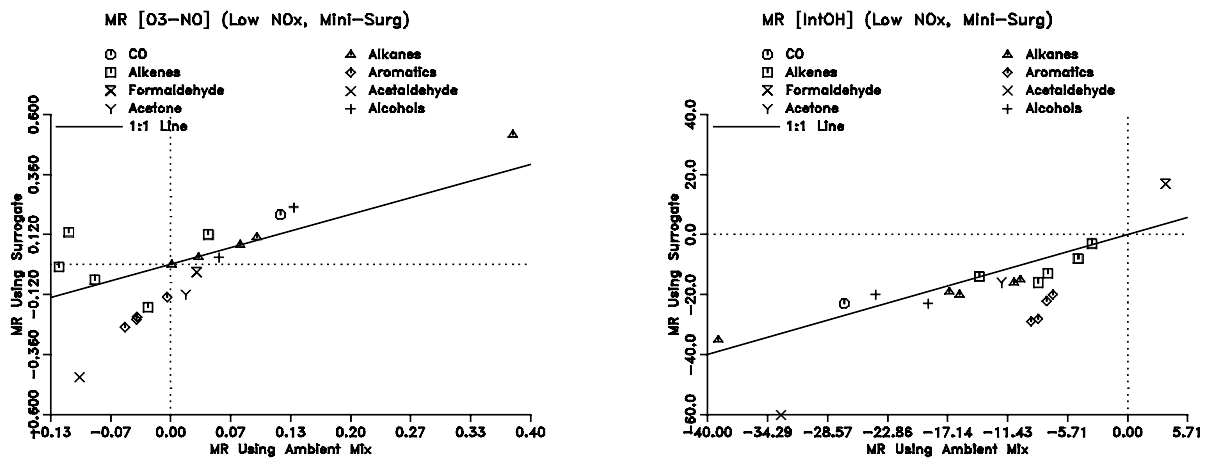


Figure 7. Plots of calculated mechanistic reactivities of representative species in  $\text{NO}_x$ -limited chamber experiments using the 3-component mini-surrogate, against calculated mechanistic reactivities for similar experiments using the ambient ROG mixture.

result is not due to the same condensed mechanism being used to simulate both mixtures.

Figure 1 also shows that the model with MEK representing the lost carbons gives essentially identical results as the standard mechanism. (The models are also almost identical in predictions for the base case experiment, except obviously for MEK.) This should alleviate concerns about the lack of representation of "lost carbon" in the ROG surrogate, at least for one day experiments. As indicated above, it is probable that MEK overstates the effect of lost carbon, so if the reactivities are insensitive to this model for the lost carbons, they should be even less sensitive to a more realistic one.

Figures 2-4 show the comparisons of the  $d(O_3-NO)$  and IntOH mechanistic reactivities for various simplifications of the lumped molecule surrogate. Different symbols are shown for the different ROG surrogates, and individual compounds where the discrepancies are the worst for the simpler surrogates are identified on selected plots. (A slightly smaller number of representative compounds are shown on these plots than on Figure 1 and subsequent figures, for easier readability.) The results show that removing acetaldehyde from the surrogate and replacing it with formaldehyde has a only a small effect compared to experimental uncertainties, suggesting that this simplification, which has significant experimental advantages, may be appropriate. Simplifying the alkanes and/or the aromatics also has only a small effect in most cases, but for some VOCs the effects may be non-negligible. For example, simplifying the alkanes has a non-negligible effect on the predicted  $d(O_3-NO)$  reactivities of toluene under low  $NO_x$  conditions and of acetaldehyde under maximum ozone conditions. Simplifying the aromatics significantly affects the predicted  $d(O_3-NO)$  and IntOH reactivities of acetaldehyde under maximum reactivity conditions, and also affects the  $d(O_3-NO)$  reactivity of ethene under maximum ozone conditions. Since the experimental advantages of simplifying alkanes or aromatics are not as great as that of removing acetaldehyde, these latter two simplifications may not be appropriate.

Figures 5-7 show the comparisons of the  $d(O_3-NO)$  and IntOH mechanistic for the 3-component mini-surrogate we used in our previous reactivity experiments. In this case, different symbols are used for different classes of compounds, and the formaldehyde and acetone reactivities have been divided by 2 on selected plots to make their magnitudes more comparable with those for the other VOCs. These figures show that the mini-surrogate yields greater differences in reactivities compared to using the ambient mixture or the "lumped molecule" surrogates. The largest effect of using the mini-surrogate is on the reactivities of formaldehyde under maximum reactivity or maximum ozone conditions, but the reactivities of the other VOCs are affected to some extent as well. This is probably due to the lack of formaldehyde in this mini-surrogate, causing a greater sensitivity of the mini-surrogate to radical initiation and radical termination effects. This greater sensitivity, however, makes experiments with

this mixture more useful for testing model predictions concerning this aspect of the mechanism.

Figure 8 shows plots of the maximum ozone in the base case experiments and mechanistic reactivities of selected VOCs against initial  $\text{NO}_x$  concentrations at a constant nominal base ROG level of 5.5 ppmC. Note that the 0.5 ppm  $\text{NO}_x$  level is taken as "maximum reactivity" conditions in the previous plots (though slightly lower  $\text{NO}_x$  may be slightly closer to the "true" MIR point for some VOCs), 0.2 ppm  $\text{NO}_x$  is used for "maximum ozone" conditions, and 0.05 ppm is used for "Low  $\text{NO}_x$ " conditions for all the surrogates. The maximum ozone and reactivities calculated for the ethylene surrogate are also shown. It can be seen that the 9-component surrogate tracks the  $\text{NO}_x$ -dependence of the maximum ozone and VOC reactivities of the ambient mixture very closely. The mini-surrogate does not track the ambient mixture as closely, particularly for formaldehyde and n-octane under maximum reactivity conditions. The discrepancies are apparently due to the greater sensitivity of the mini-surrogate experiments to radical initiation/termination effects under maximum reactivity conditions.

Figure 8 also shows that the reactivities using the simple ethylene surrogate track the reactivities using the mini-surrogate remarkably well, particularly under maximum ozone to maximum reactivity conditions. This suggests that use of ethylene as the ROG surrogate may give essentially equivalent results in reactivity experiments to use of the mini-surrogate. (It also suggests that the high  $\text{NO}_x$  reactivities measured in the previous program using the mini-surrogate may not be highly sensitive to the m-xylene mechanism, since almost the same reactivity results are calculated to occur if m-xylene were absent.) The correspondences between these two surrogates is shown for a larger variety of compounds on Figure 9, which gives plots of calculated mechanistic reactivities for experiments using the ethylene surrogate against those using the mini-surrogate for maximum reactivity, maximum ozone, and low  $\text{NO}_x$  conditions. The main difference is that reactivities tend to be lower (or more negative) under low  $\text{NO}_x$  conditions in experiments using the ethene surrogate than in those using the mini-surrogate or the ambient mixture. This is undoubtedly related to the fact that ethene has much weaker  $\text{NO}_x$  sinks in its mechanism than the other components of the mini-surrogate or the more realistic mixtures. Thus adding a compound with  $\text{NO}_x$  sinks to a  $\text{NO}_x$ -limited system with weak  $\text{NO}_x$  sinks has a greater effect than adding it to an otherwise comparable system with stronger  $\text{NO}_x$  sinks. This suggests that use of ethylene as the ROG surrogate in low  $\text{NO}_x$  reactivity experiments may provide a more sensitive test for this aspect of the mechanism than using more realistic surrogates which contain compounds which stronger  $\text{NO}_x$  sinks.

#### **D. Comparison of Predicted Experimental Reactivities with the Maximum Reactivity and Maximum Ozone Reactivity Scales.**

Figure 10 shows comparisons of mechanistic reactivities calculated for chamber conditions with those calculated for similar  $\text{NO}_x$  conditions in the

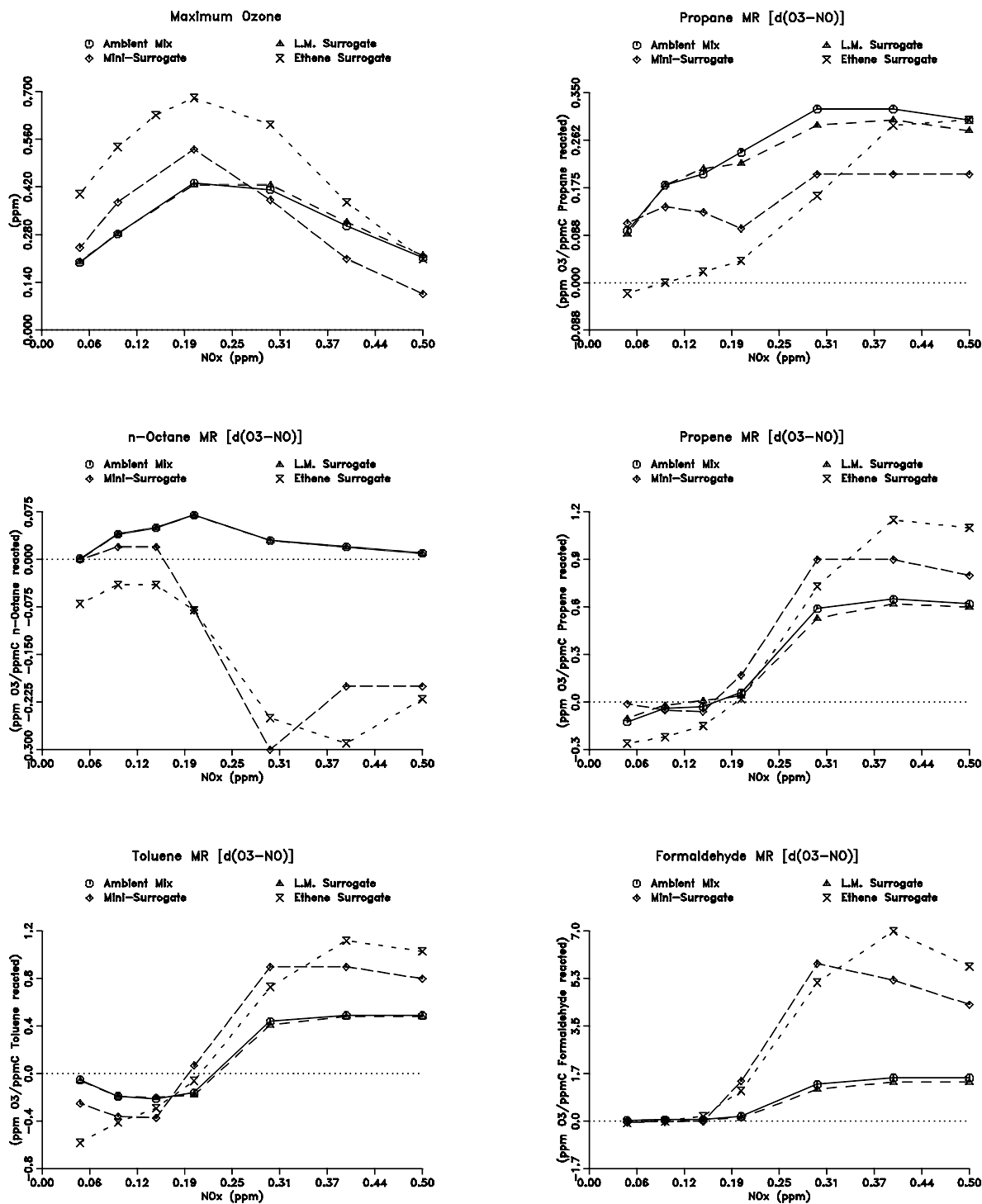


Figure 8. Plots of maximum ozone in base case experiments and of mechanistic reactivities for selected VOCs as a function of initial NO<sub>x</sub> from model simulations of reactivity experiments employing the ambient ROG mixture and selected ROG surrogates.

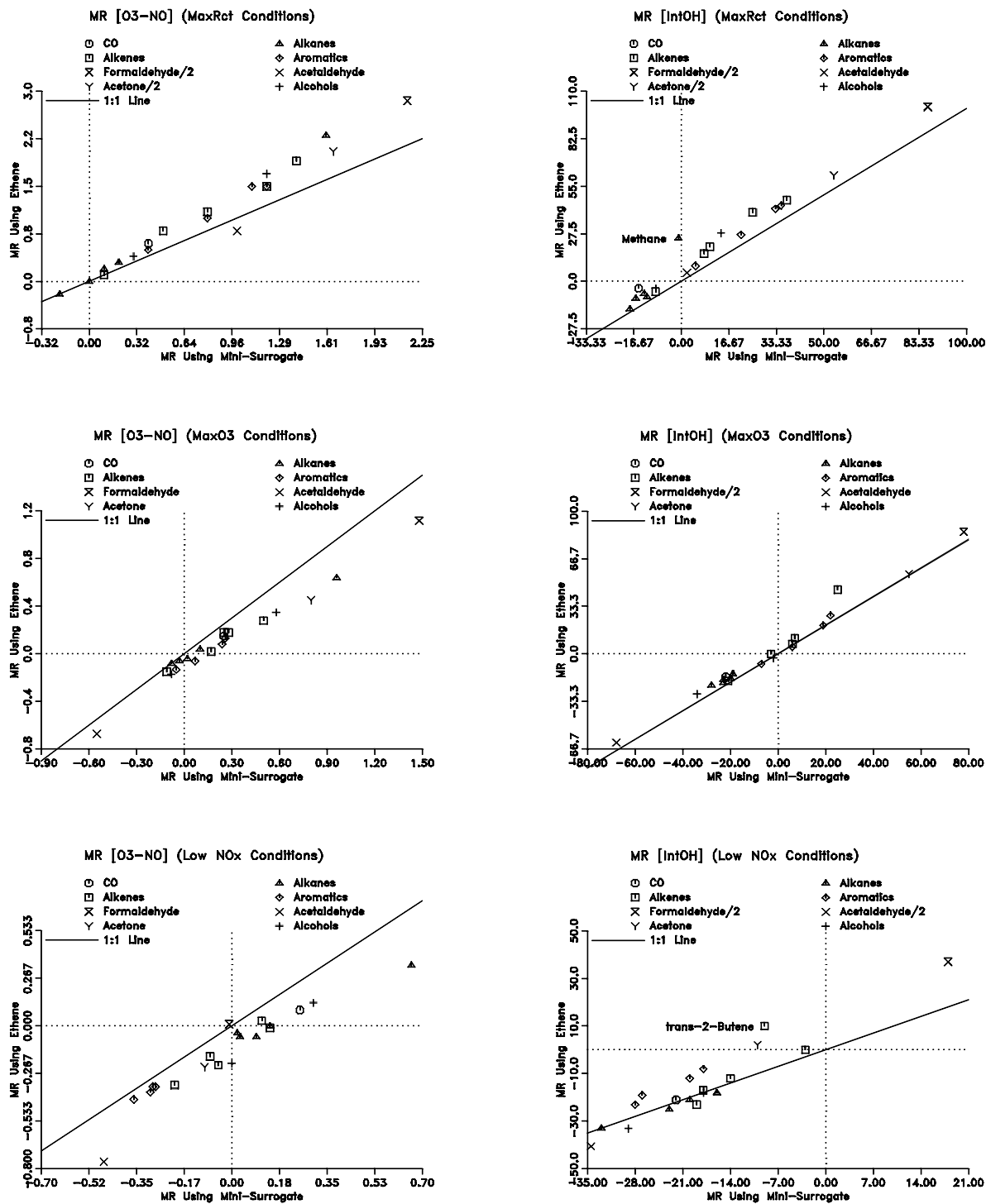


Figure 9. Plots of calculated mechanistic reactivities of selected species in chamber experiments using the ethene as the ROG surrogate against those for experiments using the mini-surrogate ROG mixture.

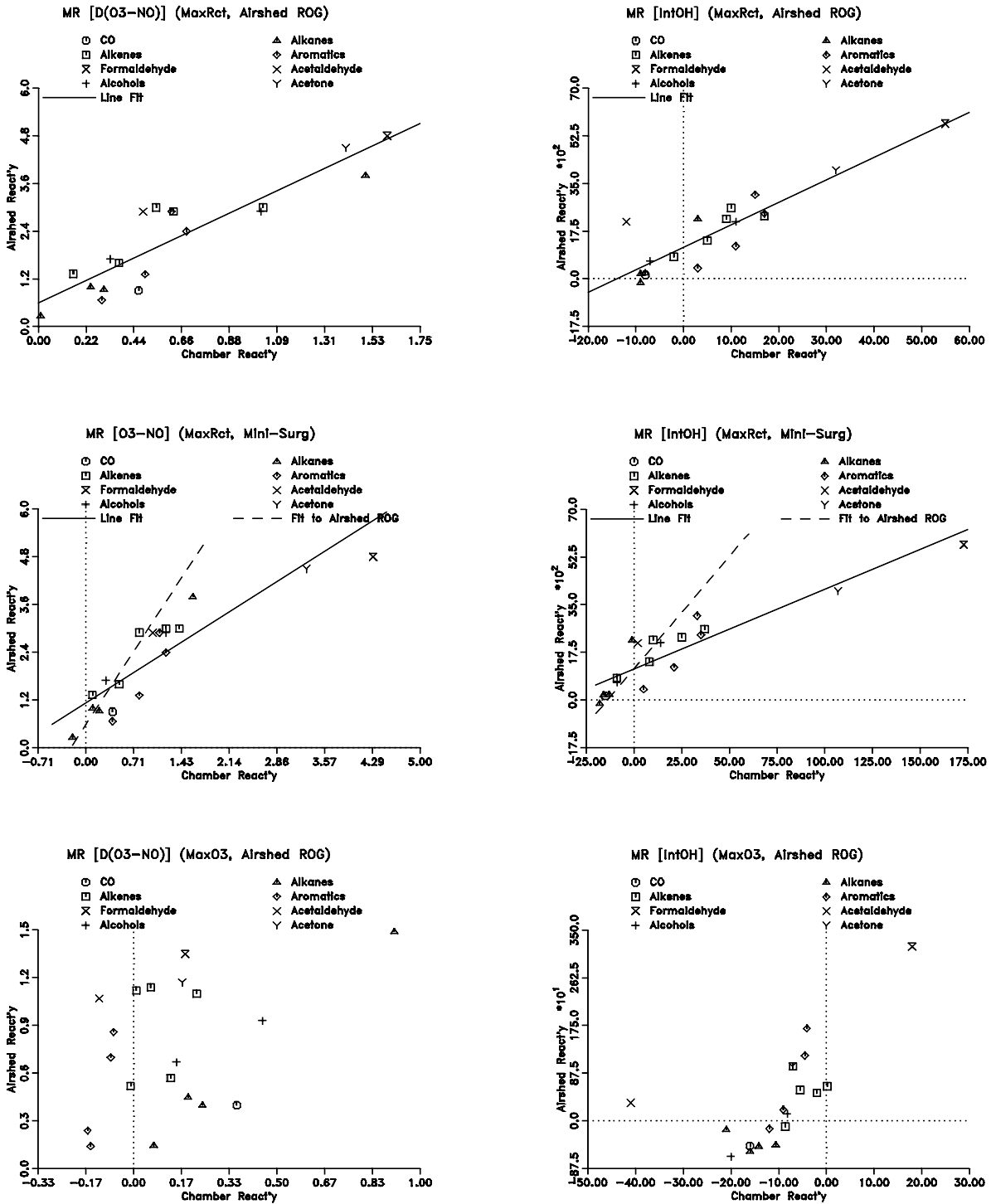


Figure 10. Plots of calculated mechanistic reactivities for chamber conditions, using either the airshed ROG or the 3-component mini-s surrogate, against those calculated for airshed conditions.

atmosphere. The top four plots show mechanistic reactivities calculated for the "maximum reactivity" experiments, plotted against mechanistic reactivities in the MIR scale (Carter, 1994).

The bottom plots on Figure 10 compare mechanistic reactivities calculated for maximum ozone experiments with corresponding reactivities in the MOIR scale (Carter, 1994). The top two and bottom two plots are calculated with the same base ROG mixture in both the chamber experiments as used in the ambient air (MIR or MOR) calculations, and thus show the differences between chamber and atmospheric reactivities with the ROG mixture held constant. It can be seen that a fair correlation is obtained in the maximum reactivity case for both  $d(O_3\text{-NO})$  and IntOH reactivities, but the slopes are less than one and the intercepts are significantly nonzero in both cases. The correlation is much worse under maximum ozone conditions, being essentially none in the case of  $d(O_3\text{-NO})$  reactivities. This is probably because the maximum ozone reactivities are determined by a balance of several, often opposing, factors, whose relative importances apparently are different in the chamber than the atmosphere. Except for acetaldehyde, the correlation of IntOH reactivities is much better, presumably because it depends on only one aspect of the mechanism. The poor correlations for acetaldehyde must be due to different effects on the importance of PAN formation in the chamber vs the atmosphere.

The middle plots on Figure 10 compare chamber reactivities using the 3-component mini-surrogate with atmospheric MIR reactivities. The dotted lines on the plots are the best fit lines for the chamber reactivities using the ambient mixture, taken from the top two plots. Although the correlation with atmospheric reactivities is not as good as the case with the experiments using the ambient mixture, they are not significantly worse. The intercepts are approximately the same, but the slopes are different because the runs with the mini-surrogate tend to be more sensitive to the VOCs (yield higher mechanistic reactivities) than those with the ambient mixture.

The results of these calculations indicate that it is not possible to obtain exact correlations between chamber reactivities and atmospheric reactivities even if the exact same ROG mixture is employed. The correlation is almost non-existent in the case of  $d(O_3\text{-NO})$  reactivities under maximum ozone or low- $NO_x$  conditions, though it is better for IntOH reactivities. Nonzero intercepts of plots of chamber reactivities against atmospheric reactivities are consistently observed, i.e., based on the calculated correlations we would predict that if a VOC has a mechanistic reactivity of zero in the chamber it have a positive reactivity in the atmosphere. Using a more realistic ROG surrogate may improve the correlation for those cases where there is a correlation, but there would still be the nonzero intercept, and the improvement may not be that significant except for compounds which photolyze.

## **E. Summary**

These calculations indicate that a 9-component "lumped" surrogate provides an excellent representation of the ambient ROG mixture for reactivity experiments, and that use of more complex mixtures would not yield experimentally distinguishable results. The effect of ignoring the "lost carbon" in the ROG surrogate was calculated to be negligible. The calculations also showed that the 9-component surrogate can be further simplified by using formaldehyde to represent both formaldehyde and acetaldehyde (on a molar basis) without yielding a measurable difference in reactivities, but that additional simplifications may have non-negligible effects. In particular, the 3-component "mini-surrogate" used in the previous study was calculated to yield measurable differences in reactivities for many species, and significantly higher reactivities for formaldehyde and acetone.

However, the calculations also showed that even if the exact same ROG mixture is used in the experiments as occurs in the atmosphere, reactivities in environmental chamber experiments would not necessarily be the same or even correlate with those in the atmosphere. The best correlations are obtained with reactivities under maximum reactivity conditions and with IntOH reactivities under various conditions. No correlation is obtained with ozone reactivities under maximum ozone or NO<sub>x</sub>-limited conditions.

Using a realistic ROG surrogate may not necessarily be of greatest utility for mechanism testing. The calculations indicated that experiments with the simpler 3-component mini-surrogates are more sensitive to effects of differences among VOCs, and thus potentially more useful for mechanism evaluation. Since the use of this surrogate for mechanism evaluation was complicated by uncertainties in the m-xylene mechanism, calculations were conducted to determine whether use of an even simpler "surrogate" - ethylene alone - might provide equivalent information while minimizing problems due to base ROG mechanism uncertainties. It was found that the ethylene surrogate gives almost equivalent maximum reactivity results, but tends to be more sensitive to NO<sub>x</sub>-sink species under NO<sub>x</sub>-limited conditions. The latter may be an advantage from the point of view of evaluating this aspect of VOC mechanisms.

It is concluded that the 8-compound surrogate, the "lumped" surrogate with acetaldehyde removed, will provide an appropriate representation of the ambient ROG mixture in reactivity experiments where maximum correlation with atmospheric reactivities is desired. Calculations indicate that using more complex mixtures would complicate the experiment and analysis without yielding measurably different results. However, if the objective is mechanism evaluation, the mini-surrogate or even ethylene alone may be the superior ROG surrogate, since reactivity experiments using it are more sensitive to differences among VOCs, and (in the case of ethylene) possibilities for compensating errors are significantly fewer. The two types of experiments should be considered complementary and of equal importance to providing comprehensive data for reactivity analysis.

Based on these results, it was determined that incremental reactivity experiments using both the lumped surrogate, and ethylene alone as the surrogate, would, in conjunction with the mini-surrogate experiments already conducted, provide useful and complementary information concerning the effect of ROG surrogate on incremental reactivity. These experiments are discussed in the following sections.

### III. EXPERIMENTAL FACILITY AND METHODS

#### A. Facility

##### 1 New Indoor and Outdoor Chamber Laboratory Facility

The work plan for this program includes conducting both indoor and outdoor chamber experiments. (The outdoor chamber experiments are discussed elsewhere [Carter et al., 1995a].) When the program started, all the SAPRC indoor chambers were located in Fawcett Laboratory, where a number of research programs besides this one were being carried out. Because of acquisition of major new equipment for these programs, the space in Fawcett Laboratory became limited, and we were required to relocate the chamber used for into a room which lacked adequate temperature control - a problem which showed up in the data (Carter et al., 1993a). Furthermore, we felt it was important to construct a new type of indoor chamber more suitable for incremental reactivity studies (see discussion of the "DTC", below), but there was insufficient space in Fawcett for this purpose. There was also insufficient office space at Fawcett for the personnel on this program, who had to use offices in a trailer about a block away. Therefore, this program needed additional laboratory and office space.

A further problem with the existing facility was that the SAPRC outdoor chamber was located approximately one block away, and duplicate instrumentation was not available to allow conducting experiments in both facilities simultaneously. This meant that there would be significant down time while moving the equipment and setting them up for outdoor experiments, moving them back and setting them up again for indoor runs, and during periods of unfavorable weather when the laboratory was set up for outdoor runs. Much greater productivity and efficient use of the available resources could be obtained if the indoor chambers could be located in a laboratory adjacent to the outdoor chamber, so equipment can simultaneously used by both, and indoor runs can alternate with outdoor runs as weather or the demands of the program dictate.

To address both these problems, for this program (under funding from the SCAQMD) we obtained a new modular building at the site of the outdoor chamber laboratory which was large enough to house the indoor chambers needed for the program. A layout of this building, which also shows its location relative to the outdoor chamber, is shown on Figure 11. The building has a main laboratory area which houses the analytical instrumentation, and also has room for the ~3000-liter indoor Teflon chamber #2 ("ETC") used in the Phase I experiments, as well as a separate unit, ~3000-liter Teflon chamber which was used for calibrations and injection test experiments. A separate room was dedicated to the new Dividable Teflon Chamber (DTC) or the new Xenon Teflon Chamber (XTC) which was used for the indoor chamber experiments in this program and which are discussed below. (The DTC was constructed first, and it was replaced by the XTC later in the program.) The continuous monitoring instruments could be attached either to

Figure 11. Diagram of SCAQMD-Funded SAPRC indoor and outdoor chamber laboratory for VOC reactivity studies.

one of the indoor chambers (ETC and XTC) or the sampling manifold for DTC and the outdoor chamber (OTC). The building also has offices which were used by the experimental personnel and for data processing. All the experiments discussed in this report were carried out using this facility and four chambers (ETC, DTC, XTC and OTC) were employed in this program..

The facility had an AADCO air purification system located nearby which provided dry pure air for all the chambers. Later in the program a second AADCO was added to provide a greater flow rate to allow more rapid flushing of more than one chamber at a time, and a drying system was added to improve the efficiency of the system and increase the useful lifetime of the air purification cartridges.

## **2. Indoor Teflon Chamber #2 (ETC)**

The Indoor Teflon Chamber #2, which is called the "ETC". This chamber was described in our previous report (Carter et al., 1993a; see also Carter et al., 1995b). Briefly, it consisted of 1 2-mil thick FEP Teflon reaction bag fitted inside an aluminum frame of dimensions of 8 ft x 4 ft x 4 ft. The light source for the chamber consisted of two diametrically opposed banks of 30 Sylvania 40-W BL blacklights, one above and the other below the chamber.

## **3. Dividable Teflon Chamber (DTC)**

The Dividable Teflon Chamber (DTC) was designed to allow irradiations of two separate mixtures at the same time and under the same reaction conditions. Such a chamber should be particularly useful for incremental reactivity experiments, which consist of repeated irradiations of the same mixture, with and without a test VOC added. In the ETC chamber, these experiments have to be carried out one at a time, with the "base case" experiment alternating with "test" experiments consisting of the same nominal reaction mixture, but with a test VOC added. Because of variability of reaction conditions (such as the variability in temperature) and slight differences in amounts of reactants injected from run-to-run, statistical regression analysis methods have to be used to correct for the differences between the runs when determining the effects of the added VOC (Carter et al., 1993a; see also below). This lead to some imprecisions in the reactivity analysis because not all the run-to-run variability could be accounted for in the regressions (Carter et al., 1993a). However, if the base case and the test experiments could be carried out simultaneously, with the same temperatures and concentrations of common reactants, then the precision of the reactivity determination could in principle be improved, and also the productivity of the program, in terms of compounds studies per run day, could be doubled.

The DTC, which is shown schematically in Figure 12, was constructed with these objectives in mind. It consists of two ~5000-liter reaction bags located adjacent to each other, and fitted inside an 8' cubic framework. The light source consisted of two diametrically opposed banks of 32 Sylvania 40-W BL

Figure 12. Diagram of SAPRC Dividable Teflon Chamber (DTC).

blacklights, whose intensity can be controlled by 16 switches, each of which operates 2 blacklights. The lights are backed by aluminum-coated plastic reflectors which are molded into the same shape as the Alzak reflectors in the SAPRC Indoor Teflon Chamber #1 (ITC) (Carter et al., 1995b). The roof, floor and the two end walls are covered with polished aluminum panels, except for a window in the middle of one of the end walls where the sampling, reactant injection, and air fill probes were located. (See also the diagram of the laboratory in Figure 11.) The light intensity in this system turned out to be so high that to achieve light intensities comparable to ambient conditions all the runs in the data base were carried out with 50% of the maximum light intensity.

A specially constructed system of two Teflon-coated fans and blowers was used to rapidly exchange and mix the contents of the two reaction bags. Each blower forces the air from one reaction bag into the other, and the fans mix the air in each bag. This results in equal concentrations of common reactants in both reaction bags, when desired. The valves connecting the two bags can be closed to isolate the two chambers after the injection of common reactants, and the fans can then be used to mix additional reactants in each of the sides separately.

Dry purified air was provided by the same AADCO air purification system discussed above. All runs were carried out under dry conditions  $RH \leq 5\%$ , except for a few runs where water vapor was manually injected to yield  $\sim 50\%$  RH.

The sampling to the continuous monitoring instruments were controlled by two computer-activated solenoid valves, which select the chamber side where air is withdrawn for analysis. One of these valves controls the sampling for the  $O_3$  and  $NO_x$  analyzers, where the sides being sampled are usually alternated every 10 minutes. The other valve is used to control sampling for formaldehyde, which usually had a 15 minute sampling time for each reaction bag. The data acquisition system controlled the sampling valves and kept track of which reaction bag is being monitored when the data are being collected. In addition, a solenoid valve attached to vacuum pump, which was located under the modular building, was employed to withdraw air from one side at the same sampling flow rate as of the continuous analyzers when the other side was being drawn for the continuous analyzers. This was important to keep withdrawing air in both sampling lines so continuous analyzers could monitor each side promptly when the side was changed, especially for the outdoor Teflon Chamber because two longer sampling lines were used.

The two reaction bags are designated as sides "A" and "B". Because two separate mixtures are being irradiated simultaneously, each DTC run consists of two separate experiments. These are designated as runs DTCnnnA and DTCnnnB, where nnn is the run number.

## **B. Experimental Procedures**

The chambers were flushed with dry purified air for 6-9 hours on the nights before the experiments. The continuous monitors were connected prior to reactant injection and the data system began logging data from the continuous monitoring systems. The reactants were injected as described previously (Carter et al, 1993a). For dual chamber (DTC) runs, the common reactants were injected in both sides simultaneously (using a "T" in the injection line) and were well mixed before the chamber was divided. In the case the DTC, the contents of side A were blown into side B and visa-versa using two separate blowers. Fans were used to mix the reactants in the indoor chambers during the injection period, but these were turned off prior to the irradiation. Dividing the DTC consisted of closing the ports which connected the two reaction sides. After the DTC was divided, the reactants for specific sides were injected and mixed. The irradiation began by turning on the lights (for the blacklight chambers), opening the cover (for the OTC), or sliding back the panels in front of the Xenon lights (which were turned on ~30 minutes previously). The irradiation proceeded for 6 hours. After the run, the contents of the chamber(s) were emptied (by allowing the bag to collapse) and flushed with purified air. A heater was turned on to preheat the ETC chamber to reach the experimental temperature desired and turned off when the irradiation began, as described in previous report (Carter et al, 1993a). Preheat for the DTC chamber was accomplished by turning on the temperature control system ~2 hours prior to the irradiation.

## **C. Analytical Methods**

Ozone and nitrogen oxides were continuously monitored using commercially available continuous analyzers with PFA Teflon and borosilicate glass sample lines inserted directly into the chambers (ca 18 in.). For DTC and OTC chamber runs, the sampling lines from each half of the chamber were connected to solenoids which switched from side to side every 10 minutes, so the instruments alternately collected data from each side. Ozone was monitored using a Dasibi Model 1003AH UV photometric ozone analyzer and NO and total oxides of nitrogen (including HNO<sub>3</sub> and organic nitrates) were monitored using either a Columbia Model 1600 or a Teco Model 14B or 43 chemiluminescent NO/NO<sub>x</sub> monitor. The output of these instruments, along with that from the temperature and (for OTC and XTC runs) light sensors were attached to a computer data acquisition system, which recorded the data at periodical intervals, using 30 second averaging times. For single mode (ETC or XTC) chamber runs, the O<sub>3</sub>, NO<sub>x</sub>, and other continuous data recorded every 15 minutes; for the divided chamber (DTC or OTC) runs, the data was collected every 10 minutes, yielding a sampling interval of 20 minutes for taking data from each side.

Organic reactants other than formaldehyde were measured by gas chromatography with FID detection as described elsewhere (Carter et al., 1993a). GC samples were taken for analysis at intervals from fifteen minutes to one hour using 100 ml gas-tight glass syringes. These samples were taken from ports directly connected to the chamber. The syringes were flushed with the chamber contents

several times before taking the sample for analysis. The various analysis systems, and their calibration data, are described in more detail elsewhere (Carter et al., 1995b).

Although we made numerous attempts to obtain a good analysis for PAN using the GC-ECD instrument acquired for this purpose (Carter et al., 1995b), during the period of this program we were not successful in obtaining reproducible data. Therefore, although PAN data are available for many of the experiments conducted for this program, we do not consider them to be sufficiently reliable for quantitative mechanism evaluation. The poorly-constructed sample injection system was subsequently rebuilt.

Formaldehyde was monitored using a diffusion scrubber system based on the design of Dasgupta and co-workers (Dasgupta et al, 1988, 1990; Dong and Dasgupta, 1987), as described elsewhere (Carter et al., 1993a). This system alternately collected data in sample (30 minutes), zero (15 minutes), and calibrate mode (15 minutes), for a one hour cycle time. The readings at the end of the time period for each mode, averaged for 30 seconds, were recorded on the computer data acquisition system, which subsequently processed the data to apply the calibration and zero corrections. A separate sampling line from the chamber was used for the formaldehyde analysis. For the DTC or OTC, a solenoid, which was separate from the one used for O<sub>3</sub> and NO<sub>x</sub> sampling, was used to select the chamber side from which the formaldehyde sample was withdrawn, which alternated every 15 minutes. This yielded formaldehyde data as frequently as every 15 minutes for single chamber (e.g., ETC) runs, and every 30 minutes for each side for divided chamber (e.g. DTC) runs. The calibration data for this instrument are discussed elsewhere (Carter et al., 1995b).

#### **D. Characterization Data**

##### **1. Light Source**

NO<sub>2</sub> Actinometry. The absolute light intensity in the chambers was determined by conducting periodic NO<sub>2</sub> actinometry experiments using the quartz tube method as employed previously (Carter et al, 1993a), except that the "effective quantum yield" factor,  $\Phi$ , was changed from 1.75 to 1.66 based on computer model simulations of a large number of such experiments as discussed in detail elsewhere (Carter et al., 1995b). The procedures for the actinometry runs in the ETC chamber were discussed previously (Carter et al., 1993a). Unless noted differently, in the actinometry runs for the DTC the quartz tube was located between the reaction bags and at about mid height, and parallel with the walls with the lights and the ceiling and the floor.

Spectral Measurements. The spectral measurements for the ETC and DTC chambers were taken periodically using a LiCor Li-1800 portable spectroradiometer. There was found to be no significant difference between the spectrum of this chamber and any other SAPRC blacklight chamber. As discussed

elsewhere (Carter et al., 1995b) a composite spectrum was developed, based on spectral measurements using several spectroradiometers, for use in modeling experiments in all SAPRC blacklight chambers. That spectrum, which gives a better representation of the sharp Hg lines than the lower resolution spectrum used previously (Carter et al., 1993a; Carter and Lurmann, 1991) was used in this work.

## **2. Temperature**

Iron-Constantan thermocouple, interfaced directly to a temperature sensor board in the Keithly A-to-D converter, were used to monitor the temperature as a function of time in these experiments. The probes were calibrated as discussed elsewhere (Carter et al., 1995b). Some additional corrections are needed to the temperature data for the individual chambers. In the cases of the ETC and DTC, one temperature sensor was located in each of the reaction bags for the ETC and DTC chambers. No shielding was used for the probes because at the time it was believed that radiative heating by the blacklights was believed to be minor. However, subsequent comparison of temperatures monitored with this method with simultaneous readings using an aspirated temperature probe indicated that temperatures measured using this method need to be corrected by  $\sim 2^{\circ}\text{C}$  (Carter et al., 1995b).

## **3. Dilution**

Dilution due to sampling is expected to be small because the flexible reaction bags can collapse as sample is withdrawn for analysis. However, some dilution occasionally occurred because of small leaks, and several runs had larger than usual dilution due to a larger leak which was subsequently found and repaired. Information concerning dilution in an experiment can be obtained from relative rates of decay of added VOCs which react significantly only with OH radicals with differing rate constants (Carter et al., 1993a). All experiments had a more reactive compound (such as m-xylene or n-octane) present either as a reactant or added in trace amounts to monitor OH radical levels. Trace amounts ( $\sim 0.1$  ppm) of n-butane was added to experiments if needed to provide a less reactive compound for the purposes of monitoring dilution. In many experiments, dilution rates were zero within the uncertainties of the determinations.

## **4. Control Experiments**

Several types of control experiments were conducted to characterize chamber conditions. Ozone decay rate measurements were conducted with new reactors, and the results were generally consistent with ozone decays observed in other Teflon bag reactors (Carter et al. 1984, 1986).  $\text{NO}_x$ -air irradiations with trace amounts of propene or isobutene, or n-butane- $\text{NO}_x$ -air experiments, were conducted to characterize the chamber radical source (Carter et al., 1982). The specific types of experiments are discussed where relevant in the section describing model calculation methods.

#### IV. EXPERIMENTAL ANALYSIS METHODS AND RESULTS

A chronological list of the experiments carried out in this phase of the program which are relevant to this report is given in Table 5, and Table 6 summarizes the types of incremental reactivity experiments which were carried out. The reactivity experiments include high NO<sub>x</sub> (i.e., maximum reactivity) ethene surrogate experiments and high and low NO<sub>x</sub> (maximum reactivity and NO<sub>x</sub>-limited) lumped surrogate runs. The ethene surrogate experiments were carried out primarily in the ETC, while all the lumped surrogate experiments were carried out in the DTC. The methods used to analyze the data from these experiments, and the results obtained, are described in the following sections.

##### A. Reactivity Analysis Methods

With a few exceptions noted below, the methods used to analyze the results of the reactivity experiments were the same as discussed in our previous report (Carter et al., 1993a). The major features of this analysis, and the modifications to this analysis method made for this program, are summarized below. For a more detailed discussion and the derivations of some of the equations used, the reader is referred to the previous report (Carter et al., 1993a).

As indicated above, two types of reactivity experiments are carried out, the "base case" experiment designed to simulate (or be a simplified representation of) a particular type of chemical environment into which a VOC might be emitted, and a "test" experiment in which an appropriate amount of a VOC whose reactivity is being assessed is added to the base case experiment. The measured quantities in these experiments which are used in the reactivity analysis are as follows:

##### 1. NO oxidized and Ozone Formed, [d(O<sub>3</sub>-NO)]

The amount of O<sub>3</sub> formed and NO oxidized as a function of time, or d(O<sub>3</sub>-NO), is defined as  $([O_3]_t - [NO]_t) - ([O_3]_0 - [NO]_0)$ , where  $[O_3]_0$ ,  $[NO]_0$ ,  $[O_3]_t$  and  $[NO]_t$  are the initial and final O<sub>3</sub> and NO concentrations, respectively. The change in [O<sub>3</sub>]-[NO] is a more useful quantity for reactivity assessment than the change in O<sub>3</sub> alone because, as discussed elsewhere (Johnson, 1983; Carter and Atkinson, 1987; Carter and Lurmann, 1990, 1991), it reflects the same chemical processes, and provides useful reactivity information even under conditions when O<sub>3</sub> is low and NO is high. These data are obtained from the simultaneous NO and O<sub>3</sub> measurements taken during the experiments, and the values after each hour of the experiments are used in the analysis. If O<sub>3</sub> and NO measurements are not available exactly on the hour for a particular run, the hourly values are obtained by interpolating the d(O<sub>3</sub>-NO) data before and after the hour. Interpolation was necessary for the DTC runs because O<sub>3</sub> and NO measurements alternated from side to side every 10 minutes.

Table 5. Listing of all environmental chamber experiments relevant to this report. Gaps in run numbers are experiments for other purposes.

Run	Date	Description and Comments
<b>ETC Experiments</b>		
<b>Characterization Experiments</b>		
	4/22/92	New reaction bag installed.
370	4/23/92	Pure-air irradiation
371	4/23/92	Ozone decay (result in normal range)
374	5/12/92	Pure-air irradiation
375	5/18/92	Propene-NO <sub>x</sub>
380	5/26/92	Tracer-NO <sub>x</sub>
381	5/27/92	Ethene-NO <sub>x</sub>
382	5/28/92	Acetaldehyde-air
448		NO <sub>2</sub> Actinometry
	10/30/92	Full (8-component, "lumped molecule") Surrogate test
455	11/2/92	Full Surrogate test
458	11/09/92	Pure air Irradiation
460	11/12/92	Full Surrogate test
461	11/13/92	NO <sub>2</sub> Actinometry
462	11/13/92	Tracer - NO <sub>x</sub>
463	11/16/92	Full Surrogate test
<b>Ethylene Surrogate Incremental Reactivity Experiments</b> (Unless noted otherwise, "Ethene" refers to 1.6 ppm Ethene, 0.5 ppm NO <sub>x</sub> .)		
464	11/20/92	Ethene
466	11/23/92	Ethene
467	11/25/92	Ethene
468	11/1/92	Ethene + Formaldehyde
469	12/2/92	Ethene
470	12/3/92	Ethene + Formaldehyde
472	12/7/92	Ethene + n-Octane
473	12/8/92	Ethene
474	12/9/92	Ethene + n-Octane
475	12/14/92	Propene - NO <sub>x</sub>
476	12/15/92	Ethene
477	12/16/92	Ethene + m-Xylene
478	12/17/92	Ethene + m-Xylene
479	12/18/92	Ethene
480	12/21/92	Ethene + Acetone
482	1/5/93	Ethene
483	1/6/93	Ethene + CO
484	1/7/93	Ethene + n-Butane
485	1/8/93	Pure-air irradiation
486	1/11/93	Ethene
487	1/12/93	Ethene + CO
488	1/13/93	Ethene + n-Butane
489	1/14/93	Ethene + HCHO
490	1/15/93	Ethene + Acetone
496	1/27/93	Ethene + Propene
499	2/2/93	Ethene + m-Xylene
500	2/3/93	Ethene + Propene
501	2/4/93	Ethene + t-2-Butene
502	2/5/93	Ethene
506	2/17/93	Ethene + Ethane

Table 5 (continued)

Run	Date	Description and Comments
<b>DTC Experiments</b>		
<b>Characterization and Preliminary Experiments</b>		
	12/9/92	NO <sub>2</sub> Actinometry 100% lights
	12/10/92	NO <sub>2</sub> Actinometry with 50% lights
	1/4/93	Dual Teflon reactor bags installed. k <sub>1</sub> tube between bags NO <sub>2</sub> Actinometry. (50% lights for all subsequent runs unless noted)
	1/4/93	O <sub>3</sub> conditioning and decay determination: Initial [O <sub>3</sub> ]=0.63 ppm, in chamber for 15 hours. Decay rate in last 9 hours: 2.0 and 2.4%/hr in sides A, and B respectively.
	1/6/93	Test temperature system
001	1/21/93	Pure air photolysis.
002	1/22/93	O <sub>3</sub> decay. 1.63±0.08%/hr side A; 1.69±0.10%/hr, side B
003	1/27/93	Pure air photolysis
004	1/28/93	NO <sub>2</sub> Actinometry, variable positions
005	1/29/93	NO <sub>2</sub> Actinometry, variable positions
006	2/11/93	Ethene-NO <sub>x</sub> , side equivalency. test.
007	2/18/93	Preliminary full surrogate - NO <sub>x</sub> , side equivalency. test. (Unless indicated otherwise, "surrogate" means 8-component "lumped molecule" surrogate.)
008	2/24/93	Preliminary surrogate - NO <sub>x</sub> (injection and analysis tests)
009	3/2/93	Preliminary surrogate - NO <sub>x</sub> (injection and analysis tests)
010	3/4/93	Preliminary surrogate - NO <sub>x</sub> (injection and analysis tests)
011	3/5/93	Preliminary surrogate - NO <sub>x</sub> (injection and analysis tests)
012	3/10/93	Preliminary surrogate - NO <sub>x</sub> (injection and analysis tests)
013	3/11/93	High NO <sub>x</sub> surrogate, both sides. (Unless indicated otherwise, "High NO <sub>x</sub> surrogate" is 0.5 ppm NO <sub>x</sub> and 4 ppmC "lumped molecule" surrogate.)
<b>Lumped Molecule Surrogate Incremental Reactivity Experiments</b>		
014	3/12/93	High NO <sub>x</sub> surrogate + CO (149 ppm added to side A)
015	3/16/93	High NO <sub>x</sub> surrogate + CO (149 ppm, B)
016	3/17/93	High NO <sub>x</sub> surrogate + CO (71.5 ppm, A)
017	3/18/93	High NO <sub>x</sub> surrogate + Ethene (B)
018	3/22/93	High NO <sub>x</sub> surrogate + Propene (A)
019	3/24/93	High NO <sub>x</sub> surrogate + n-Butane (B)
020	3/25/93	High NO <sub>x</sub> surrogate w/o formaldehyde + CO (96.7 ppm, B)
021	3/26/93	High NO <sub>x</sub> surrogate + <u>trans</u> -2-Butene (B)
022	3/29/93	High NO <sub>x</sub> surrogate + formaldehyde (B)
023	3/30/93	High NO <sub>x</sub> surrogate + toluene (A)
024	3/31/93	High NO <sub>x</sub> surrogate + n-Octane (B)
025	4/1/93	High NO <sub>x</sub> surrogate + m-Xylene (A)
026	4/6/93	Propene-NO <sub>x</sub>
027	4/7/93	Low NO <sub>x</sub> surrogate side equivalency. test. (Unless indicated otherwise, "Low NO <sub>x</sub> surrogate" is 0.17 ppm NO <sub>x</sub> and 4 ppmC lumped molecule surrogate.)
028	4/8/93	High NO <sub>x</sub> surrogate + Acetone (A)
029	4/9/93	Low NO <sub>x</sub> surrogate + CO (A)
030	4/12/93	Low NO <sub>x</sub> surrogate + Toluene (B)
031	4/13/93	Low NO <sub>x</sub> surrogate + n-Butane (A)
032	4/15/93	Low NO <sub>x</sub> surrogate + Propene (B)
033	4/16/93	Low NO <sub>x</sub> surrogate + t-2-Butene (A)
034	4/19/93	Low NO <sub>x</sub> surrogate + α-Pinene (B)
035	4/20/93	Low NO <sub>x</sub> surrogate + m-Xylene (A)

Table 5 (continued)

Run	Date	Description and Comments
<b>DTC</b>		
036	4/21/93	Low NO <sub>x</sub> surrogate + Formaldehyde (A)
037	4/21/93	Low NO <sub>x</sub> surrogate + n-Octane (A)
038	4/26/93	Low NO <sub>x</sub> surrogate + Ethene (B)
039	4/27/93	Low NO <sub>x</sub> surrogate + Benzene (B)
040	4/30/93	surrogate w/o NO <sub>x</sub> (control)
041	5/03/93	Low NO <sub>x</sub> ethene surrogate + t-2-Butene (A)
042	5/05/93	Toluene + NO <sub>x</sub>
043	5/06/93	High NO <sub>x</sub> ethene surrogate + t-2-Butene (B)
049	5/17/93	Pure Air Irradiation (Temperature control test)
052	5/25/93	NO <sub>x</sub> + propene (A); NO <sub>x</sub> + Isobutene (B)
054	5/28/93	NO <sub>x</sub> + propene (A); NO <sub>x</sub> + Acetone (B)
055	6/01/93	NO <sub>x</sub> + acetone (A); NO <sub>x</sub> + Acetaldehyde (B)
064	7/15/93	High NO <sub>x</sub> Surrogate + Acetone (B)
065	7/17/93	High NO <sub>x</sub> surrogate + Acetaldehyde (A)
066	7/19/93	Low NO <sub>x</sub> surrogate + Acetaldehyde (B)
067	7/20/93	Low NO <sub>x</sub> surrogate + m-Xylene (B)
068	7/21/93	High NO <sub>x</sub> surrogate + m-Xylene (B)
069	7/23/93	High NO <sub>x</sub> Full-surrogate + t-2-butene (A)
070	7/26/93	High NO <sub>x</sub> Full-Surrogate + n-C8 (A)
071	7/27/93	Low NO <sub>x</sub> Full-Surrogate + n-C8 (B)
072	7/28/93	High NO <sub>x</sub> Ethene Surrogate + n-C6 (A)

Table 6. Summary of reactivity experiments carried out for this program.

Test VOC	Number of Experiments		
	Ethene Surg. High NO <sub>x</sub> (ETC)	Lumped Molecule High NO <sub>x</sub> (DTC)	Surrogate Low NO <sub>x</sub> (DTC)
Carbon Monoxide	3	4	1
Ethane	1		
n-Butane	2	1	1
n-Hexane	1 [a]		
n-Octane	2	2	2
Ethene		1	1
Propene	2	1	1
<u>trans</u> -2-Butene	3	2	1
Benzene			1
Toluene		1	1
m-Xylene	3	2	2
Formaldehyde	3	1	1
Acetaldehyde		1	1

[a] DTC used

## 2. Integrated OH Radicals (IntOH)

The integrated OH radicals, or IntOH, is useful in providing information on the effect of the VOC on radical levels, which in turn provides information on the chemical basis for a VOC's reactivity (Carter et al, 1993a; see also below.) The IntOH can be derived from the measured concentrations of any compound present in the experiment which reacts only with OH radicals, provided (1) that its OH radical rate constant is well known and (2) that it reacts sufficiently rapidly that the amount consumed due to reaction can be determined as a function of time with a reasonable degree of precision. If  $[\text{Tracer}]_0$  and  $[\text{Tracer}]_t$  are the initial and time t concentration of the compound used as the "OH tracer",  $k_{\text{OH}}^{\text{tracer}}$  is its OH rate constant, and D is the dilution rate of the experiment (derived as discussed below), then  $\text{IntOH}_t$  is given by (Carter et al, 1993a):

$$\text{IntOH}_t = \int_0^t [\text{OH}]_t dt = \frac{\ln \left( \frac{[\text{tracer}]_0}{[\text{tracer}]_t} \right) - Dt}{k_{\text{OH}}^{\text{tracer}}}. \quad (\text{I})$$

m-Xylene was used as the OH tracer in the experiments where this compound was present as a surrogate constituent. In the ethene surrogate runs, small amounts (75-100 ppb) of cyclohexane or methylcyclohexane were added as the OH radical tracer. (The specific tracer used in the ethene experiments is given in the tabulations of the results.) The rate constants used to derive the IntOH values in this work are:  $3.46 \times 10^4 \text{ ppm}^{-1} \text{ min}^{-1}$  for m-xylene,  $1.11 \times 10^4 \text{ ppm}^{-1} \text{ min}^{-1}$  for cyclohexane, and  $1.51 \times 10^4 \text{ ppm}^{-1} \text{ min}^{-1}$  for methylcyclohexane (Atkinson, 1989; Carter, 1990).

Hourly IntOH values were used in the data analysis. In our previous work, the  $\ln([\text{tracer}])$  data were fit by linear or quadratic function, and this function was then used for deriving the hourly IntOH values. This approach was useful in smoothing the data and also provided a means for using the scatter of the data to give uncertainty estimates. However, we subsequently found that this can sometimes introduce artifacts into the IntOH estimates for early time periods, particularly in runs with strong radical inhibitors. Therefore, this approach was not used in this work. Instead, the IntOH values were calculated for the times for which tracer data were available, and hourly values were determined by linear interpolation. The stated uncertainties in the IntOH values were derived by estimating a 2% minimum imprecision uncertainty in the tracer measurements. This is a minimum uncertainty estimate since it does not include uncertainties in the OH radical rate constant, nor does it take into account possible experiments where measurement scatter was greater than 2%.

### 3. Base Case d(O<sub>3</sub>-NO) and IntOH

For each "test" experiment where a test VOC is added, there is a corresponding "base case" experiment where the conditions are the same except that the test VOC is not present. In the DTC experiments, where two mixtures could be irradiated simultaneously and where the common NO<sub>x</sub> and base ROG reactants can be added and mixed equally in both reactors prior to adding the test compound to one, the base case experiment was carried out simultaneously with each test experiment. In this case, the d(O<sub>3</sub>-NO)<sub>t</sub><sup>base</sup> and IntOH<sub>t</sub><sup>base</sup> data corresponding to any test experiment are simply derived from the results of the simultaneous irradiation of the base case mixture.

In the ETC experiments, where only one mixture could be irradiated at a time, and where there is run-to-run variability in temperature and initial reactant concentrations, there is not necessarily a base case experiment which corresponds as closely to the conditions of any given test experiment as is possible in dual chamber runs. In this case, a linear regression analysis is used to derive the dependencies of the base case d(O<sub>3</sub>-NO)<sub>t</sub> and IntOH<sub>t</sub> data on the variable run conditions, and the results of this analysis is used to derive the d(O<sub>3</sub>-NO)<sub>t</sub><sup>base</sup> and IntOH<sub>t</sub><sup>base</sup> values corresponding to the condition of any given test experiment. This is the approach used in our previous incremental reactivity experiments in this chamber (Carter et al., 1993a). Note that when this approach is used, the analysis can also give uncertainty estimates for d(O<sub>3</sub>-NO) and IntOH due to variations in run conditions which are not accounted for by the regressions.

### 4. Amounts of Test VOC Added and Reacted

The amounts of test VOC added, [VOC]<sub>0</sub>, was obtained from the measured test VOC concentration at or immediately prior to the start of the irradiation. The amount of VOC reacted at time=t, [VOC reacted]<sub>t</sub>, was determined either from the experimental measurements of the VOC as a function of time during the experiment, corrected for dilution as shown below, or, for VOCs which react only with OH radicals, from the measured IntOH values and the VOC's OH radical rate constant. In the "direct" method, the amount reacted at time t is given by:

$$(\text{VOC reacted})_t = [\text{VOC}]_0 - [\text{VOC}]_t - D \int_0^t [\text{VOC}] dt \quad (\text{II})$$

where D is the dilution and [VOC]<sub>t</sub> is the measured VOC concentration at time t. In the IntOH method the amount reacted is given by

$$(\text{VOC reacted})_t = [\text{VOC}]_0 \frac{k\text{OH}^{\text{VOC}} \text{IntOH}_t}{k\text{OH}^{\text{VOC}} \text{IntOH}_t + Dt} \left( 1 - e^{-k\text{OH}^{\text{VOC}} \text{IntOH}_t - Dt} \right) \quad (\text{III})$$

where kOH<sup>VOC</sup> is the VOC's OH radical rate constant. (See Carter et al. [1993a] for the derivations of these equations.) As with the previous study (Carter et

al., 1993a), if the amount reacted could be estimated by either method, the method estimated to have the least uncertainty was used.

The uncertainties in the amounts reacted using the direct method (Equation II) were derived by assuming a minimum 2% imprecision uncertainty in the VOC measurements, together with the uncertainty in the dilution derived as discussed below. (The actual imprecision uncertainties for some VOCs were different from this, but this was not taken into account in this analysis.) The uncertainties in the amounts reacted derived from the IntOH method (Equation III) were derived from the uncertainties derived for IntOH and D, and also, for determining which estimation approach is least uncertain, by assuming a 20% uncertainty in  $kOH^{VOC}$ . The estimated uncertainty in  $kOH^{VOC}$  was used only in making the choice between Equation (II) or (III), and was not used in the minimum uncertainties in the amounts reacted given with the data tabulations (Carter et al., 1993a).

Amounts reacted could be estimated for all the test VOCs used in this study except for formaldehyde. Amounts of formaldehyde could not be estimated from Equation (III) because formaldehyde is consumed to a significant extent by photolysis, and could not be estimated from the measured formaldehyde concentrations because a significant amount of this compound is formed from the reactions of the base ROG surrogate. However, for VOCs which are strong radical inhibitors, the amounts of test VOC or OH tracer compound reacted are small relative to analytical imprecisions, and thus estimates of amounts reacted become uncertain.

## 5. Dilution

Note that the derivations of IntOH and VOC reacted require an estimate of the dilution rate, D, for each experiment. Although in principal experiments in flexible Teflon reaction chambers should not have dilution because the chamber can collapse as samples are withdrawn for analysis, in practice we find that some non-negligible dilution is occurring. The analysis of dilution in ETC experiments has been discussed in detail previously (Carter et al., 1993a), and an approximate dilution rate of  $0.48 \pm 0.25$  %/hour was derived for experiments in this chamber. This value was used for the ETC experiments in this study as well.

For the DTC chamber, the dilution rate was derived from the rate of consumption of n-butane (a component of the full surrogate), corrected for its reaction with OH radicals by using its OH radical rate constant and the m-xylene data and its rate constant. The general method employed has been discussed previously (Carter et al., 1993a). If necessary data were missing or the data appeared to be too scattered for a reliable dilution estimate, the dilution rate was estimated based on results for other runs in the same side of the DTC carried out at approximately the same time. (In those cases, the dilutions were given uncertainty estimates of  $\sim 1$  %/hour.) The dilution rates generally ranged from

highs of ~1-2 %/hr for the initial experiments to averages of ~0.3 %/hour in the later runs. Thus they were usually comparable to dilution rates in the ETC.

Uncertainties in dilution were taken into account in the estimates in the minimum uncertainties in the IntOH and amounts reacted data. Generally, the dilution corrections were not large contributors to the overall uncertainties in these quantities.

#### 6. Total or d(O<sub>3</sub>-NO) incremental reactivities

The term "total" incremental reactivity is used to refer to incremental reactivity relative to d(O<sub>3</sub>-NO) because it reflects all aspects of a VOC's reaction mechanism which affects O<sub>3</sub>. It is given by

$$IR_t^{\text{total}} = \frac{d(O_3\text{-NO})_t^{\text{test}} - d(O_3\text{-NO})_t^{\text{base}}}{[VOC]_0} \quad (\text{IV})$$

where d(O<sub>3</sub>-NO)<sub>t</sub><sup>test</sup> and d(O<sub>3</sub>-NO)<sub>t</sub><sup>base</sup> are the d(O<sub>3</sub>-NO)<sub>t</sub> measured in the test experiment and either measured or derived for the corresponding base case experiment, respectively, for time t, and [VOC]<sub>0</sub> is the initial VOC concentration.

The minimum uncertainties in the overall incremental reactivities are estimated differently depending on whether the experiment is a divided chamber (DTC) or single mode (e.g., ETC) chamber run. If it is a single mode run, the regression analysis used to derive the d(O<sub>3</sub>-NO)<sup>base</sup> data also yields an uncertainty estimate for these data. The d(O<sub>3</sub>-NO)<sup>test</sup> are assumed to have the same uncertainty for the purpose of estimating uncertainties in IR. For divided chamber runs, there is no uncertainty estimate for d(O<sub>3</sub>-NO)<sup>base</sup> or d(O<sub>3</sub>-NO)<sup>test</sup>. In this case, we assume they each have a ~3% uncertainty for the purpose of estimating a minimum uncertainty for IR. This is based on the approximate level of equivalence observed when the same mixture is irradiated on both sides of the chamber.

Unless otherwise indicated, the overall incremental reactivities in this work are given in units of moles of ozone per mole of VOC. Note that this is not the same as gram basis or carbon basis incremental reactivities, which are more often used in a regulatory context. However, molar units are preferred in this work because they have a more direct relationship to the chemical basis of reactivity.

#### 7. IntOH Incremental Reactivities.

The IntOH incremental reactivity is a measure of the effect of the VOC on OH radical levels. It is given by:

$$IR_t^{\text{IntOH}} = \frac{\text{IntOH}_t^{\text{test}} - \text{IntOH}_t^{\text{base}}}{[VOC]_0} \quad (\text{V})$$

where  $\text{IntOH}^{\text{test}}$  is the  $\text{IntOH}$  measured in the test experiment with the added VOC and  $\text{IntOH}^{\text{base}}$  is the  $\text{IntOH}$  measured or derived for the corresponding base case run. The  $\text{IntOH}$  reactivity results are given in units of ppt-min OH per ppm VOC added. The minimum uncertainties in the  $\text{IR}^{\text{IntOH}}$  values are derived from the uncertainties in the  $\text{IntOH}^{\text{test}}$  and  $\text{IntOH}^{\text{base}}$  data derived from either assuming a 2% imprecision uncertainty in the tracer data (for all the  $\text{IntOH}^{\text{test}}$  data and the DTC  $\text{IntOH}^{\text{base}}$  data), or (for the ETC  $\text{IntOH}^{\text{base}}$  data) from the uncertainty in the regression estimate.

### 8. Direct and Indirect Incremental Reactivities

As discussed previously (Carter et al., 1993a), the total  $d(\text{O}_3\text{-NO})$  incremental reactivity can be broken down into its "direct" and "indirect" components,

$$\text{IR}^{\text{total}} = \text{IR}^{\text{direct}} + \text{IR}^{\text{indirect}} \quad (\text{VI})$$

where the "Direct" incremental reactivity is defined as the amount of  $\text{O}_3$  formation and  $\text{NO}$  oxidation caused directly by the reactions of the radicals formed from the reactions of the test VOC and its reactive products, and the "indirect" incremental reactivity is the change in  $\text{O}_3$  formation and  $\text{NO}$  oxidation resulting from the effect of the test VOC on the reactions of the other VOCs present, in both cases relative to the amount of test VOC added. In an incremental reactivity experiment, the "other VOCs" are the components of the base ROG mixture used in the base case experiments. An estimate of how the reactions of the test VOC effect  $d(\text{O}_3\text{-NO})$  from the reactions of the base ROG can be obtained if it is assumed that the relationship between  $\text{IntOH}$  and the  $d(\text{O}_3\text{-NO})$  formed from the reactions of the base ROG mixture is the same in the test experiments as it is in the base case runs. This is a reasonable assumption in high  $\text{NO}_x$  experiments where the addition of the test VOC does not cause a large perturbation on the system, but is not valid under  $\text{NO}_x$ -limited conditions where the effect of the VOC on  $\text{NO}_x$  levels will also affect ozone formation from the base ROG surrogate. If this is assumed, then

$$\text{IR}^{\text{indirect}} \approx \text{IR}^{\text{IntOH}} \frac{d(\text{O}_3\text{-NO})_t^{\text{base}}}{\text{IntOH}_t^{\text{base}}} \quad (\text{VII})$$

and thus, from (VI)

$$\text{IR}^{\text{direct}} \approx \text{IR}^{\text{total}} - \text{IR}^{\text{IntOH}} \frac{d(\text{O}_3\text{-NO})_t^{\text{base}}}{\text{IntOH}_t^{\text{base}}} \quad (\text{VIII})$$

Because the assumptions behind these equations are not valid under  $\text{NO}_x$ -limited conditions, direct and indirect reactivities are only reported for high  $\text{NO}_x$  experiments, or portions of lower  $\text{NO}_x$  experiments where ozone formation is not  $\text{NO}_x$ -limited.

The  $d(O_3-NO)^{base}/IntOH^{base}$  ratios for the DTC experiments were taken directly from the results of the base case experiment conducted along with the test run. For the single chamber ETC runs, a linear regression analysis was used to determine how this ratio depended on reaction conditions, and this was used to derive the  $d(O_3-NO)^{base}/IntOH^{base}$  ratios for the conditions of each test experiment. The ratio tended to be less variable than  $d(O_3-NO)^{base}$  or  $IntOH^{base}$ , so the ratio for a test run derived based on the regression analysis on the base case ratio tended to have less uncertainty than the ratio of the  $d(O_3-NO)^{base}$  and  $IntOH^{base}$  derived from the separate regressions on each.

### 9. Mechanistic Reactivities

Mechanistic reactivities are analogous to incremental reactivities except they are relative to the amount of test VOC reacted up to the time of the observation, rather than the amount added. Thus

$$MR_t^{total} = \frac{d(O_3-NO)_t^{test} - d(O_3-NO)_t^{base}}{(VOC\ Reacted)_t} \quad (IX)$$

$$MR_t^{IntOH} = \frac{IntOH_t^{test} - IntOH_t^{base}}{(VOC\ reacted)_t} \quad (X)$$

$$MR^{total} = MR^{direct} + MR^{indirect} \quad (XI)$$

$$MR^{indirect} \approx MR^{IntOH} \frac{d(O_3-NO)_t^{base}}{IntOH^{base}} \quad (XII)$$

and

$$MR^{direct} \approx MR^{total} - MR^{IntOH} \frac{d(O_3-NO)_t^{base}}{IntOH^{base}} \quad (XIII)$$

Mechanistic reactivities are useful because, to a first approximation, they are independent on how rapidly the VOC reacts, and thus allow comparisons of reactivity characteristics of VOCs which react at different rates. However, measurements of mechanistic reactivities are useful only for VOCs where the amount reacted can be determined with a reasonable degree of precision. Thus, no mechanistic reactivity data could be obtained for formaldehyde, and determinations of mechanistic reactivities in some experiments with strong radical inhibition are probably insufficiently precise to be useful for mechanism evaluation.

## B. Ethene Surrogate Reactivity Results

### 1. Base Case results

The conditions and selected results of the ethene surrogate reactivity experiments are summarized on Table 7. The base case experiments consisted of irradiations of  $0.43 \pm 0.04$  ppm  $\text{NO}_x$  and  $1.66 \pm 0.10$  ppm ethene, with  $\sim 100$  ppb each of cyclohexane (or methylcyclohexane) and n-butane as dilution and radical tracers. Concentration-time plots for  $\text{O}_3$ , NO,  $\text{NO}_2$  and ethene in a typical "ethene surrogate" base case experiment is shown in Figure 13. Results of model simulations of the experiment, discussed later in this report, are also shown. It can be seen that this can be considered a "high  $\text{NO}_x$ " experiment since  $\text{NO}_2$  is still being consumed and  $\text{O}_3$  is still forming when the run is ended at 6 hours. The continued formation of  $\text{O}_3$  and the presence of reacting  $\text{NO}_2$  means that  $\text{O}_3$  is not  $\text{NO}_x$ -limited. Thus the base case for experiments can be considered to approximate "maximum reactivity" conditions, though, as discussed below, this is not true for many of the added test VOC runs.

Table 7 shows that except for run ETC467, which had higher than the usual NO levels, good reproducibility was observed in these ethene- $\text{NO}_x$  base case experiments. Nevertheless, there was sufficient variability in the results that the uncertainties in the incremental reactivity derivations could be reduced by using linear regression analyses to take into account the dependencies of the results on the variable reaction conditions. The set of parameters used for the regressions depended on the base case result being predicted, being chosen to minimize the uncertainty in the predictions using the regressions. (Note that while using the maximum number of dependent parameters in the regression may give the best fits of the predictions to the base case data, it does not necessarily give the least uncertain estimates of the predicted values because increasing the number of degrees of parameters beyond the optimum number tends to increase uncertainties of the predictions). The set of parameters which gave the least uncertainties in the predictions were as follows:

<u>Predicted Quantity</u>	<u>Parameters Used</u>
hour 1 $d(\text{O}_3\text{-NO})$	none (simple average used)
hour 2-6 $d(\text{O}_3\text{-NO})$	average temperature, initial $\text{NO}_2$ and ethene
hour 1-5 IntOH	average temperature, initial NO and ethene
hour 6 IntOH	average temperature, initial NO, $\text{NO}_2$ and ethene
hour 1 $d(\text{O}_3\text{-NO})/\text{IntOH}$	none
hour 2-3 $d(\text{O}_3\text{-NO})/\text{IntOH}$	average temperature, initial $\text{NO}_2$ and ethene
hour 4-6 $d(\text{O}_3\text{-NO})/\text{IntOH}$	average temperature, initial NO and $\text{NO}_2$ .

Figure 14 shows plots of the predicted vs. observed 6-hour  $d(\text{O}_3\text{-NO})$ , IntOH and  $d(\text{O}_3\text{-NO})/\text{IntOH}$  results of the base case experiments, with the error bars showing the uncertainties of the regression predictions.

It is interesting to note that although the range of average temperatures in these experiments was less than  $2^\circ\text{C}$ , the variation in temperature was found

Table 7. Summary of conditions and selected results of the ETC ethene surrogate reactivity experiments.

ETC Run No.	Test VOC		Avg. T (K)	Initial Reactants [a]				Results (t=6 hrs) [b]		
	Name	(ppm)		NO	NO <sub>2</sub>	NO <sub>x</sub>	Ethene	d(O <sub>3</sub> -NO)	IntOH	Ratio
464 [c]			301.7	279	96	375	1.48	1.162	41.1	28.3
466 [c]			301.0	308	105	413	1.48	1.080	35.0	30.9
467 [c,d]			301.0	400	125	525	1.46	0.732	20.5	35.8
469			301.4	341	114	455	1.77	1.136	32.6	34.8
471			302.3	342	110	452	1.77	1.268	42.1	30.1
473			301.4	344	116	460	1.86	1.233	38.3	32.2
476			301.1	300	131	431	1.68	1.043	32.8	31.8
479			301.3	312	106	418	1.75	1.150	37.5	30.7
482			301.2	315	95	410	1.57	1.139	33.7	33.8
486			301.4	339	101	440	1.56	1.076	32.1	33.5
497			301.9	319	135	454	1.74	1.184	38.4	30.9
505			301.0	283	115	398	1.61	1.080	38.4	28.1
487	CO	107	301.8	335	122	457	1.64	1.431	33.4	
483	CO	155	300.7	312	111	423	1.58	1.475	25.9	
506	ETHANE	50	300.6	290	122	412	1.54	1.209	20.0	
488	N-C4	10.3	300.5	311	108	419	1.56	1.323	16.9	
484	N-C4	15	300.7	338	118	456	1.67	1.400	14.2	
472	N-C8	1.6	301.4	314	107	421	1.78	0.966	13.6	
474	N-C8	2.3	301.4	318	138	456	1.76	0.920	11.6	
500	PROPENE	0.21	300.7	303	116	419	1.66	1.270	36.5	
496	PROPENE	0.30	301.5	280	96	376	1.59	1.226	45.0	
501	T-2-BUTE	0.066	300.9	303	120	423	1.70	1.274	48.6	
493	T-2-BUTE	0.14	301.4	314	110	424	1.79	1.247	55.0	
478	M-XYLENE	0.097	300.9	301	128	429	1.70	1.298	48.7	
499	M-XYLENE	0.16	301.2	317	112	429	1.73	1.274	39.5	
477	M-XYLENE	0.19	301.4	319	142	461	1.75	1.295	53.9	
468	FORMALD	0.11	301.2	324	104	428	1.67	1.280	40.7	
470	FORMALD	0.26	301.8	294	96	390	1.63	1.371	56.8	
489	FORMALD	0.29	302.0	314	105	419	1.63	1.377	56.1	
Average			301.3	313	114	430	1.66			
Std. Deviation			0.5	6%	11%	5%	5%			

[a] Initial NO, NO<sub>2</sub>, and NO<sub>x</sub> in ppb; initial ethene in ppm.

[b] d(O<sub>3</sub>-NO) in units of ppm; IntOH in units of ppt-min; Ratio is base case d(O<sub>3</sub>-NO)/IntOH in units of 10<sup>3</sup> min<sup>-1</sup>

[c] Initial ethene appears to be anomalously low. Model more constant with entire set if these runs are assumed to have the same ethene as the other runs.

[d] Initial NO unusually high. Results not used for base case results regression.

to be a statistically significant factor in affecting the results, with both d(O<sub>3</sub>-NO) and IntOH (though not their ratio) increasing with temperature. The temperature dependence indicated by the regression analysis for t=6 hour d(O<sub>3</sub>-NO) corresponds to an apparent activation energy of 19 kcal/mole. As discussed elsewhere (Carter et al., 1995a), this is comparable to the temperature dependence observed in the phase I mini-surrogate runs (Carter et al., 1993a), and in both cases the temperature dependence is far greater than can be accounted for in the mechanism, even after considering possible temperature-dependent chamber effects.

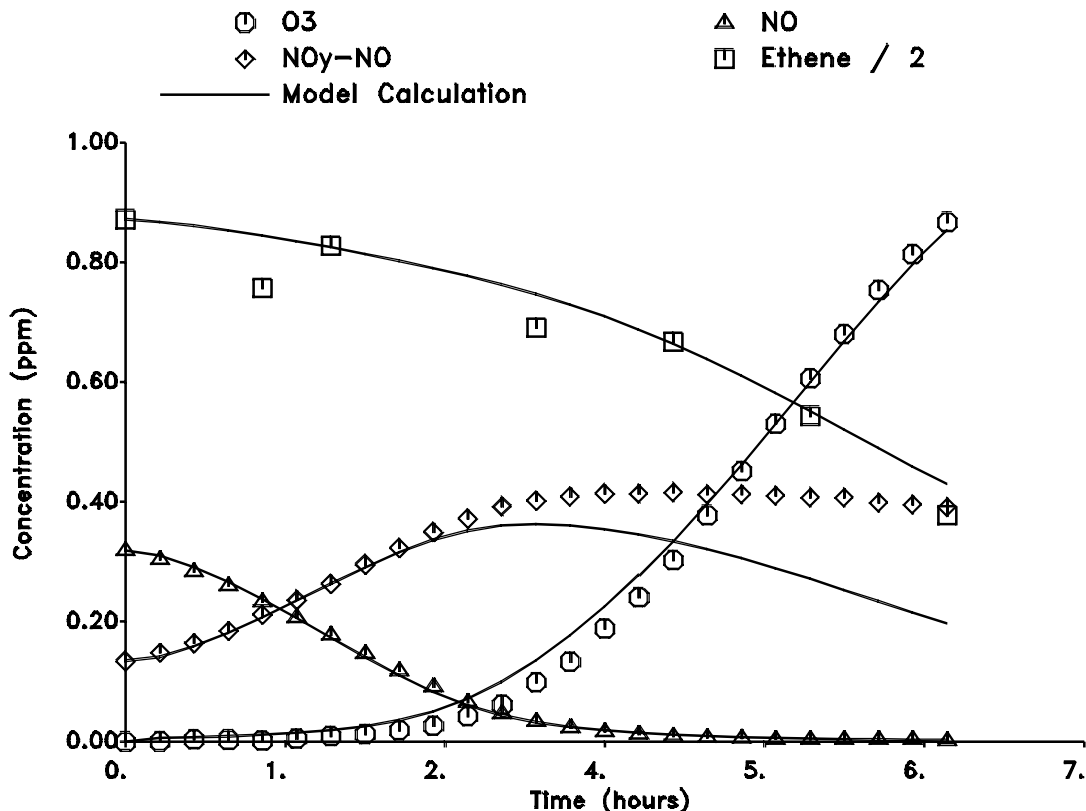


Figure 13. Concentration time plots of selected species in a representative "base case" ethene surrogate run. Results of model simulations are also shown.

## 2. Reactivity Results

As indicated in Table 6, ethene surrogate reactivity experiments were carried out for carbon monoxide, ethane, n-butane, n-octane, propene, trans-2-butene, m-xylene and formaldehyde, in most cases with two experiments for each VOC. The conditions and selected results of the added test VOC runs are included on Table 7, the detailed results of the ethene surrogate reactivity experiments are shown on Tables 8-10. These include, for each hour in the experiment, the estimated amount of test VOC reacted and its uncertainty, the method used to estimate the amount reacted, the  $d(\text{O}_3\text{-NO})$  and  $\text{IntOH}$  observed in the added VOC run and their corresponding base case values derived from linear regressions of the base case experiments for the conditions of the added VOC runs, the corresponding  $d(\text{O}_3\text{-NO})$  and  $\text{IntOH}$  incremental and mechanistic reactivities, the  $d(\text{O}_3\text{-NO})^{\text{base}}/\text{IntOH}^{\text{vase}}$  ratio derived from the linear regression of this ratio in the base case runs, the amount of  $d(\text{O}_3\text{-NO})$  formed from the reactions of the base ROG estimated using  $d(\text{O}_3\text{-NO})^{\text{base}}/\text{IntOH}^{\text{vase}}$  and  $\text{IntOH}^{\text{test}}$ , and the corresponding estimated

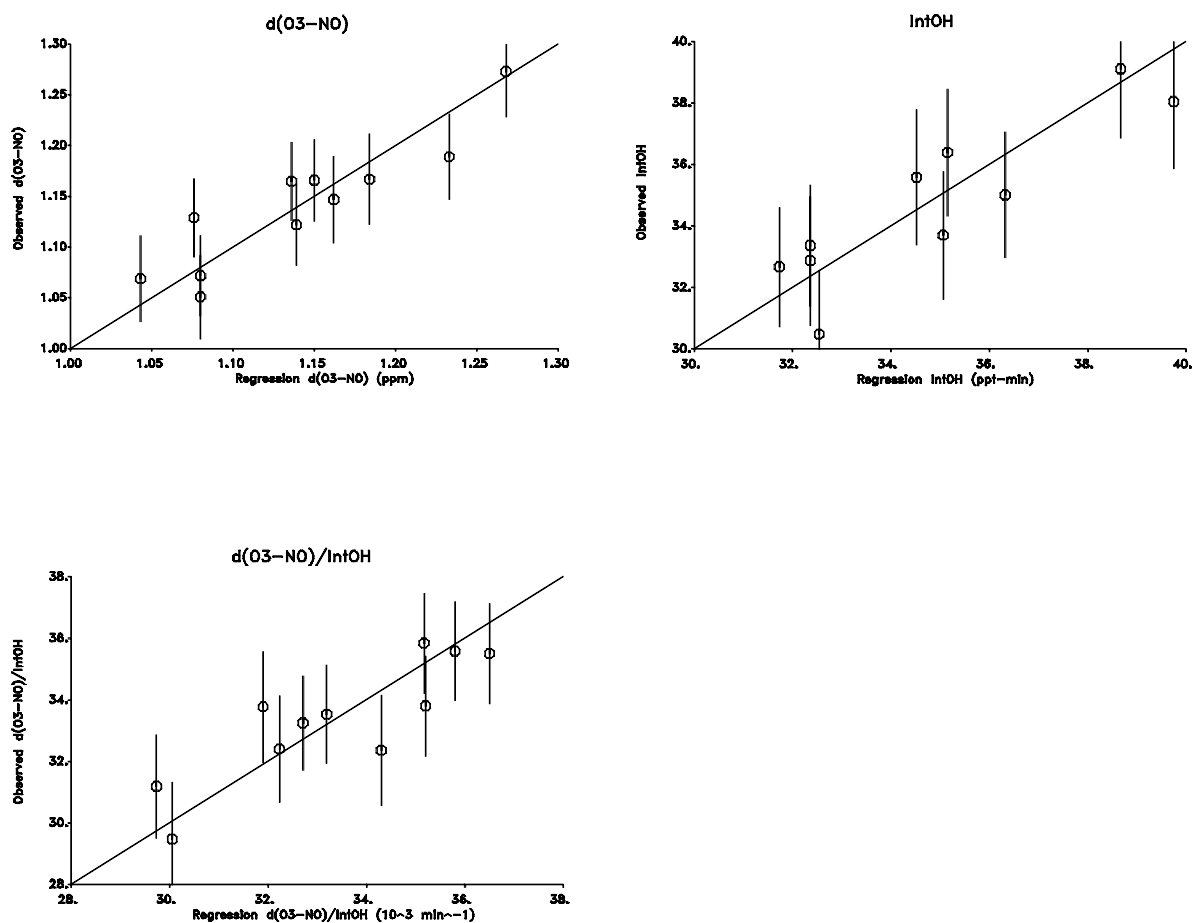


Figure 14. Plots of observed vs regression predicted 6-hour d(O<sub>3</sub>-NO), IntOH and d(O<sub>3</sub>-NO)/IntOH ratios for the base case ethene surrogate experiments.

direct incremental and mechanistic reactivities. Data whose estimated minimum uncertainties are too large to be meaningful are not shown.

Plots of representative results for the added VOC ethene surrogate experiments are shown on Figures 15-23. Results of model calculations, discussed later, are also shown. Except as noted, the figures include the following plots for each VOC:

- (1) The concentration-time plots of d(O<sub>3</sub>-NO) for the added VOC runs and the hourly average base case d(O<sub>3</sub>-NO) results. The standard deviations of the averages for the base case are also shown.

Table 8. Derivation of hourly d(O<sub>3</sub>-NO) reactivities from the results of the ethene surrogate experiments.

ETC Run No.	Added (ppm)	Time (hr)	Reacted [a]		d(O <sub>3</sub> -NO) (ppm)			Reactivity (mol/mol)	
			(ppm)	Deriv.	Test	Base Fit	Change	Incremental	Mechanistic
<b>Carbon Monoxide</b>									
487	107. ± 2.	1		[b]	0.168	0.088 ± 0.015	0.080 ± 0.022	0.0007 ± 28%	
		2		[b]	0.412	0.216 ± 0.019	0.196 ± 0.027	0.0018 ± 14%	
		3	0.326 ± 0.099	IntOH	0.752	0.379 ± 0.028	0.373 ± 0.039	0.0035 ± 11%	1.14 ± 32%
		4	0.547 ± 0.102	IntOH	1.115	0.605 ± 0.045	0.510 ± 0.063	0.0048 ± 13%	0.93 ± 22%
		5	0.803 ± 0.106	IntOH	1.352	0.894 ± 0.059	0.458 ± 0.083	0.0043 ± 18%	0.57 ± 23%
		6	1.121 ± 0.113	IntOH	1.431	1.151 ± 0.041	0.280 ± 0.058	0.0026 ± 21%	0.25 ± 23%
483	155. ± 3.	1		[b]	0.184	0.088 ± 0.015	0.096 ± 0.022	0.0006 ± 23%	
		2	0.261 ± 0.141	IntOH	0.446	0.210 ± 0.020	0.236 ± 0.028	0.0015 ± 12%	0.90 ± 55%
		3	0.461 ± 0.143	IntOH	0.825	0.350 ± 0.028	0.475 ± 0.040	0.0031 ± 9%	1.03 ± 32%
		4	0.713 ± 0.147	IntOH	1.198	0.528 ± 0.046	0.670 ± 0.065	0.0043 ± 10%	0.94 ± 23%
		5	0.979 ± 0.153	IntOH	1.392	0.777 ± 0.060	0.615 ± 0.085	0.0040 ± 14%	0.63 ± 21%
		6	1.223 ± 0.160	IntOH	1.475	1.038 ± 0.042	0.437 ± 0.059	0.0028 ± 14%	0.36 ± 19%
<b>Ethane</b>									
506	49.7 ± 1.0	1		[b]	0.130	0.088 ± 0.015	0.042 ± 0.022	0.0008 ± 53%	
		2	0.101 ± 0.051	IntOH	0.317	0.197 ± 0.022	0.120 ± 0.030	0.0024 ± 25%	1.19 ± 57%
		3	0.181 ± 0.052	IntOH	0.547	0.328 ± 0.031	0.219 ± 0.044	0.0044 ± 20%	1.21 ± 35%
		4	0.211 ± 0.054	IntOH	0.827	0.494 ± 0.050	0.333 ± 0.070	0.0067 ± 21%	1.58 ± 33%
		5	0.241 ± 0.056	IntOH	1.076	0.729 ± 0.066	0.346 ± 0.093	0.0070 ± 27%	1.44 ± 35%
		6	0.382 ± 0.058	IntOH	1.209	0.991 ± 0.046	0.218 ± 0.065	0.0044 ± 30%	0.57 ± 34%
<b>n-Butane</b>									
488	10.31 ± 0.21	1		[b]	0.130	0.088 ± 0.015	0.042 ± 0.022	0.0040 ± 53%	
		2		[b]	0.320	0.209 ± 0.021	0.111 ± 0.030	0.0108 ± 27%	
		3	0.221 ± 0.100	IntOH	0.594	0.344 ± 0.030	0.250 ± 0.042	0.024 ± 17%	1.13 ± 48%
		4	0.316 ± 0.101	IntOH	0.945	0.514 ± 0.049	0.431 ± 0.069	0.042 ± 16%	1.37 ± 36%
		5	0.462 ± 0.104	IntOH	1.209	0.753 ± 0.064	0.456 ± 0.090	0.044 ± 20%	0.99 ± 30%
		6	0.504 ± 0.107	IntOH	1.323	1.015 ± 0.045	0.308 ± 0.063	0.030 ± 21%	0.61 ± 30%
484	15.2 ± 0.3	1		[b]	0.183	0.088 ± 0.015	0.095 ± 0.022	0.0062 ± 23%	
		2		[b]	0.451	0.210 ± 0.020	0.241 ± 0.028	0.0159 ± 12%	
		3	0.341 ± 0.146	IntOH	0.828	0.353 ± 0.029	0.475 ± 0.041	0.031 ± 9%	1.39 ± 44%
		4	0.410 ± 0.149	IntOH	1.206	0.532 ± 0.047	0.674 ± 0.066	0.044 ± 10%	1.64 ± 38%
		5	0.425 ± 0.154	IntOH	1.374	0.786 ± 0.061	0.587 ± 0.087	0.039 ± 15%	1.38 ± 39%
		6	0.645 ± 0.158	IntOH	1.400	1.051 ± 0.043	0.349 ± 0.061	0.023 ± 18%	0.54 ± 30%
<b>n-Octane</b>									
472	1.60 ± 0.03	1		[b]	0.057	0.088 ± 0.015	-0.031 ± 0.022	-0.0196 ± 70%	
		2		[b]	0.154	0.235 ± 0.019	-0.081 ± 0.027	-0.050 ± 33%	
		4	0.123 ± 0.046	Direct	0.452	0.625 ± 0.044	-0.173 ± 0.062	-0.108 ± 36%	-1.40 ± 52%
		5	0.185 ± 0.047	Direct	0.700	0.920 ± 0.058	-0.220 ± 0.081	-0.137 ± 37%	-1.19 ± 45%
		6	0.278 ± 0.047	Direct	0.966	1.183 ± 0.040	-0.217 ± 0.057	-0.135 ± 26%	-0.78 ± 31%
		474	2.27 ± 0.05	1		[b]	0.053	0.088 ± 0.015	-0.035 ± 0.022
2				[b]	0.147	0.206 ± 0.020	-0.059 ± 0.029	-0.026 ± 49%	
3				[b]	0.273	0.361 ± 0.029	-0.088 ± 0.041	-0.039 ± 47%	
4	0.128 ± 0.066			Direct	0.429	0.566 ± 0.047	-0.137 ± 0.067	-0.060 ± 49%	-1.07 ± 71%
5	0.172 ± 0.068			Direct	0.656	0.847 ± 0.062	-0.191 ± 0.088	-0.084 ± 46%	-1.11 ± 61%
6	0.286 ± 0.068			Direct	0.920	1.111 ± 0.044	-0.191 ± 0.062	-0.084 ± 32%	-0.67 ± 40%
<b>n-Hexane</b>									
72A [c]	2.88 ± 0.06	1		[b]	0.057	0.067 ± 0.002	-0.010 ± 0.003	-0.0035 ± 26%	
		2		[b]	0.140	0.180 ± 0.005	-0.040 ± 0.007	-0.0139 ± 17%	
		3		[b]	0.256	0.326 ± 0.010	-0.070 ± 0.012	-0.024 ± 18%	
		4		[b]	0.405	0.492 ± 0.015	-0.087 ± 0.019	-0.030 ± 22%	
		5		[b]	0.608	0.718 ± 0.022	-0.110 ± 0.028	-0.038 ± 26%	
		6	0.166 ± 0.121	IntOH	0.914	1.022 ± 0.031	-0.108 ± 0.041	-0.037 ± 38%	-0.65 ± 82%
<b>Propene</b>									
500	0.213 ± 0.004	1	0.011 ± 0.006	Direct	0.136	0.088 ± 0.015	0.048 ± 0.022	0.22 ± 46%	4.48 ± 72%
		2	0.050 ± 0.005	Direct	0.349	0.211 ± 0.020	0.138 ± 0.028	0.65 ± 21%	2.75 ± 23%
		3	0.121 ± 0.005	Direct	0.681	0.354 ± 0.029	0.327 ± 0.041	1.53 ± 13%	2.71 ± 13%
		4	0.174 ± 0.005	Direct	1.003	0.534 ± 0.046	0.469 ± 0.066	2.2 ± 14%	2.70 ± 14%
		5	0.201 ± 0.005	Direct	1.192	0.788 ± 0.061	0.404 ± 0.086	1.89 ± 21%	2.01 ± 21%
		6	0.208 ± 0.005	Direct	1.270	1.052 ± 0.043	0.218 ± 0.060	1.02 ± 28%	1.05 ± 28%
496	0.301 ± 0.006	1	0.032 ± 0.008	Direct	0.149	0.088 ± 0.015	0.061 ± 0.022	0.20 ± 36%	1.92 ± 44%
		2	0.104 ± 0.007	Direct	0.451	0.232 ± 0.018	0.219 ± 0.026	0.73 ± 12%	2.10 ± 14%
		3	0.222 ± 0.006	Direct	0.873	0.396 ± 0.026	0.477 ± 0.037	1.58 ± 8%	2.15 ± 8%
		4		[b]	1.114	0.619 ± 0.043	0.495 ± 0.060	1.65 ± 12%	
		5	0.301 ± 0.006	Direct	1.205	0.903 ± 0.056	0.302 ± 0.080	1.00 ± 26%	1.00 ± 26%
		6	0.301 ± 0.006	Direct	1.226	1.158 ± 0.039	0.068 ± 0.056	0.23 ± 82%	0.23 ± 82%

Table 8 (continued)

ETC Run No.	Added (ppm)	Time (hr)	Reacted [a]		d(O3-NO) (ppm)			Reactivity (mol/mol)	
			(ppm)	Deriv.	Test	Base Fit	Change	Incremental	Mechanistic
<b>trans-2-Butene</b>									
501	0.066 ±0.001	1	0.038 ±0.001	Direct	0.319	0.088 ±0.015	0.231 ±0.022	3.5 ± 10%	6.07 ± 10%
		2	0.066 ±0.001	Direct	0.638	0.212 ±0.019	0.426 ±0.027	6.5 ± 7%	6.47 ± 7%
		3	0.066 ±0.001	Direct	0.881	0.360 ±0.027	0.521 ±0.039	7.9 ± 8%	7.92 ± 8%
		4	0.066 ±0.001	Direct	1.096	0.549 ±0.044	0.547 ±0.063	8.3 ± 12%	8.32 ± 12%
		5	0.066 ±0.001	Direct	1.219	0.812 ±0.059	0.407 ±0.083	6.2 ± 20%	6.18 ± 20%
		6	0.066 ±0.001	Direct	1.274	1.076 ±0.041	0.198 ±0.058	3.0 ± 29%	3.01 ± 29%
43B [c]	0.097 ±0.002	1	0.066 ±0.002	Direct	0.350	0.063 ±0.002	0.287 ±0.011	3.0 ± 4%	4.36 ± 5%
		2	0.097 ±0.002	Direct	0.715	0.174 ±0.005	0.541 ±0.022	5.6 ± 5%	5.60 ± 5%
		3	0.097 ±0.002	Direct	0.979	0.318 ±0.010	0.661 ±0.031	6.8 ± 5%	6.84 ± 5%
		4	0.097 ±0.002	Direct	1.224	0.485 ±0.015	0.739 ±0.039	7.6 ± 6%	7.65 ± 6%
		5	0.097 ±0.002	Direct	1.363	0.712 ±0.021	0.651 ±0.046	6.7 ± 7%	6.74 ± 7%
		6	0.097 ±0.002	Direct	1.410	1.009 ±0.030	0.401 ±0.052	4.1 ± 13%	4.15 ± 13%
493	0.142 ±0.003	1	0.142 ±0.003	Direct	0.674	0.088 ±0.015	0.586 ±0.022	4.1 ± 4%	4.14 ± 4%
		2	0.142 ±0.003	Direct	0.932	0.233 ±0.019	0.699 ±0.026	4.9 ± 4%	4.94 ± 4%
		3	0.142 ±0.003	Direct	1.117	0.400 ±0.027	0.717 ±0.038	5.1 ± 6%	5.07 ± 6%
		4	0.142 ±0.003	Direct	1.218	0.621 ±0.043	0.597 ±0.061	4.2 ± 10%	4.22 ± 10%
		5	0.142 ±0.003	Direct	1.244	0.916 ±0.057	0.328 ±0.080	2.3 ± 25%	2.32 ± 25%
		6	0.142 ±0.003	Direct	1.247	1.179 ±0.040	0.068 ±0.056	0.48 ± 82%	0.48 ± 82%
<b>m-Xylene</b>									
478	0.095 ±0.002	1	0.013 ±0.003	Direct	0.125	0.088 ±0.015	0.037 ±0.022	0.39 ± 60%	2.72 ± 63%
		2	0.027 ±0.002	Direct	0.393	0.205 ±0.020	0.188 ±0.028	1.99 ± 15%	6.86 ± 17%
		3	0.045 ±0.002	Direct	0.736	0.349 ±0.029	0.387 ±0.040	4.1 ± 11%	8.66 ± 12%
		4	0.059 ±0.002	Direct	1.056	0.534 ±0.046	0.522 ±0.065	5.5 ± 13%	8.90 ± 13%
		5	0.070 ±0.002	Direct	1.232	0.794 ±0.061	0.438 ±0.086	4.6 ± 20%	6.28 ± 20%
		6	0.075 ±0.002	Direct	1.298	1.059 ±0.043	0.239 ±0.060	2.5 ± 25%	3.18 ± 25%
499	0.147 ±0.003	1	0.015 ±0.004	Direct	0.192	0.088 ±0.015	0.104 ±0.022	0.71 ± 21%	6.84 ± 34%
		2	0.046 ±0.004	Direct	0.544	0.225 ±0.018	0.320 ±0.026	2.2 ± 8%	7.01 ± 11%
		4	0.097 ±0.003	Direct	1.182	0.591 ±0.042	0.591 ±0.059	4.0 ± 10%	6.12 ± 11%
		5	0.108 ±0.003	Direct	1.261	0.872 ±0.055	0.390 ±0.078	2.7 ± 20%	3.61 ± 20%
		6	0.117 ±0.003	Direct	1.274	1.134 ±0.039	0.140 ±0.055	0.95 ± 39%	1.20 ± 39%
		477	0.173 ±0.003	1	0.023 ±0.005	Direct	0.249	0.088 ±0.015	0.161 ±0.022
2	0.062 ±0.004	Direct	0.690	0.202 ±0.022	0.488 ±0.030	2.8 ± 7%	7.85 ± 9%		
3	0.098 ±0.004	Direct	1.083	0.354 ±0.031	0.729 ±0.044	4.2 ± 6%	7.45 ± 7%		
4	0.118 ±0.004	Direct	1.259	0.558 ±0.050	0.701 ±0.070	4.1 ± 10%	5.93 ± 11%		
5	0.133 ±0.004	Direct	1.295	0.835 ±0.066	0.460 ±0.093	2.7 ± 20%	3.46 ± 20%		
6	0.139 ±0.004	Direct	1.295	1.099 ±0.046	0.196 ±0.065	1.13 ± 33%	1.41 ± 33%		
<b>Formaldehyde</b>									
468	0.108 ±0.002	1	[b]		0.161	0.088 ±0.015	0.073 ±0.022	0.67 ± 30%	
		2	[b]		0.336	0.228 ±0.018	0.108 ±0.026	1.00 ± 24%	
		3	[b]		0.542	0.387 ±0.026	0.155 ±0.037	1.44 ± 24%	
		4	[b]		0.812	0.596 ±0.042	0.216 ±0.060	2.0 ± 28%	
		5	[b]		1.085	0.875 ±0.055	0.210 ±0.078	1.95 ± 37%	
		6	[b]		1.280	1.135 ±0.039	0.145 ±0.055	1.35 ± 38%	
470	0.260 ±0.005	1	[b]		0.262	0.088 ±0.015	0.174 ±0.022	0.67 ± 13%	
		2	[b]		0.563	0.239 ±0.019	0.324 ±0.027	1.25 ± 9%	
		3	[b]		0.916	0.412 ±0.027	0.505 ±0.039	1.94 ± 8%	
		4	[b]		1.193	0.650 ±0.044	0.543 ±0.063	2.1 ± 12%	
		5	[b]		1.320	0.950 ±0.058	0.371 ±0.083	1.42 ± 22%	
		6	[b]		1.371	1.204 ±0.041	0.167 ±0.058	0.64 ± 35%	
489	0.286 ±0.006	1	[b]		0.216	0.088 ±0.015	0.128 ±0.022	0.45 ± 17%	
		2	[b]		0.511	0.233 ±0.019	0.278 ±0.027	0.97 ± 10%	
		3	[b]		0.880	0.407 ±0.028	0.473 ±0.039	1.66 ± 9%	
		4	[b]		1.182	0.649 ±0.045	0.533 ±0.063	1.86 ± 12%	
		5	[b]		1.328	0.953 ±0.059	0.375 ±0.083	1.31 ± 22%	
		6	[b]		1.377	1.206 ±0.041	0.171 ±0.058	0.60 ± 34%	

[a] Derivation methods: "IntOH" = hourly amounts reacted computed from the experimentally measured IntOH and VOC's OH rate constant; "Direct" = hourly amounts reacted determined by interpolating experimental measurements of the VOC, with a correction for dilution.

[b] Amount reacted could not be determined for this VOC, or amount reacted could not be determined for this time with sufficient precision to be useful.

[c] This is a DTC run. "Base fit" data is from base case run carried out in the other side of the chamber.

Table 9. Derivation of hourly IntOH reactivities from the results of the ethene surrogate experiments.

ETC Run No	Added (ppm)	Time (hr)	Reacted (ppm)	IntOH (ppt-min)			Reactivity (ppt-min/ppm)	
				Test Run	Base Fit	Change	Incremental	Mechanistic
<b>Carbon Monoxide</b>								
487	107.	1	[a]	1.1 ±2.6	1.0 ±1.0	0.1 ±2.8	(0.0007 ±0.03)	
		2	[a]	2.8 ±2.6	3.7 ±1.5	-0.9 ±3.0	(-0.008 ±0.03)	
		3	0.326 ±0.099	8.7 ±2.6	7.6 ±1.6	1.1 ±3.1	(0.010 ±0.03)	(3. ± 10.)
		4	0.547 ±0.102	14.7 ±2.7	12.8 ±2.6	1.9 ±3.8	(0.02 ±0.04)	(3. ± 7.)
		5	0.803 ±0.106	21.6 ±2.8	22.0 ±2.2	-0.3 ±3.5	(-0.003 ±0.03)	(0. ± 4.)
		6	1.121 ±0.113	30.3 ±2.9	32.5 ±2.2	-2.2 ±3.6	(-0.02 ±0.03)	(-2. ± 3.)
483	155.	1	[a]	1.4 ±2.6	3.2 ±1.1	-1.8 ±2.8	(-0.012 ±0.02)	
		2	0.261 ±0.141	4.8 ±2.6	5.5 ±1.6	-0.7 ±3.0	(-0.004 ±0.02)	(-3. ± 12.)
		3	0.461 ±0.143	8.5 ±2.6	9.2 ±1.7	-0.7 ±3.1	(-0.005 ±0.02)	(-2. ± 7.)
		4	0.713 ±0.147	13.2 ±2.8	13.2 ±2.8	0.0 ±3.9	(0.0003 ±0.03)	(0. ± 5.)
		5	0.979 ±0.153	18.2 ±2.8	20.8 ±2.3	-2.6 ±3.6	(-0.02 ±0.02)	(-3. ± 4.)
		6	1.223 ±0.160	22.8 ±2.9	29.5 ±2.1	-6.7 ±3.6	-0.043 ± 53%	-5. ± 55%
<b>Ethane</b>								
506	49.7	1	[a]	1.2 ±2.6	4.0 ±1.1	-2.8 ±2.8	(-0.06 ±0.06)	
		2	0.101 ±0.051	5.1 ±2.6	6.0 ±1.6	-0.9 ±3.1	(-0.02 ±0.06)	(-9. ± 31.)
		3	0.181 ±0.052	9.2 ±2.6	10.4 ±1.7	-1.3 ±3.2	(-0.03 ±0.06)	(-7. ± 18.)
		4	0.211 ±0.054	10.7 ±2.8	14.7 ±2.8	-4.0 ±4.0	(-0.08 ±0.08)	(-19. ± 20.)
		5	0.241 ±0.056	12.3 ±2.8	22.6 ±2.3	-10.3 ±3.6	-0.21 ± 35%	-43. ± 42%
		6	0.382 ±0.058	19.5 ±2.9	29.9 ±2.3	-10.4 ±3.7	-0.21 ± 35%	-27. ± 38%
<b>n-Butane</b>								
488	10.31	1	[a]	1.6 ±2.6	3.4 ±1.1	-1.8 ±2.8	(-0.2 ± 0.3)	
		2	[a]	3.4 ±2.6	5.7 ±1.7	-2.3 ±3.1	(-0.2 ± 0.3)	
		3	0.221 ±0.100	5.8 ±2.6	9.3 ±1.8	-3.5 ±3.2	-0.34 ± 92%	(-16. ± 16.)
		4	0.316 ±0.101	8.4 ±3.0	12.8 ±3.0	-4.5 ±4.2	-0.43 ± 94%	(-14. ± 99%)
		5	0.462 ±0.104	12.3 ±2.8	20.0 ±2.5	-7.7 ±3.7	-0.74 ± 49%	(-17. ± 53%)
		6	0.504 ±0.107	13.5 ±2.9	28.4 ±2.3	-14.9 ±3.7	-1.44 ± 25%	(-30. ± 32%)
484	15.2	1	[a]	1.2 ±2.6	2.6 ±1.2	-1.4 ±2.8	(-0.09 ± 0.2)	
		2	[a]	2.9 ±2.6	5.0 ±1.7	-2.1 ±3.1	(-0.14 ± 0.2)	
		3	0.341 ±0.146	6.1 ±2.6	7.9 ±1.8	-1.9 ±3.2	(-0.12 ± 0.2)	(-5. ± 10.)
		4	0.410 ±0.149	7.4 ±3.0	11.6 ±3.0	-4.2 ±4.2	(-0.3 ± 0.3)	(-10. ± 11.)
		5	0.425 ±0.154	7.7 ±2.8	19.0 ±2.5	-11.4 ±3.7	-0.75 ± 33%	(-27. ± 49%)
		6	0.645 ±0.158	11.7 ±2.9	27.0 ±2.3	-15.3 ±3.7	-1.01 ± 24%	(-24. ± 34%)
<b>n-Hexane</b>								
72A [b]	2.88	3	[a]	3.7 ±3.2	3.9 ±2.4	-0.2 ±4.0	(-0.07 ± 1.4)	
		4	[a]	3.9 ±3.8	7.9 ±2.6	-4.0 ±4.7	(-1.4 ± 2. )	
		5	[a]	5.3 ±4.5	9.0 ±2.8	-3.7 ±5.3	(-1.3 ± 2. )	
		6	0.166 ±0.121	7.3 ±5.2	17.2 ±3.1	-10.0 ±6.1	-3.5 ± 61%	(-60. ± 95%)
<b>n-Octane</b>								
472	1.60	1	[a]	2.7 ±2.2	2.9 ±1.0	-0.2 ±2.4	(-0.14 ± 2. )	
		2	[a]	3.0 ±2.2	4.8 ±1.5	-1.9 ±2.7	(-1.2 ± 2. )	
		3	0.095 ±0.046	4.8 ±2.3	9.2 ±1.6	-4.5 ±2.8	-2.8 ± 62%	(-47. ± 78%)
		4	0.123 ±0.046	6.3 ±2.6	15.5 ±2.6	-9.2 ±3.6	-5.7 ± 39%	(-75. ± 54%)
		5	0.185 ±0.047	9.6 ±2.4	25.5 ±2.1	-15.9 ±3.2	-9.9 ± 20%	(-86. ± 32%)
		6	0.278 ±0.047	15.1 ±2.5	37.0 ±2.1	-22.0 ±3.2	-13.7 ± 15%	(-79. ± 22%)
474	2.27	1	[a]	1.0 ±2.2	2.7 ±1.0	-1.6 ±2.4	(-0.7 ± 1.1)	
		2	[a]	1.7 ±2.2	4.7 ±1.5	-3.1 ±2.7	-1.35 ± 87%	
		3	[a]	2.8 ±2.3	9.0 ±1.5	-6.2 ±2.7	-2.7 ± 44%	
		4	0.128 ±0.066	4.6 ±2.5	14.9 ±2.5	-10.4 ±3.5	-4.6 ± 34%	(-81. ± 62%)
		5	0.172 ±0.068	6.2 ±2.4	24.7 ±2.1	-18.5 ±3.2	-8.1 ± 17%	(-107. ± 43%)
		6	0.286 ±0.068	10.6 ±2.5	32.8 ±2.2	-22.2 ±3.3	-9.8 ± 15%	(-78. ± 28%)
<b>Propene</b>								
500	0.213	1	0.011 ±0.006	0.9 ±2.6	3.8 ±1.1	-2.9 ±2.8	-13.5 ± 96%	(-272. ±302.)
		2	0.050 ±0.005	2.1 ±2.6	5.8 ±1.6	-3.7 ±3.1	-17.2 ± 83%	(-73. ± 84%)
		3	0.121 ±0.005	10.2 ±2.6	9.9 ±1.7	0.3 ±3.1	(2. ± 15. )	(3. ± 26. )
		4	0.174 ±0.005	21.3 ±2.8	14.7 ±2.8	6.6 ±3.9	31. ± 59%	(38. ± 59%)
		5	0.201 ±0.005	30.9 ±2.8	23.1 ±2.3	7.8 ±3.6	37. ± 46%	(39. ± 46%)
		6	0.208 ±0.005	33.9 ±2.9	31.5 ±2.1	2.3 ±3.6	(11. ± 17. )	(11. ± 17. )
496	0.301	1	0.032 ±0.008	1.7 ±2.6	3.3 ±1.1	-1.5 ±2.8	(-5. ± 9. )	(-49. ± 89. )
		2	0.104 ±0.007	7.7 ±2.6	5.2 ±1.6	2.5 ±3.0	(8. ± 10. )	(24. ± 29. )
		3	0.222 ±0.006	18.2 ±2.6	10.7 ±1.7	7.4 ±3.1	25. ± 42%	(33. ± 42%)
		4	[a]	27.6 ±2.7	17.1 ±2.7	10.6 ±3.8	35. ± 36%	
		5	0.301 ±0.006	37.0 ±2.8	27.0 ±2.3	10.0 ±3.6	33. ± 36%	(33. ± 36%)
		6	0.301 ±0.006	42.5 ±2.9	39.8 ±2.3	2.7 ±3.7	(9. ± 12. )	(9. ± 12. )

Table 9 (continued)

ETC Run No	Added (ppm)	Time (hr)	Reacted (ppm)	IntOH (ppt-min)			Reactivity (ppt-min/ppm)	
				Test Run	Base Fit	Change	Incremental	Mechanistic
<b>trans-2-Butene</b>								
501	0.066	1	0.038 ±0.001	3.5 ±2.6	3.7 ±1.0	-0.1 ±2.8	( -2. ± 42. )	( -4. ± 73. )
		2	0.066 ±0.001	12.6 ±2.6	5.6 ±1.6	7.0 ±3.0	106. ± 43%	106. ± 43%
		3	0.066 ±0.001	19.0 ±2.6	9.9 ±1.6	9.1 ±3.1	138. ± 34%	138. ± 34%
		4	0.066 ±0.001	31.8 ±2.7	15.2 ±2.7	16.6 ±3.8	252. ± 23%	252. ± 23%
		5	0.066 ±0.001	38.8 ±2.8	24.2 ±2.2	14.6 ±3.6	222. ± 24%	222. ± 24%
		6	0.066 ±0.001	41.9 ±2.9	32.9 ±2.0	9.0 ±3.5	137. ± 39%	137. ± 39%
43B [b]	0.097	1	0.066 ±0.002	6.3 ±2.3	1.2 ±2.3	5.1 ±3.3	52. ± 65%	77. ± 65%
		2	0.097 ±0.002	15.9 ±2.7	3.9 ±2.7	12.0 ±3.8	124. ± 32%	124. ± 32%
		3	0.097 ±0.002	24.1 ±3.2	8.5 ±3.2	15.7 ±4.6	162. ± 29%	162. ± 29%
		4	0.097 ±0.002	32.3 ±3.8	13.6 ±3.8	18.7 ±5.4	193. ± 29%	194. ± 29%
		5	0.097 ±0.002	38.5 ±4.5	17.1 ±4.5	21.5 ±6.4	222. ± 30%	222. ± 30%
		6	0.097 ±0.002	41.8 ±5.2	24.4 ±5.2	17.5 ±7.4	180. ± 42%	181. ± 42%
493	0.142	1	0.142 ±0.003	7.1 ±2.6	2.9 ±1.0	4.2 ±2.7	30. ± 65%	30. ± 65%
		2	0.142 ±0.003	14.9 ±2.6	4.8 ±1.5	10.1 ±3.0	71. ± 30%	71. ± 30%
		3	0.142 ±0.003	22.9 ±2.6	9.2 ±1.6	13.7 ±3.1	97. ± 23%	97. ± 23%
		4	0.142 ±0.003	28.3 ±2.7	15.5 ±2.6	12.7 ±3.7	90. ± 29%	90. ± 29%
		5	0.142 ±0.003	34.0 ±2.8	25.6 ±2.1	8.4 ±3.5	59. ± 42%	59. ± 42%
		6	0.142 ±0.003	58.0 ±2.9	36.9 ±2.1	21.2 ±3.5	150. ± 17%	150. ± 17%
<b>m-Xylene</b>								
478	0.095	1	0.013 ±0.003	4.5 ±1.0	3.7 ±1.0	0.7 ±1.5	( 8. ± 16. )	( 53. ±110. )
		2	0.027 ±0.002	9.9 ±1.6	5.6 ±1.6	4.3 ±2.2	46. ± 52%	157. ± 52%
		3	0.045 ±0.002	18.7 ±1.6	10.0 ±1.6	8.7 ±2.3	92. ± 27%	195. ± 27%
		4	0.059 ±0.002	28.5 ±2.7	15.4 ±2.7	13.1 ±3.8	139. ± 29%	223. ± 29%
		5	0.070 ±0.002	39.7 ±2.2	24.4 ±2.2	15.3 ±3.2	162. ± 21%	219. ± 21%
		6	0.075 ±0.002	47.5 ±2.1	32.2 ±2.1	15.3 ±3.0	162. ± 20%	203. ± 20%
499	0.147	1	0.015 ±0.004	3.2 ±1.0	2.8 ±1.0	0.3 ±1.4	( 2. ± 9. )	( 21. ± 90. )
		2	0.046 ±0.004	10.8 ±1.5	4.9 ±1.5	5.9 ±2.1	40. ± 35%	129. ± 36%
		3	0.076 ±0.003	21.4 ±1.5	9.0 ±1.5	12.4 ±2.2	84. ± 18%	162. ± 18%
		4	0.097 ±0.003	31.5 ±2.5	14.5 ±2.5	17.0 ±3.5	116. ± 21%	176. ± 21%
		5	0.108 ±0.003	39.3 ±2.1	23.8 ±2.1	15.6 ±2.9	106. ± 19%	144. ± 19%
		6	0.117 ±0.003	47.1 ±1.9	34.1 ±1.9	13.1 ±2.7	89. ± 21%	112. ± 21%
477	0.173	1	0.023 ±0.005	4.2 ±1.0	2.6 ±1.0	1.6 ±1.4	9.2 ± 86%	69. ± 88%
		2	0.062 ±0.004	13.0 ±1.4	4.7 ±1.4	8.3 ±2.0	48. ± 25%	134. ± 25%
		3	0.098 ±0.004	24.5 ±1.5	8.9 ±1.5	15.6 ±2.1	90. ± 14%	159. ± 14%
		4	0.118 ±0.004	34.0 ±2.5	14.8 ±2.5	19.3 ±3.5	112. ± 18%	163. ± 18%
		5	0.133 ±0.004	43.5 ±2.1	24.4 ±2.1	19.1 ±2.9	111. ± 15%	144. ± 16%
		6	0.139 ±0.004	48.8 ±2.3	32.1 ±2.3	16.7 ±3.2	97. ± 20%	120. ± 20%
<b>Formaldehyde</b>								
468	0.108	1	[a]	3.0 ±2.6	2.4 ±1.0	0.6 ±2.7	( 6. ± 25. )	
		2	[a]	6.1 ±2.6	4.7 ±1.4	1.4 ±3.0	( 13. ± 28. )	
		3	[a]	12.2 ±2.6	8.5 ±1.5	3.7 ±3.0	34. ± 83%	
		4	[a]	18.3 ±2.7	13.4 ±2.5	4.8 ±3.7	45. ± 76%	
		5	[a]	29.3 ±2.8	22.1 ±2.1	7.1 ±3.5	66. ± 49%	
		6	[a]	37.8 ±2.9	33.1 ±1.9	4.7 ±3.5	43. ± 75%	
470	0.260	1	[a]	6.0 ±2.6	2.5 ±1.0	3.5 ±2.8	13.3 ± 80%	
		2	[a]	13.2 ±2.6	4.6 ±1.6	8.6 ±3.0	33. ± 35%	
		3	[a]	22.0 ±2.6	9.9 ±1.7	12.0 ±3.1	46. ± 26%	
		4	[a]	32.3 ±2.7	16.5 ±2.7	15.8 ±3.8	61. ± 24%	
		5	[a]	44.7 ±2.8	26.8 ±2.2	17.9 ±3.6	69. ± 20%	
		6	[a]	52.8 ±2.9	40.4 ±2.2	12.4 ±3.7	48. ± 30%	
489	0.286	1	[a]	2.1 ±2.6	1.5 ±1.0	0.6 ±2.8	( 2. ± 10. )	
		2	[a]	8.0 ±2.6	3.9 ±1.6	4.1 ±3.0	14.2 ± 74%	
		3	[a]	16.5 ±2.6	8.7 ±1.6	7.7 ±3.1	27. ± 40%	
		4	[a]	29.4 ±2.7	14.9 ±2.7	14.4 ±3.8	51. ± 26%	
		5	[a]	39.0 ±2.8	24.9 ±2.2	14.1 ±3.6	49. ± 25%	

[a] Amount reacted could not be determined for this VOC, or amount reacted could not be determined for this time with sufficient precision to be useful.

[b] This is a DTC run. "Base fit" data is from base case run carried out in the other side of the chamber.

Table 10. Derivation of the hourly direct reactivities from the results of the ethene surrogate reactivity experiments. [a]

ETC Run No.	Added (ppm)	Time (hr)	Reacted (ppm)	IntOH (ppt-min)	d(O <sub>3</sub> -NO)/IntOH (base) (10 <sup>3</sup> min <sup>-1</sup> )	d(O <sub>3</sub> -NO) (ppm)		Direct d(O <sub>3</sub> -NO) Incremental (mol d(O <sub>3</sub> -NO)/mol VOC)	Reactivity Mechanistic (mol VOC)
						Total	From Base ROG		
<b>Carbon Monoxide</b>									
487	107. ± 2.	2	[b]	2.8±2.6	46.2±15.1	0.412	0.131±0.127	0.0026 ± 45%	
		3	0.326±30%	8.7±2.6	41.5± 8.8	0.752	0.361±0.133	0.0036 ± 34%	1.2 ±46%
		4	0.547±19%	14.7±2.7	44.4± 5.0	1.115	0.652±0.141	0.0043 ± 30%	0.8 ±36%
483	155. ± 3.	2	0.261±54%	4.8±2.6	38.3±15.4	0.446	0.184±0.124	0.0017 ± 47%	1.0 ±72%
		3	0.461±31%	8.5±2.6	37.0± 8.9	0.825	0.316±0.124	0.0033 ± 24%	1.1 ±39%
		4	0.713±21%	13.2±2.8	41.0± 5.4	1.198	0.542±0.134	0.0042 ± 20%	0.9 ±29%
<b>Ethane</b>									
506	49.7 ±1.0	2	0.101±51%	5.1±2.6	25.4±16.8	0.317	0.129±0.108	0.0038 ± 57%	1.9 ±77%
		3	0.181±29%	9.2±2.6	30.5± 9.7	0.547	0.279±0.120	0.0054 ± 45%	1.5 ±53%
		4	0.211±25%	10.7±2.8	34.8± 5.7	0.827	0.373±0.116	0.0091 ± 26%	2.1 ±36%
<b>n-Butane</b>									
488	10.31 ±0.21	2	[b]	3.4±2.6	36.5±16.4	0.320	0.123±0.109	0.0191 ± 56%	
		3	0.221±45%	5.8±2.6	35.9± 9.5	0.594	0.209±0.109	0.037 ± 28%	1.7 ±53%
		4	0.316±32%	8.4±3.0	41.1± 5.8	0.945	0.343±0.131	0.058 ± 22%	1.9 ±39%
484	15.2 ±0.3	2	[b]	2.9±2.6	40.1±15.7	0.451	0.117±0.113	0.022 ± 34%	
		3	0.341±43%	6.1±2.6	39.2± 9.1	0.828	0.238±0.117	0.039 ± 20%	1.7 ±47%
		4	0.410±36%	7.4±3.0	44.2± 5.9	1.206	0.326±0.139	0.058 ± 16%	2.1 ±40%
<b>n-Hexane</b>									
72A [c]	2.88	6	0.166±73%	7.3±5.2	59.4±10.6	0.914	0.431±0.320	0.168 ± 66%	( 2.9 ±2.9)
<b>n-Octane</b>									
472	1.60 ±0.03	4	0.123±37%	6.3±2.6	43.1± 4.7	0.452	0.270±0.114	0.114 ± 63%	1.5 ±73%
		5	0.185±25%	9.6±2.4	38.2± 1.9	0.700	0.367±0.093	0.21 ± 28%	1.8 ±38%
		6	0.278±17%	15.1±2.5	33.2± 1.5	0.966	0.500±0.086	0.29 ± 18%	1.7 ±25%
474	2.27 ±0.05	3	[b]	2.8±2.3	39.8± 9.3	0.273	0.110±0.094	0.072 ± 58%	
		4	0.128±52%	4.6±2.5	37.8± 5.5	0.429	0.172±0.098	0.113 ± 38%	2.0 ±64%
		5	0.172±39%	6.2±2.4	33.7± 2.2	0.656	0.209±0.082	0.197 ± 18%	2.6 ±43%
		6	0.286±24%	10.6±2.5	33.3± 1.8	0.920	0.354±0.085	0.25 ± 15%	2.0 ±28%

[a] Data are not shown for times in runs where it appears that O<sub>3</sub> formation is becoming NO<sub>x</sub>-limited, because the assumptions behind the derivation of direct reactivities are not valid for such conditions. Data are also not shown when the uncertainties of the direct reactivity estimates are too high to provide meaningful data.

[b] Amount reacted could not be determined for this time with sufficient precision to be useful.

[c] This is a DTC run. "Base fit" data is from base case run carried out in the other side of the chamber.